

The Large Scale Structure of the Universe 3: Baryon Acoustic Oscillations

Eusebio Sánchez Álvaro
CIEMAT

UniCamp Winter School on Observational Cosmology
Sao Paulo
July 2018

LSS 03: Baryon Acoustic Oscillations

Remainder: Probes of dark Energy

What are BAO? How do they measure dark energy?

BAO as standard ruler and cosmology with BAO (D_A and H)

Past and current results review

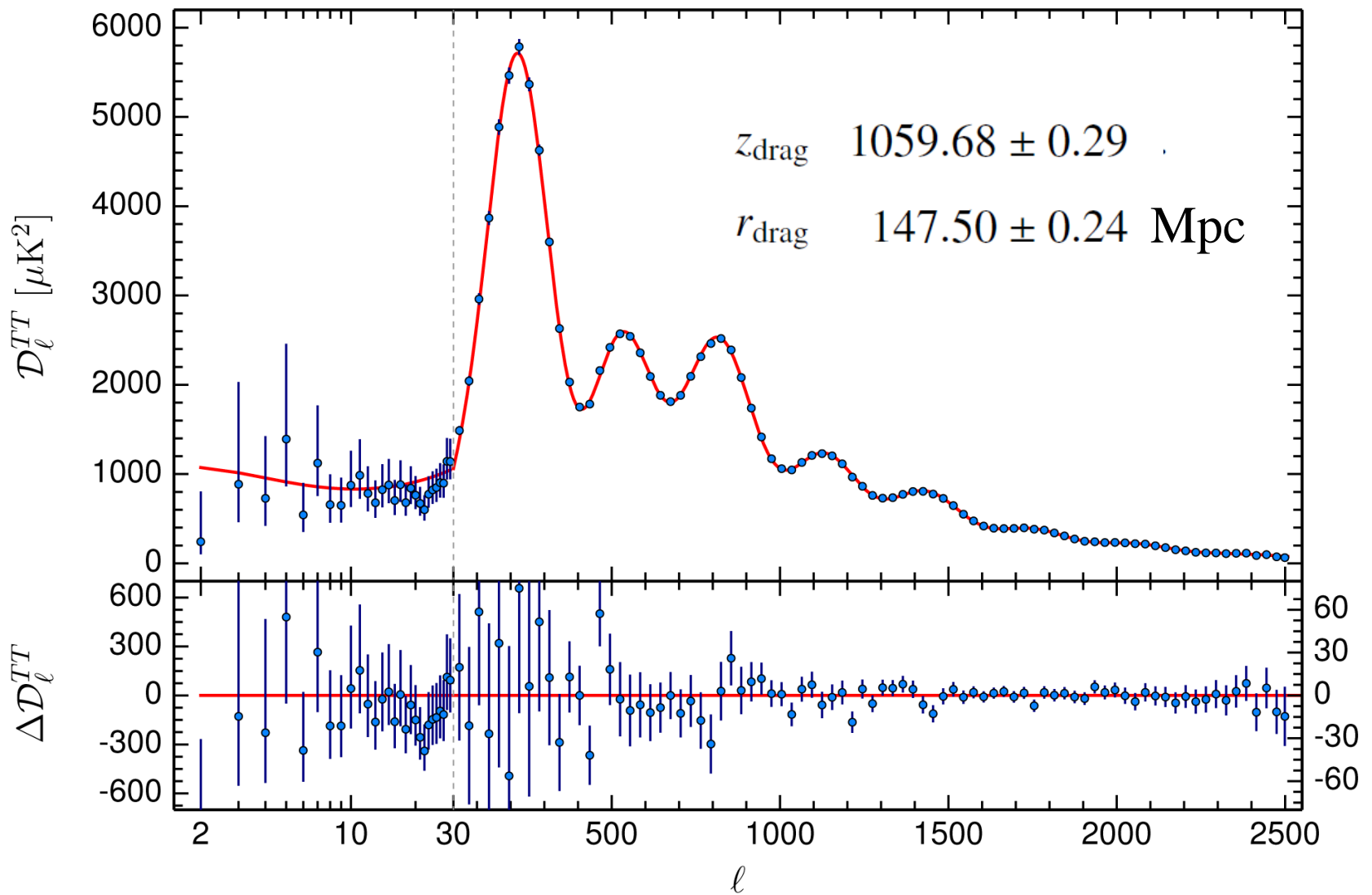
Cosmology with BAO: Some cosmological parameters

Probes of dark energy

	Expansion rate	Growth
Imaging	Supernovae/BAO	Lensing/Clusters
Spectro	BAO	Redshift Space Distortions

Robustness from combination of different probes

Acoustic oscillations seen



Not coincidentally the sound horizon is extremely well determined by the structure of the acoustic peaks in the CMB.

Although there are fluctuations on all scales, there is a characteristic angular scale.

Sound waves in the early Universe

Before recombination:

- Universe is ionized.
- Photons provide enormous pressure and restoring force.
- Perturbations oscillate as acoustic waves.

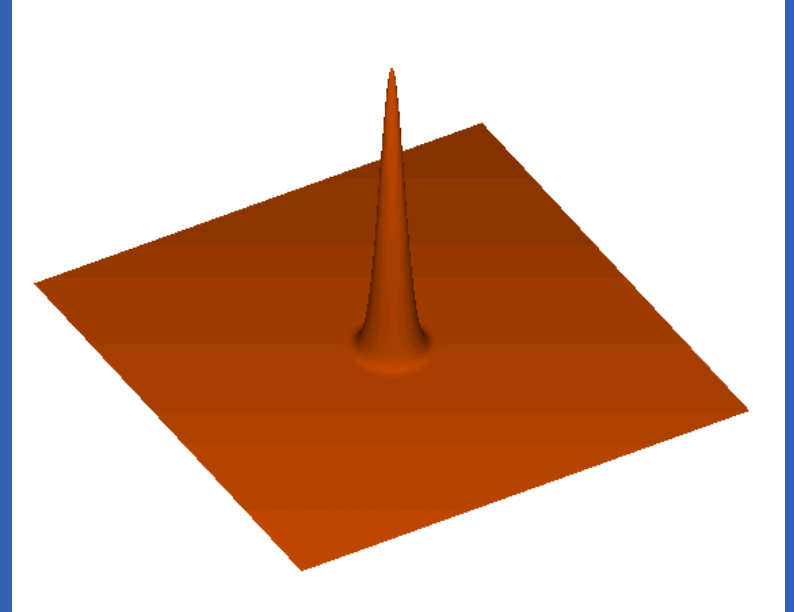
After recombination:

- Universe is neutral.
- Photons can travel freely past the baryons.
- Perturbations grow by gravitational instability.



Sound waves in the early Universe

- Each initial overdensity (in DM & gas) is an overpressure that launches a spherical sound wave.
- This wave travels outwards at 57% of the speed of light.
- Pressure-providing photons decouple at recombination. Sound speed plummets. Wave stalls at a radius of 150 Mpc.
- We see the decoupling photons as the CMB, with the modulations due to the sound waves!

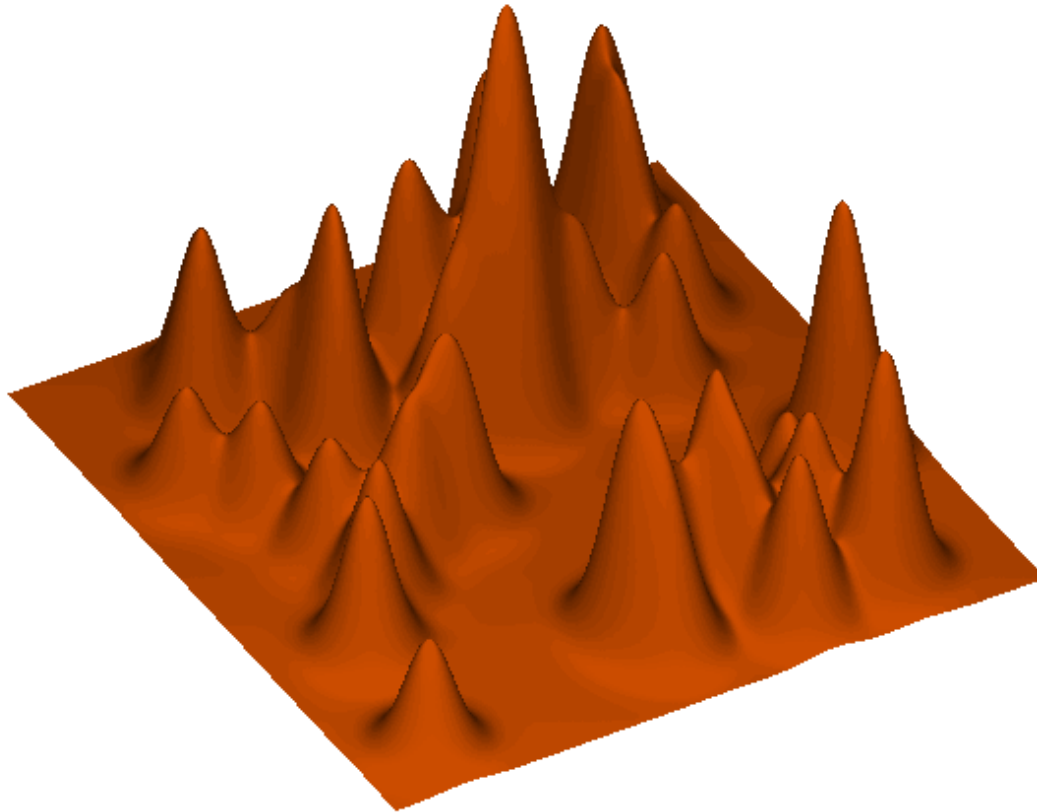


- Overdensity in shell (gas) and in the original center (dark matter) both seed the formation of galaxies. Preferred separation of 150 Mpc (500 million light-years).

Sound waves in the early Universe

A statistical signal

The Universe is a superposition of many acoustic shells
We don't expect to see bullseyes in the Galaxy distribution
We get a 1% bump in the correlation function

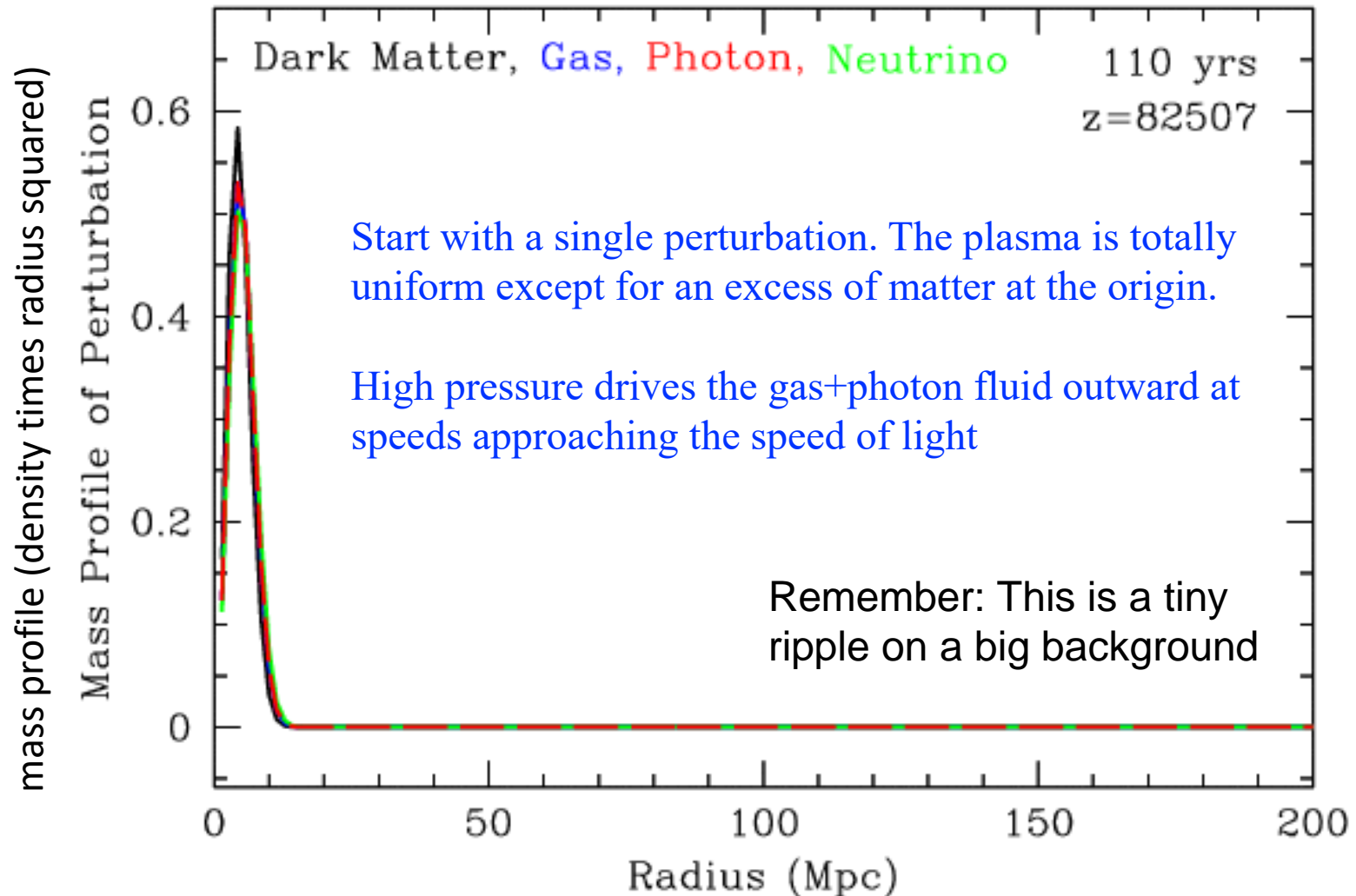


BAO Origin

Initial perturbation in the energy density field at $z = 82507$.

The perturbation is dominated by the photons and neutrinos but there is still a tightly coupled baryon-photon fluid and cold dark matter.

“Mass Profile” of the perturbation as a function of co-moving radius

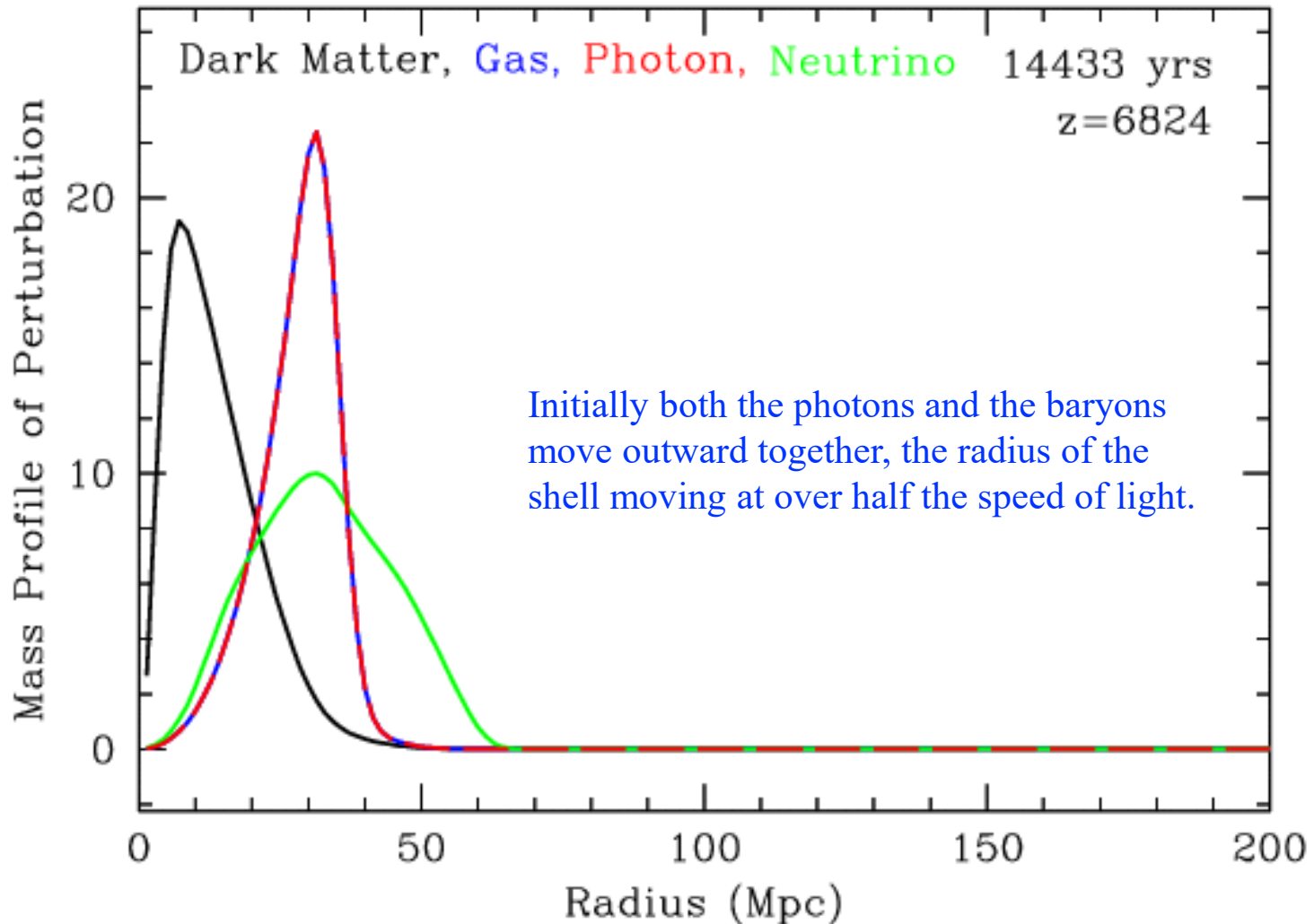


BAO before decoupling

The neutrinos freely stream away from the initial perturbation.

The dark matter stays stationary (but back-reacts to the gravitational pull of the other species.)

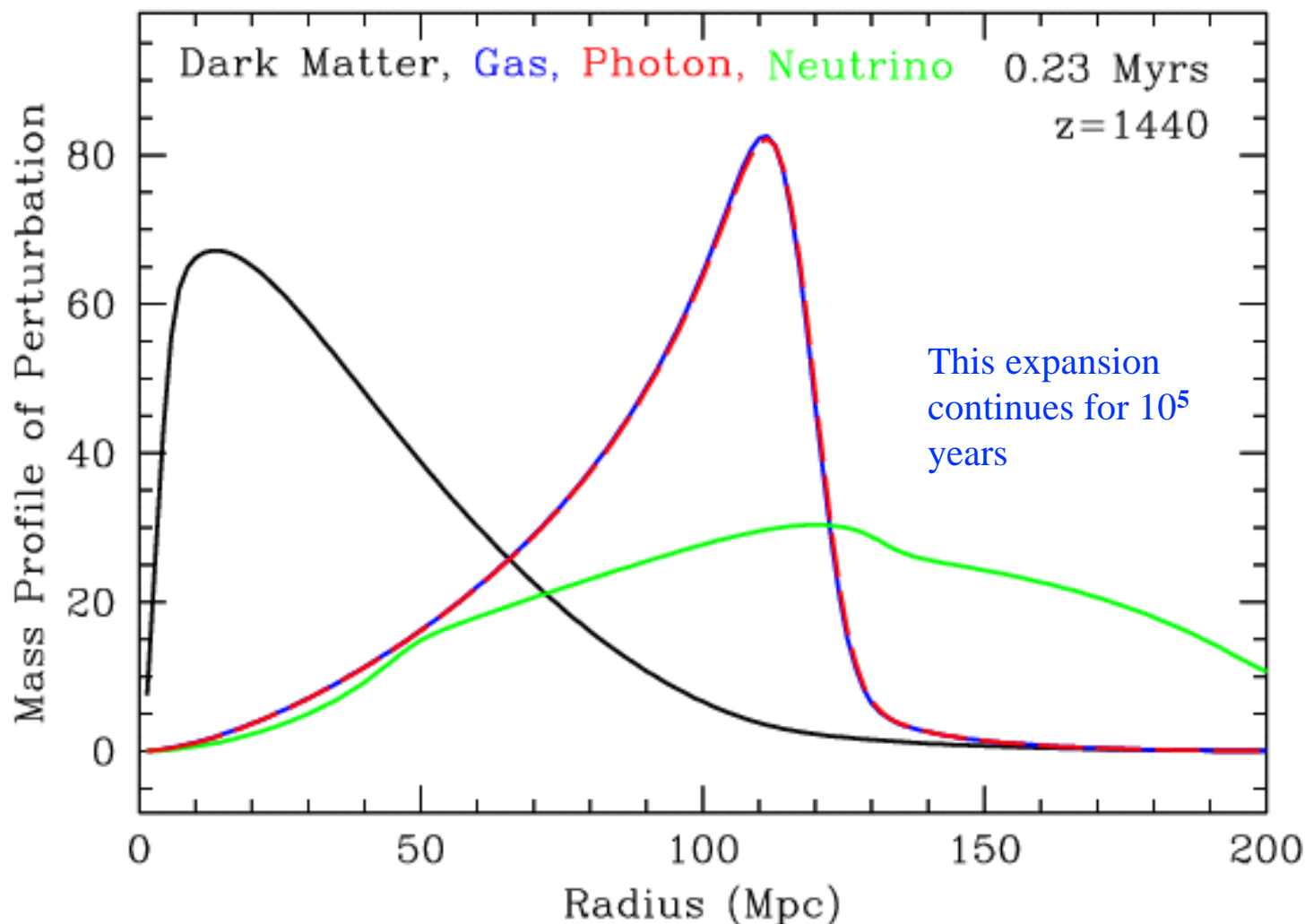
The baryon-photon fluid, which is compressed and highly over-pressured, starts expanding like a spherical sound wave. The speed of sound at this z is 57% the speed of light.



BAO at decoupling

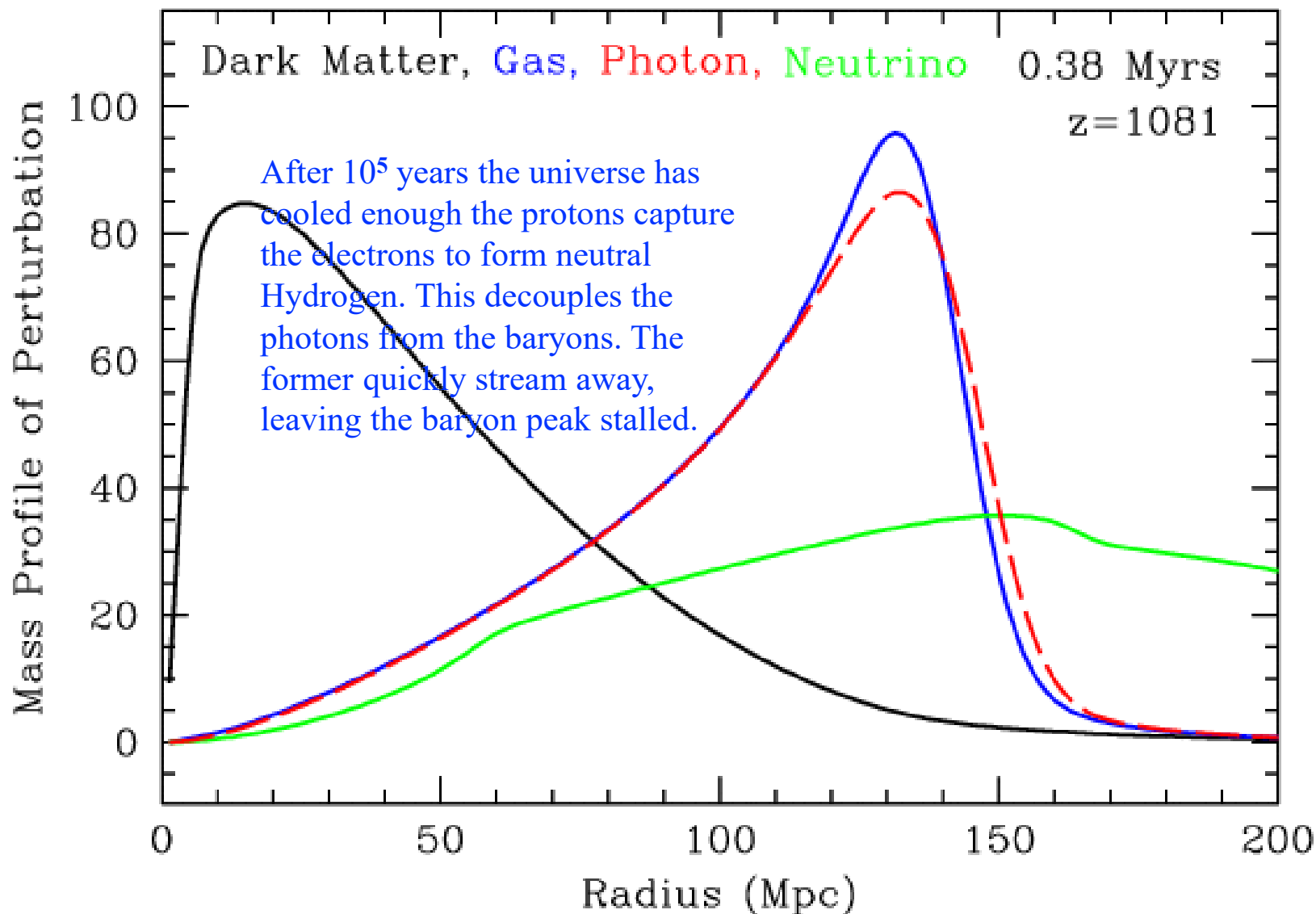
- The neutrinos have gotten spread out due to the metric perturbation.
- The baryon-photon fluid has continued to expand like a spherical sound wave.
- The dark matter perturbation has become more smeared out.

All perturbations have grown due to background matter continuing to fall in



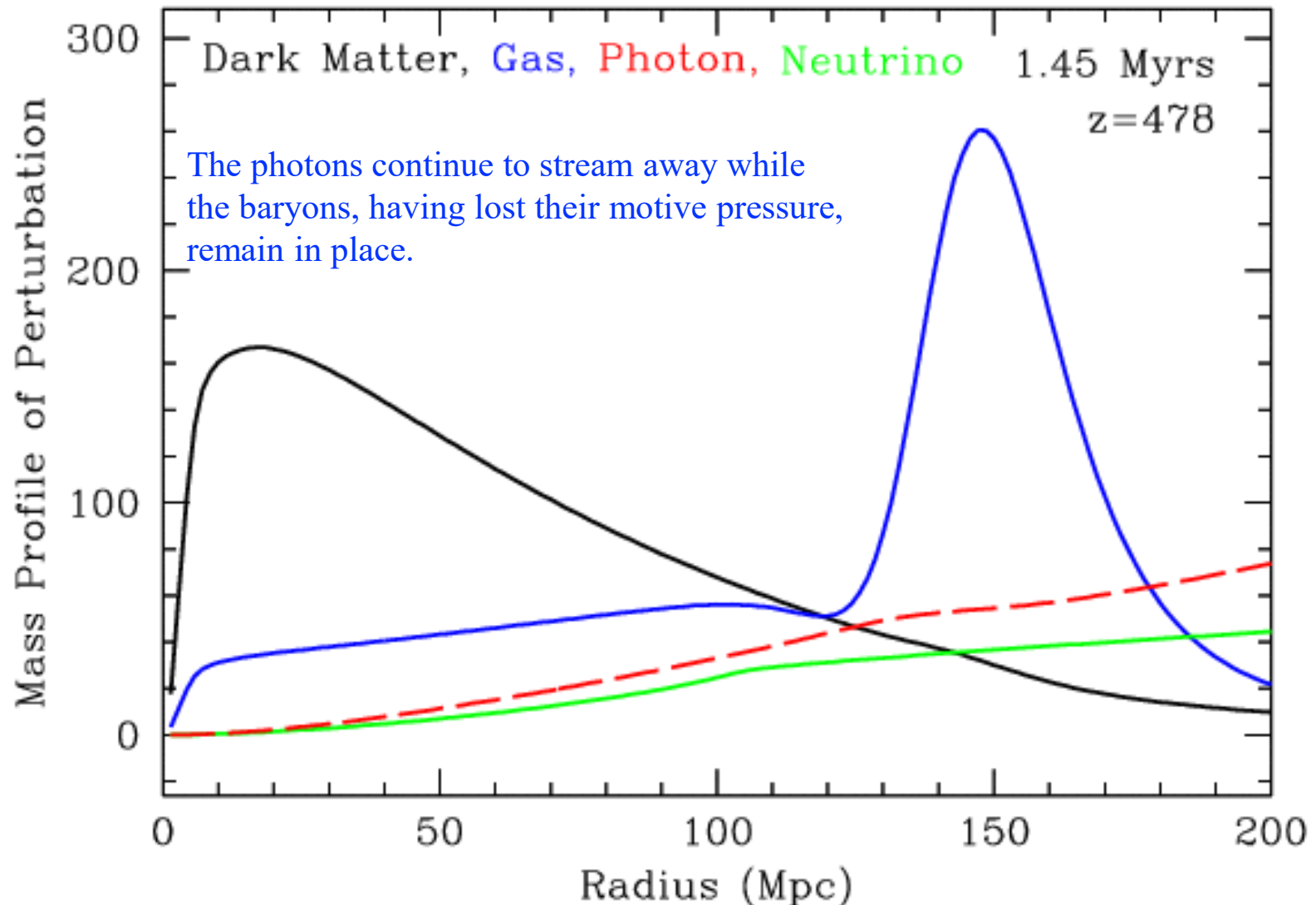
BAO at decoupling

At decoupling ($z = 1089$) the photons begin to decouple from the baryons. The sound speed drops and the pressure wave slows.



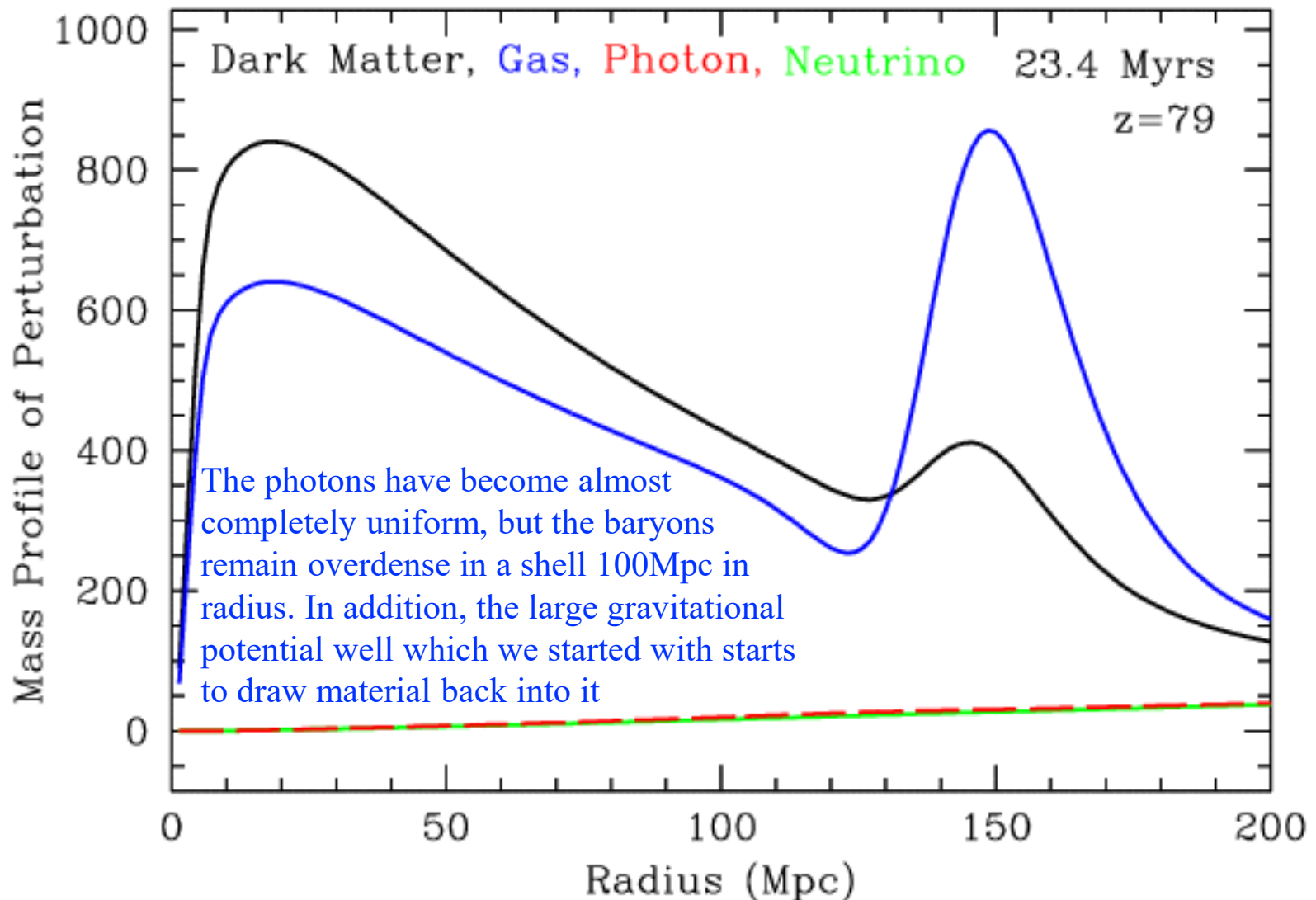
BAO

By $z = 478$ the photons have leaked out of the perturbation and smoothed themselves out. The pressure wave stalls completely. Note the continued “knowledge” of the CDM perturbation by the baryon perturbation (and visa versa).



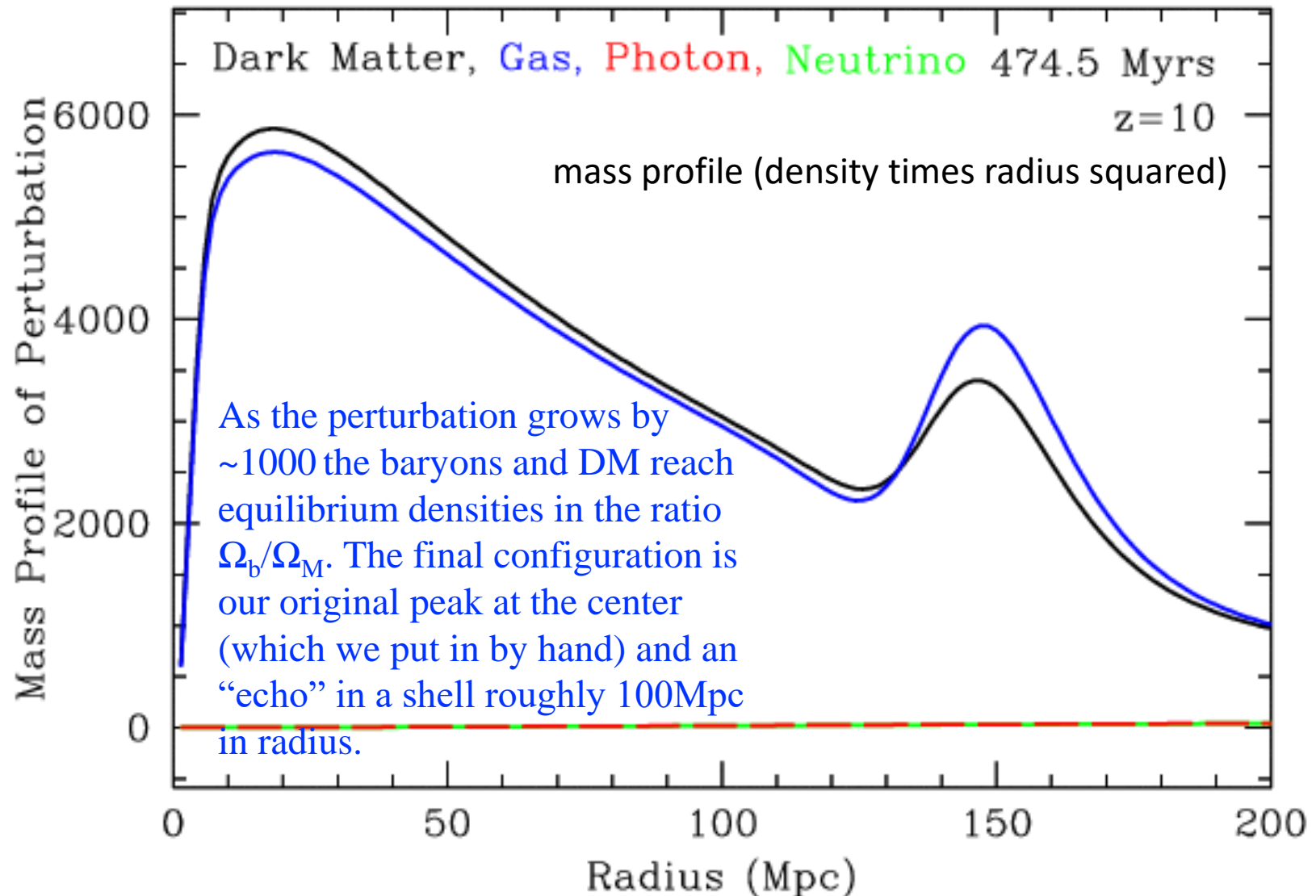
BAO

We are left with a dark matter perturbation around the original center and a gas perturbation in a shell about 150 Mpc in radius. Both perturbations continue to grow.

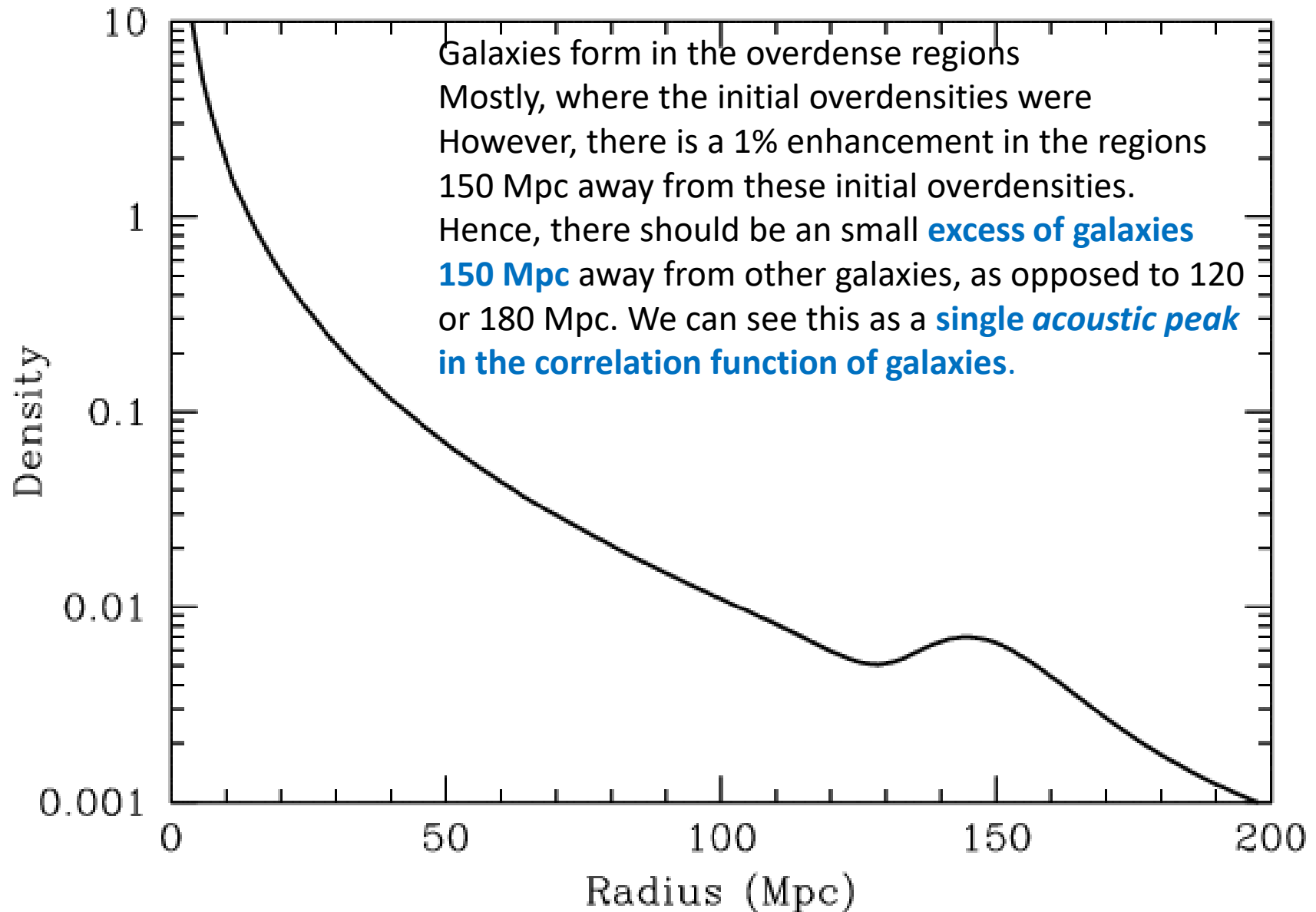


BAO

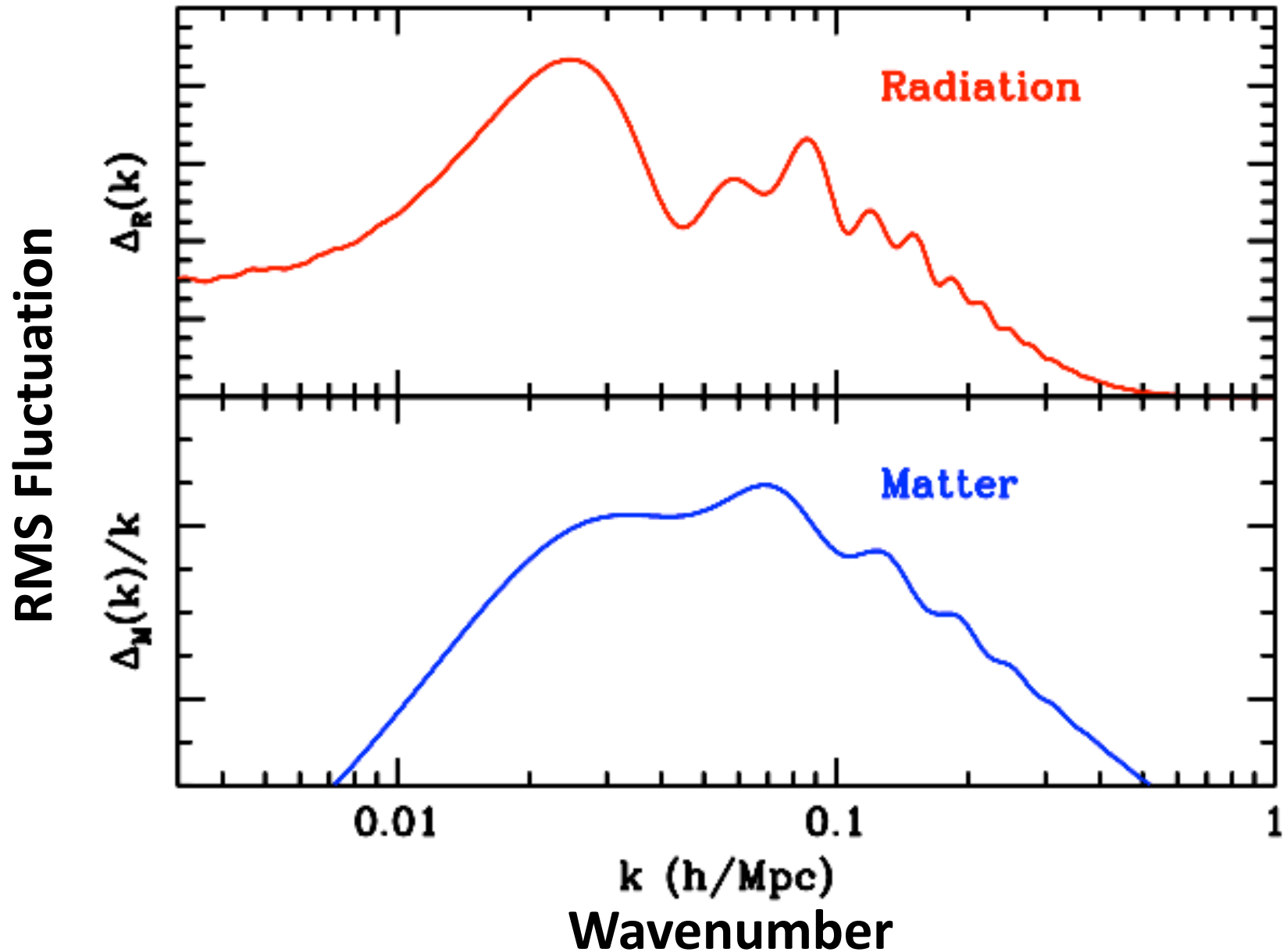
Eventually, the perturbations in the baryons and the dark matter look identical (at least on scales where linear physics dominates). The acoustic peak in the baryons is smoothed out by the much heavier dark matter distribution.



Plotting the density profile we see that the peak is indeed very weak, but measurable

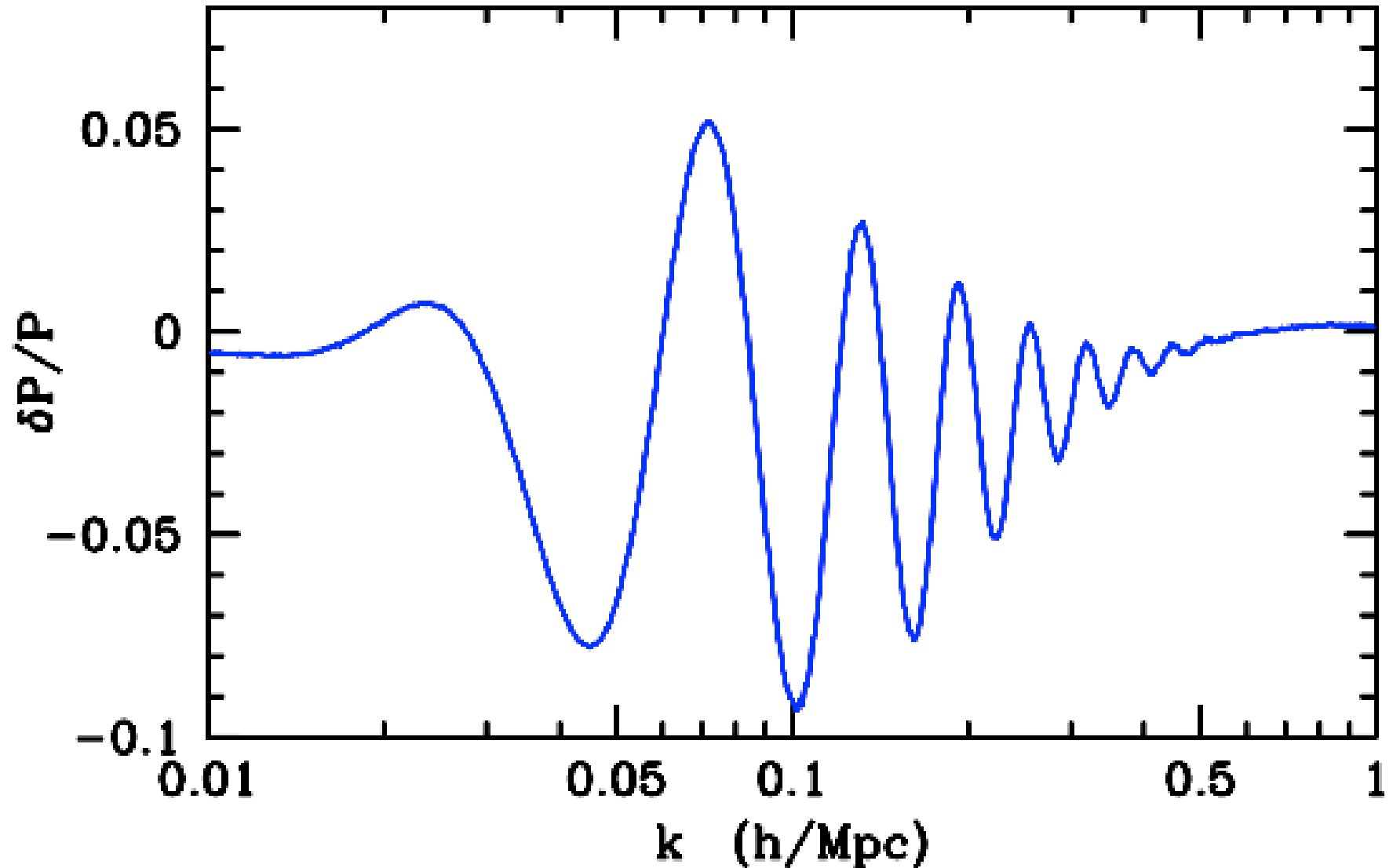


Both CMB and Matter power spectra have the imprint of acoustic oscillations

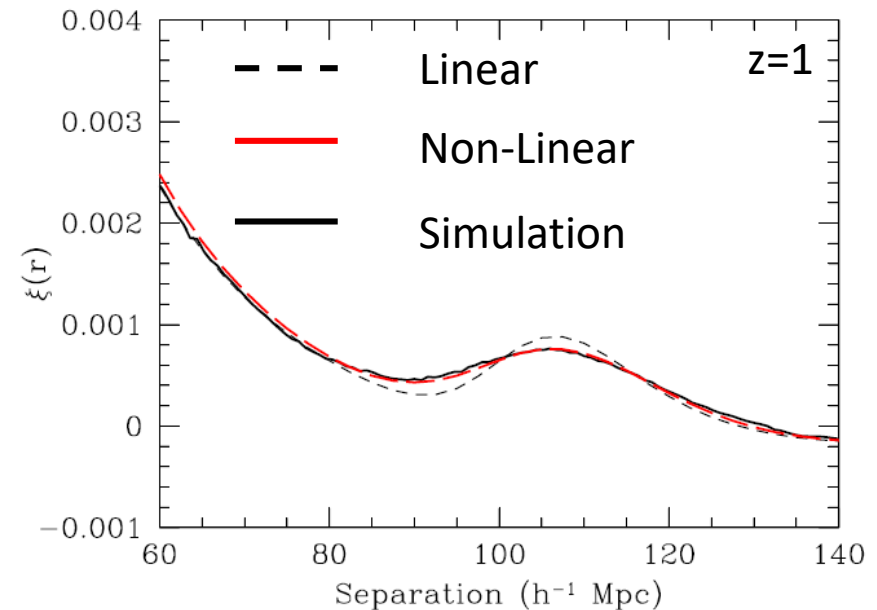
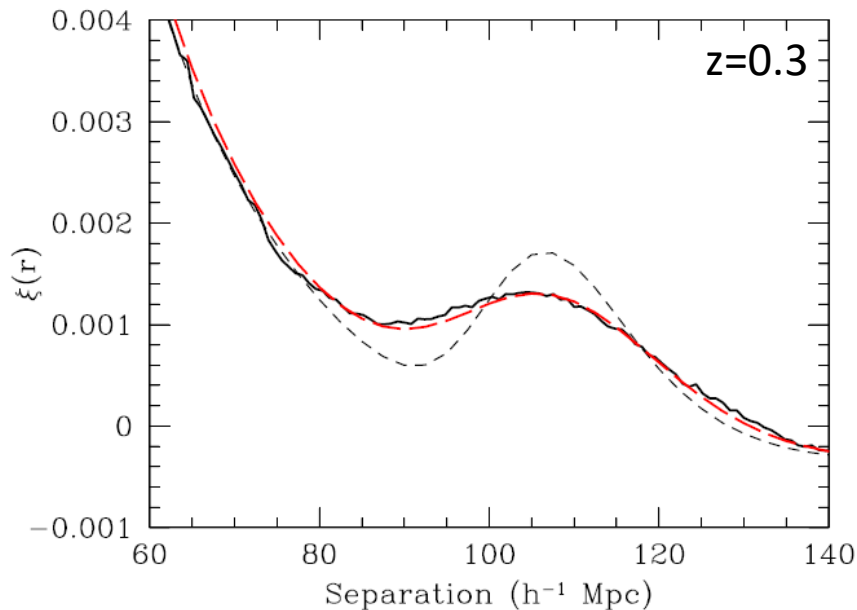


Divide out the gross trend ...

A damped, almost harmonic sequence of “wiggles” in the power spectrum of the mass perturbations of amplitude $O(10\%)$.



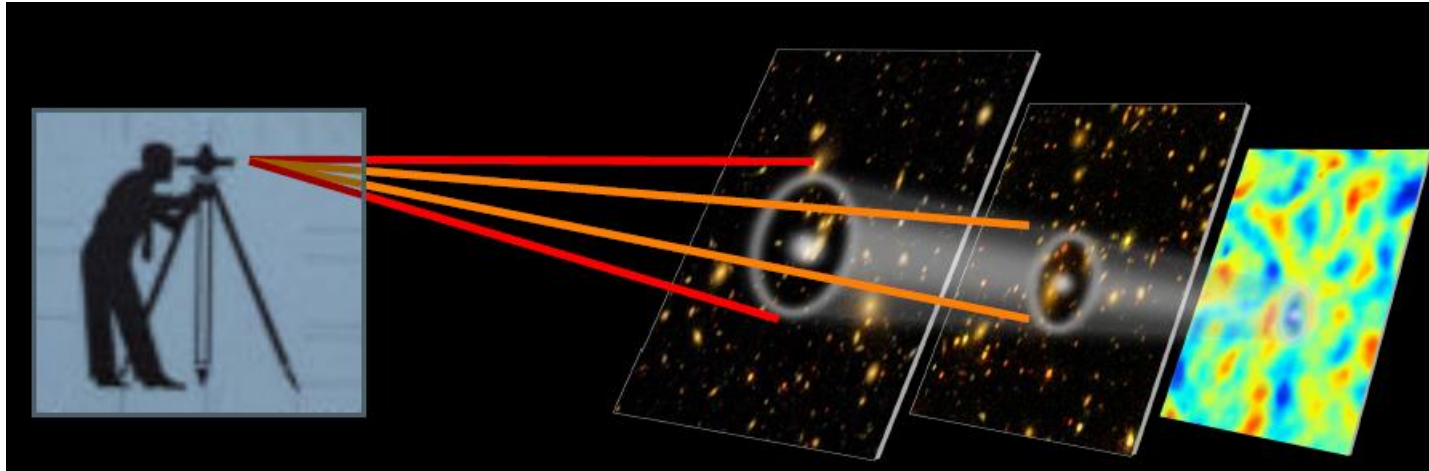
The peak is indeed very weak, but measurable as a bump in the correlation function



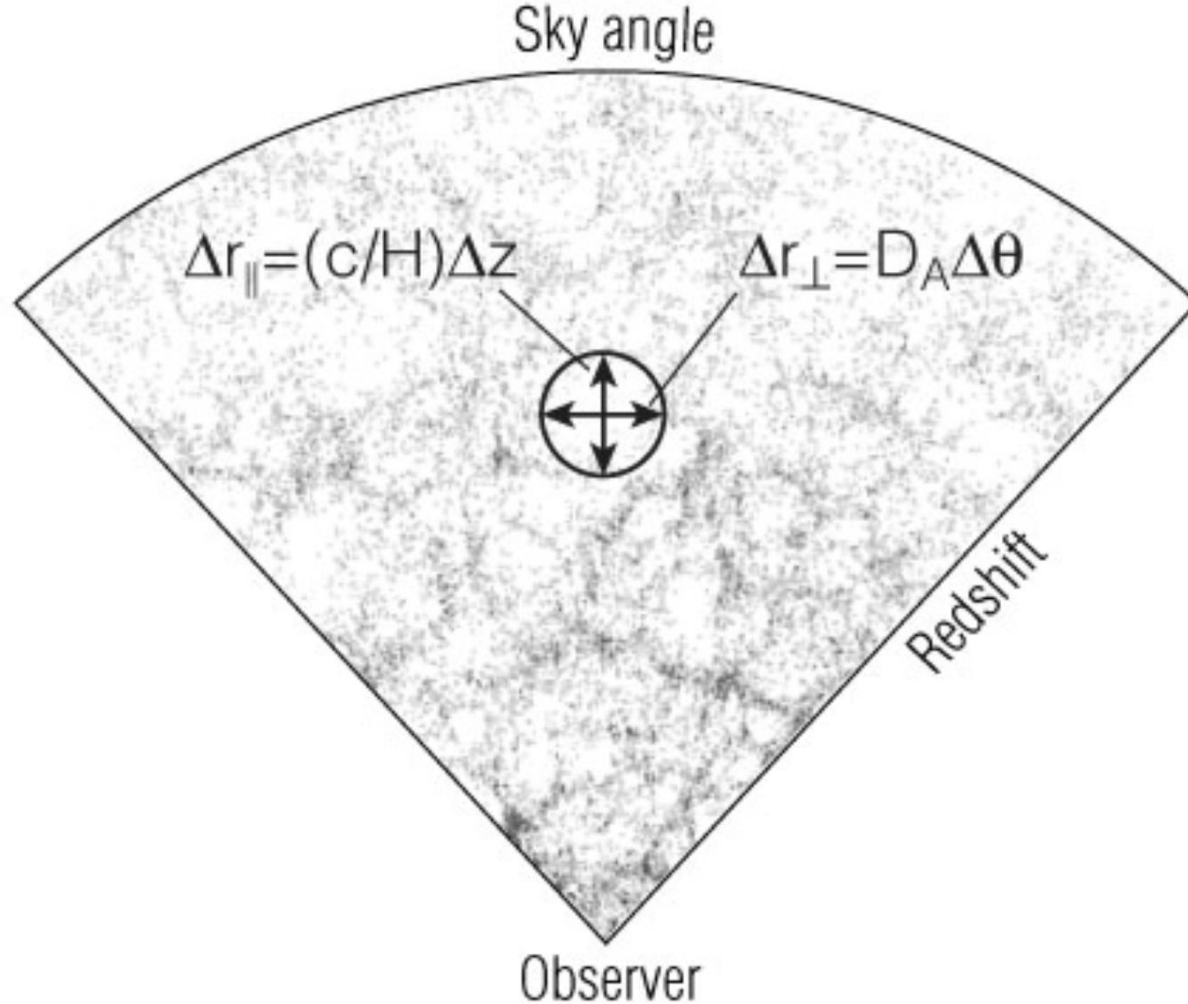
Further (non-linear) processing of the density field acts to broaden and very slightly shift the peak -- but galaxy formation is a local phenomenon with a length scale ~ 10 Mpc, so the action at $r = 0$ and $r \sim 100$ Mpc are essentially decoupled.

Why is this interesting?

- BAO are a standard ruler
- We can study cosmic expansion history using it



- In a galaxy redshift survey, we can measure this along and across the line of sight \rightarrow Yields $H(z)$ and $D_A(z)$!
- Measuring the acoustic peaks across redshift gives a purely geometrical measurement of cosmological distance.
- It is a robust method. Not very sensitive to systematic errors.
- However, the peaks are weak in amplitude and are only available on large scales. Require huge survey volumes.



Measuring 2 distances with standard rulers:

Angular diameter distance $\rightarrow D_A(z; \Omega_M, \Omega_B, \Omega_{\Lambda}, w...)$

Expansion rate (along the LoS) $\rightarrow H(z; \Omega_M, \Omega_B, \Omega_{\Lambda}, w...)$

Different sensitivity and systematic errors

GALAXY REDSHIFT SURVEYS

Redshift surveys are the main way of measuring the 3D clustering of matter

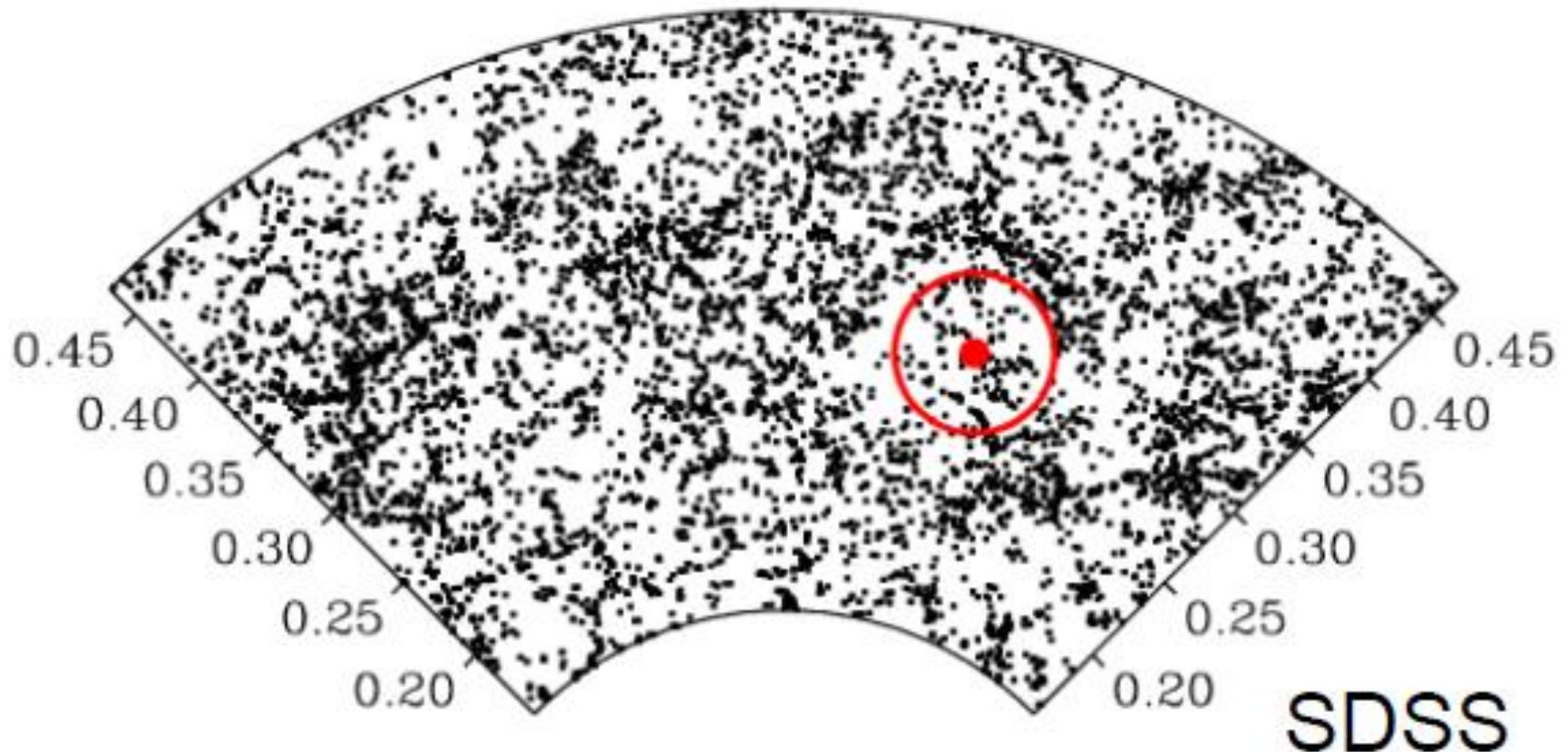
But there are some complications:

Non-linear structure formation

Bias (light does not trace mass)

Redshift space distortions

All these effects partially degrade the BAO peak, but systematics are small because BAO is a very large scale



Non-linear Structure Formation

The acoustic signature is carried by pairs of galaxies separated by 150 Mpc

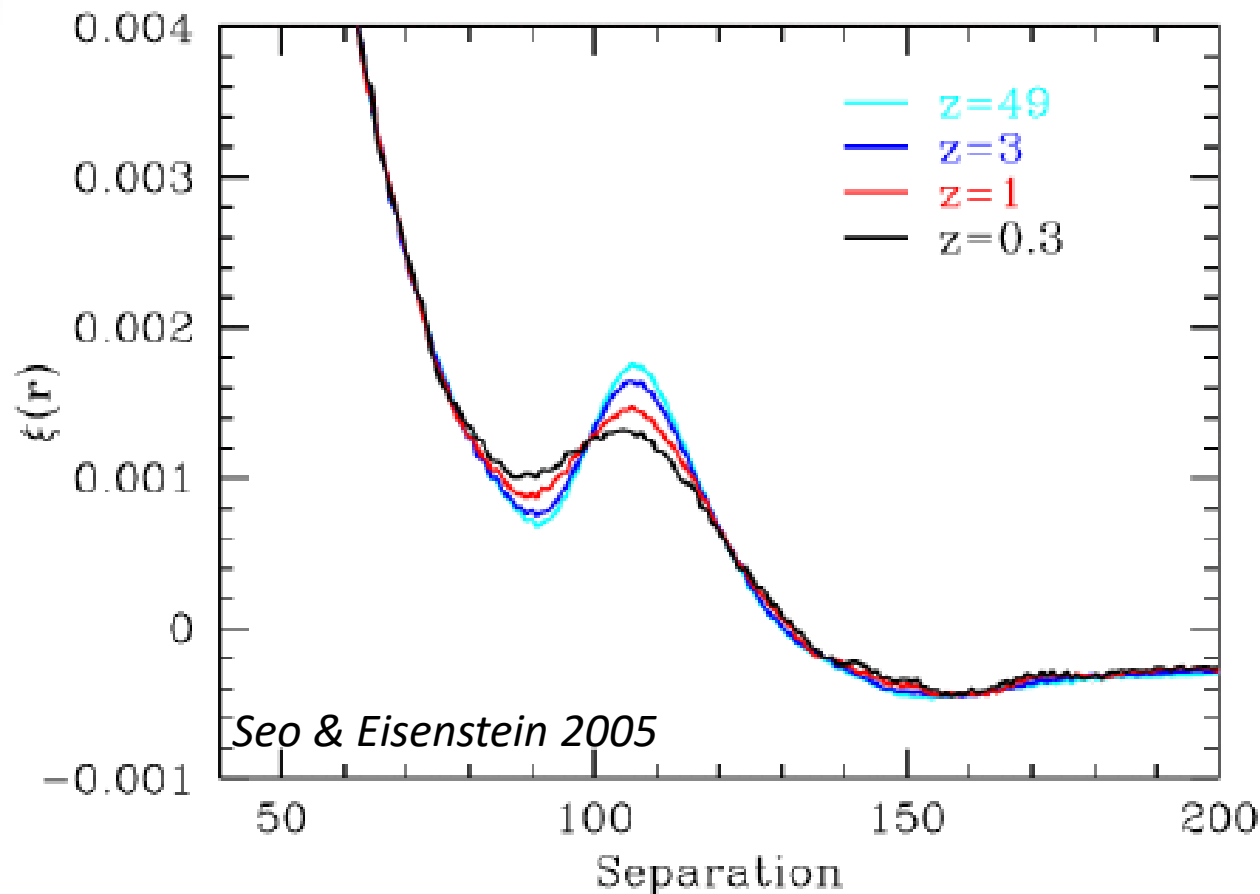
Non-linearities push galaxies around by 3-10 Mpc → broadens the peak

Non-linearities are increasingly negligible for higher z

Moving the scale would require net infall on 150 Mpc scales

This depends on the overdensity inside the sphere which is about 1%

Over and underdensities cancel, so mean shift is $<0.5\%$ → Confirmed by simulations



Virtues of the Acoustic Peaks

Since the acoustic signature is created by physics at $z=1000$ when the perturbations are 1 in 10^5 , the *linear perturbation theory is an excellent description*.

Measuring the acoustic peaks across redshift gives a geometrical measurement of cosmological distance.

The acoustic peaks are a manifestation of a *preferred scale*. Still a very large scale today, so non-linear effects are mild and we can simulate them very accurately.

Measures absolute distance, including that to $z=1000$.

Method has intrinsic cross-check between $H(z)$ & $D_A(z)$, since D_A is an integral of H .

Measuring BAO in real data

2 possibilities for
galaxy surveys:

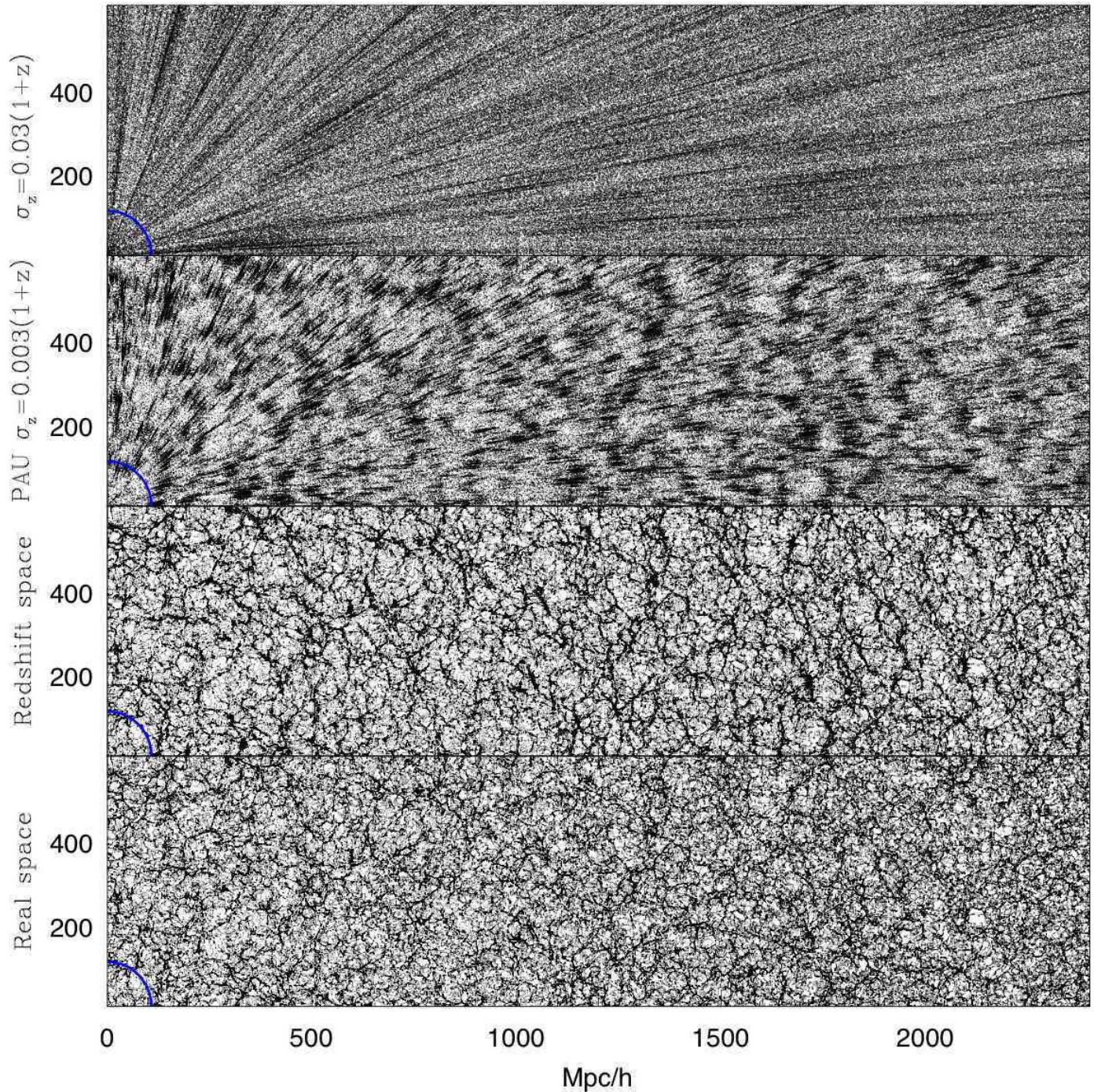
Spectroscopic
Photometric

Angular BAO:

spectro and
photo

Radial BAO:

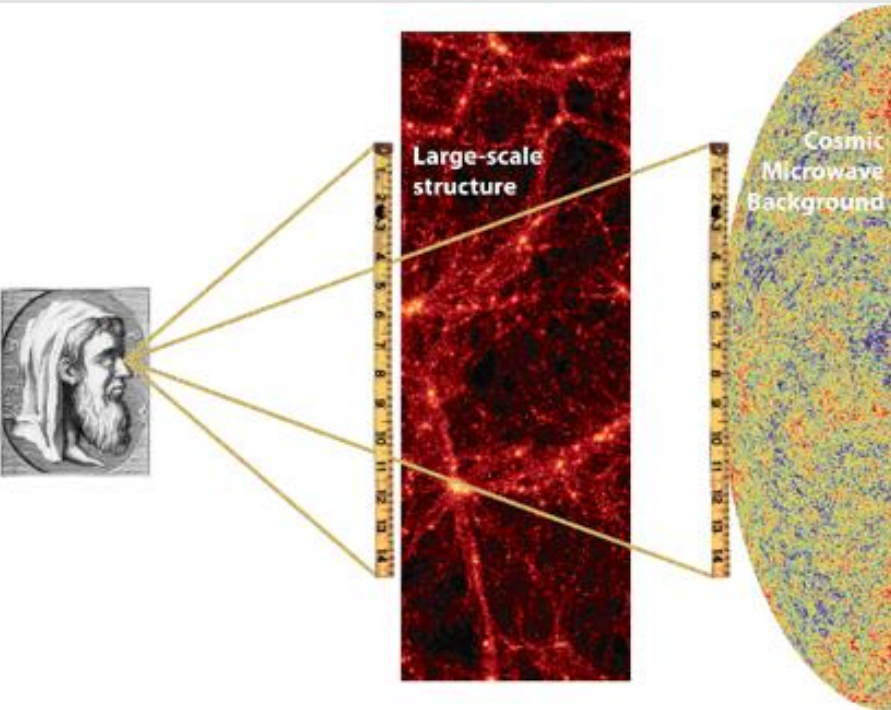
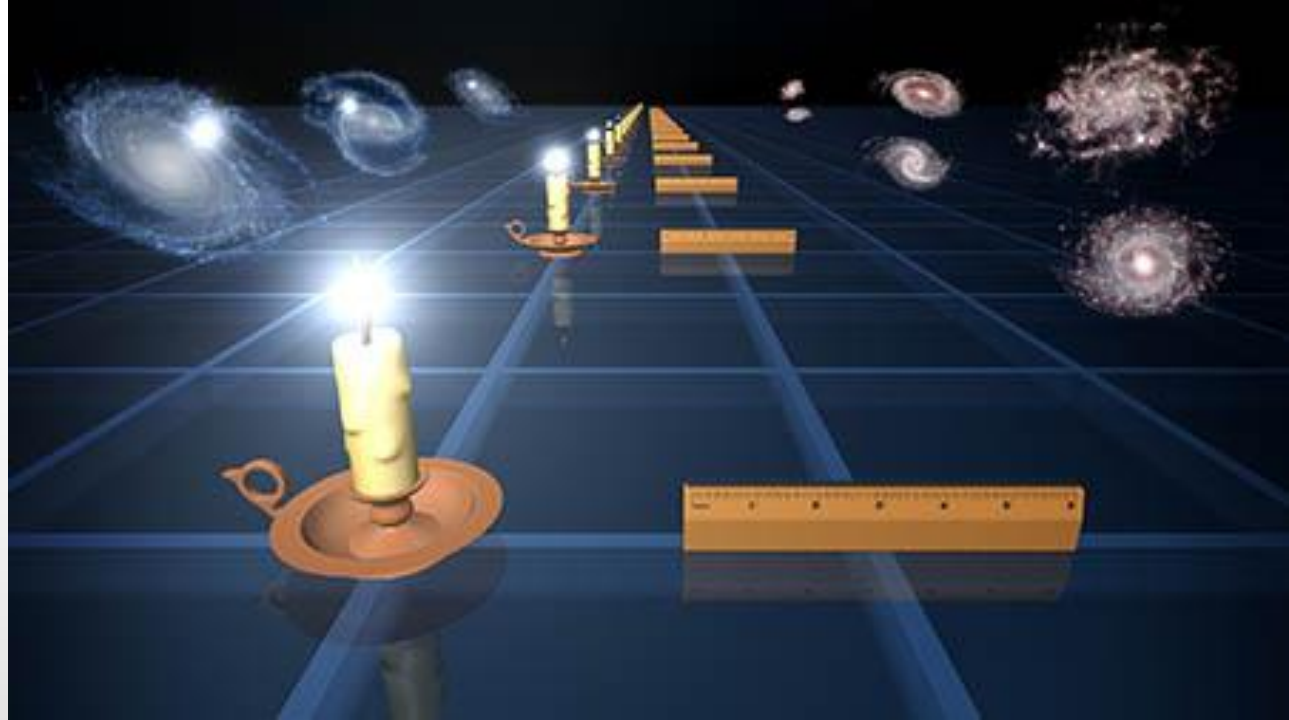
spectro



Standard rulers

Angular
diameter
distance:

$$d_A = R/\theta$$



Calibrate the BAO ruler
using the CMB, a very
well-known physics

Cosmological distances

The comoving distance to a light source at redshift z is:

$$r(z) = \frac{c}{H_0} \int_0^z \frac{dz'}{\sqrt{\Omega_\Lambda + \Omega_k(1+z')^2 + \Omega_M(1+z')^3 + \Omega_r(1+z')^4}}$$

And the Hubble parameter as a function of redshift is:

$$H(z)^2 = H_0^2 [\Omega_\Lambda + \Omega_k(1+z)^2 + \Omega_M(1+z)^3 + \Omega_r(1+z)^4]$$

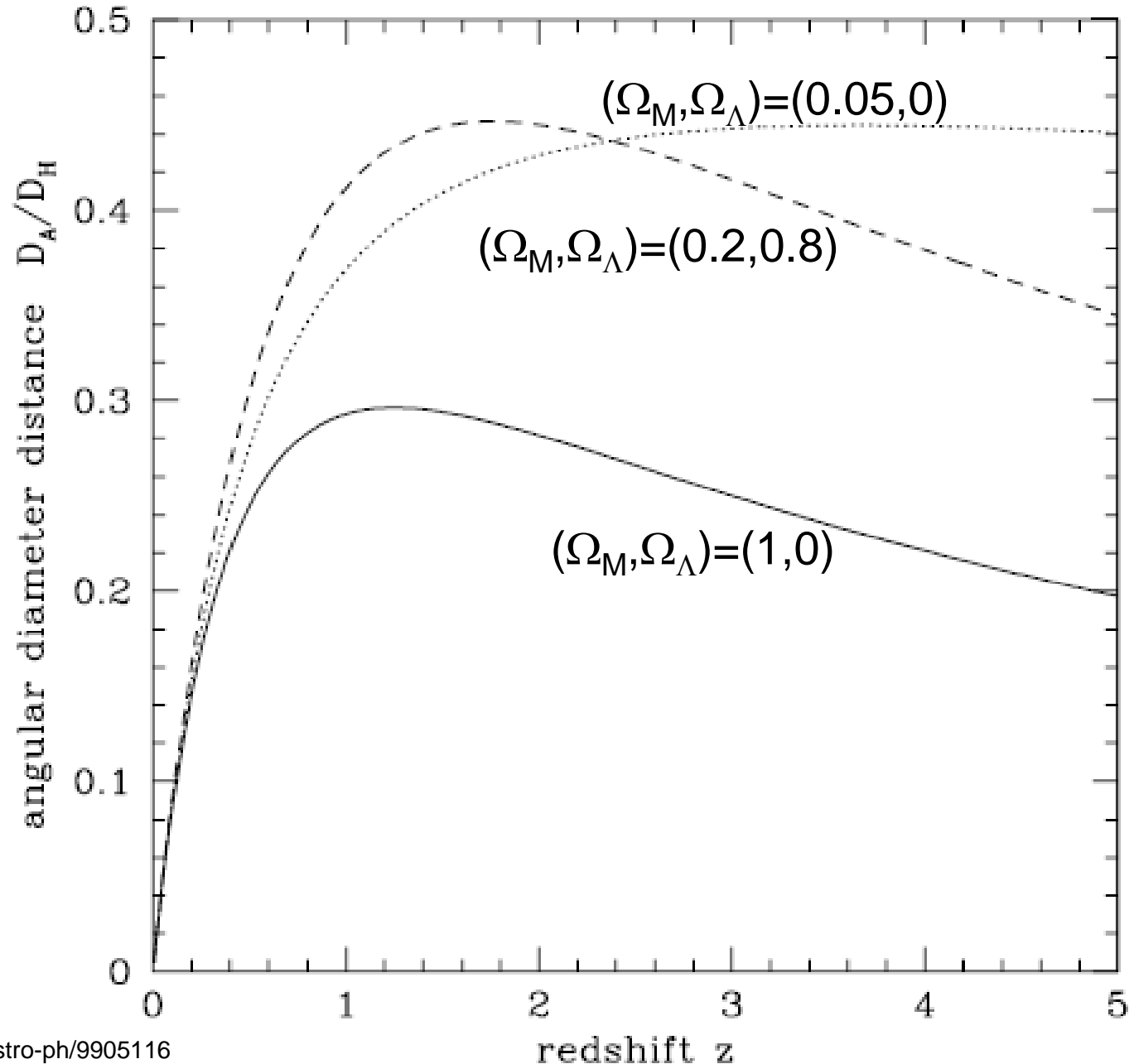
For a Euclidean Universe, the angular diameter distance is : $d_A = r(z)/(1+z)$

Therefore, from a set of standard ruler measurements at different redshifts, we will have many values of $r(z)$, and we can fit the cosmological parameters

The diagram illustrates the relationship between the angular diameter distance d_A , the standard ruler size s_\perp , and the Hubble parameter $H(z)$. The equation $\Delta\theta = \frac{s_\perp}{d_A}$ is shown on the left. A blue arrow points from the text "Standard ruler size" to s_\perp . Another blue arrow points from the same text to the denominator d_A . On the right, the equation $H(z) = \frac{c\Delta z}{s_\parallel}$ is shown, with a blue arrow pointing from the text "Standard ruler size" to s_\parallel .

$$\Delta\theta = \frac{s_\perp}{d_A} \quad \text{Standard ruler size} \quad H(z) = \frac{c\Delta z}{s_\parallel}$$

Angular diameter distance for several models

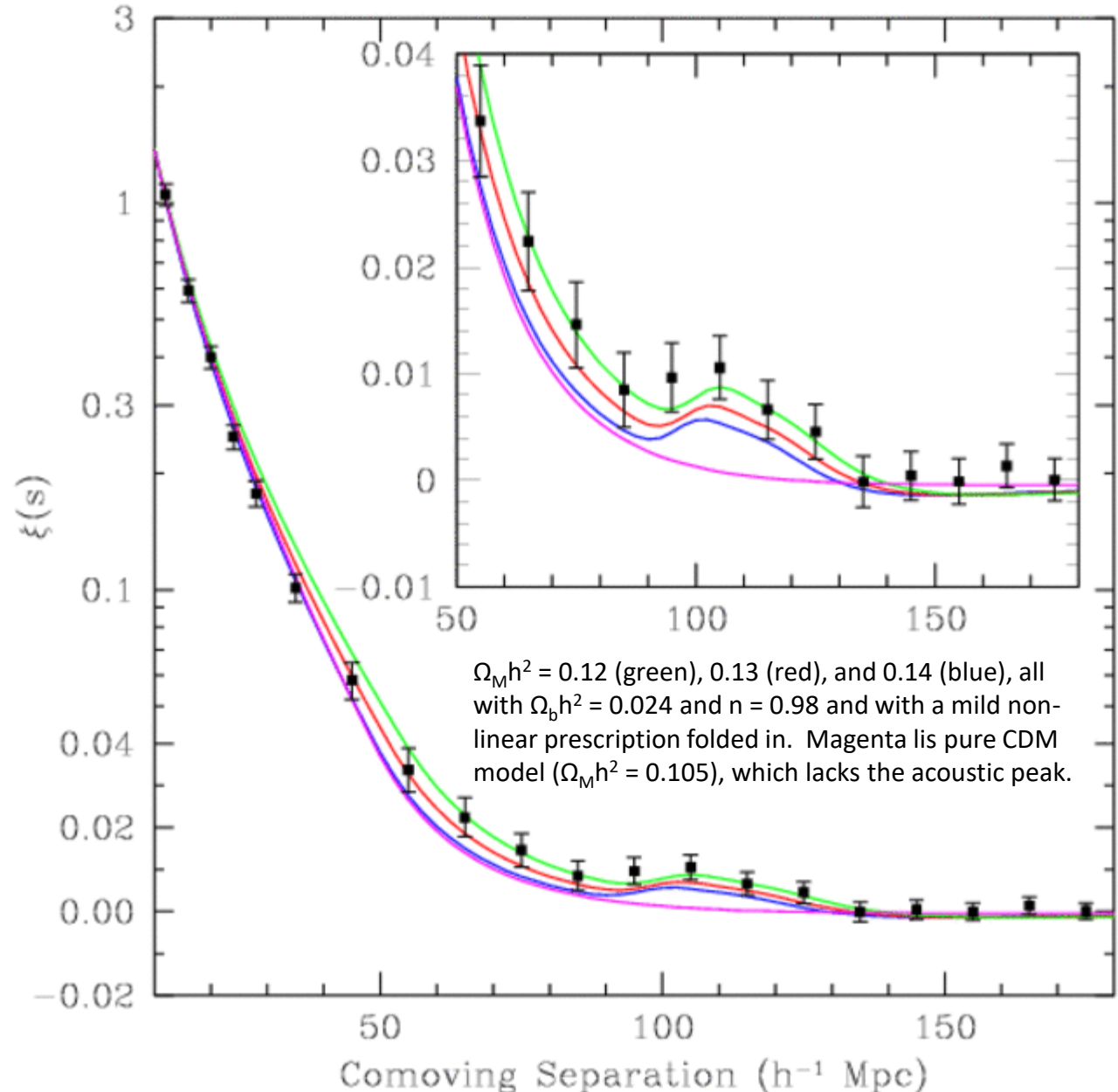


For the BAO case, the measurements are the position of the BAO peak in the correlation function for different redshifts

How to measure angular BAO

First detection in
2005, in SDSS
(Eisenstein et al)
Since then, many
observations and a
much better
understanding of
the measurement
Today we have a
Hubble diagram
using BAO

Measure angular
BAO in reshift
shells



The concrete expressions in the BAO case are

$$r_s(z_{dec}) = \frac{c}{\sqrt{3}} \int_0^{1/(1+z_{dec})} \frac{da}{a^2 H(a) \sqrt{1 + (3\Omega_b/4\Omega_\gamma)a}} \text{ Mpc h}^{-1}$$

$$z_{dec} = 1291 \frac{(\Omega_m h^2)^{0.251}}{1 + 0.659(\Omega_m)^{0.828}} \left[1 + b_1 (\Omega_b h^2)^{b_2} \right]$$

$$b_1 = 0.313 (\Omega_m h^2)^{-0.419} \left[1 + 0.607 (\Omega_m h^2)^{0.674} \right]$$

$$b_2 = 0.238 (\Omega_m h^2)^{0.223}$$

**The
observable
quantities
are angles
and
redshifts**

$$\theta_{BAO} = \frac{r_S(\Omega_M, w_0, w_a \dots)}{(1+z) d_A(z, \Omega_M, w_0, w_a \dots)}$$

$$\Delta z_{BAO} = H(z) r_s$$

Many of the BAO measurements give the geometric average of distances (angular and radial), a quantity called d_V :

$$d_V(z) \equiv ((1+z)^2 d_A^2(z) z / H(z))^{1/3}$$

Fit the coefficient α that makes the BAO peak for the fiducial model to fit the data:

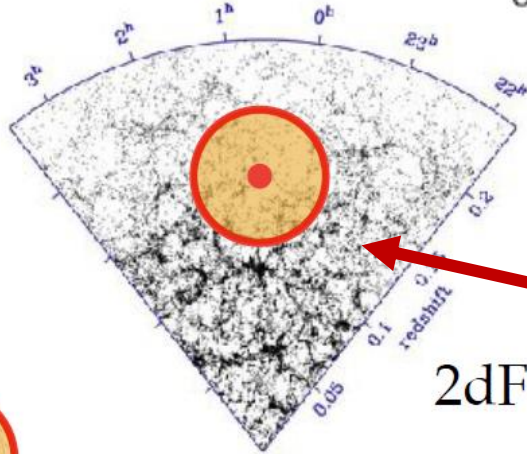
$$\frac{d_V(z)}{r_s} = \alpha \frac{d_V^{\text{fid}}(z)}{r_s^{\text{fid}}}$$

BAO measurements require large volumes!

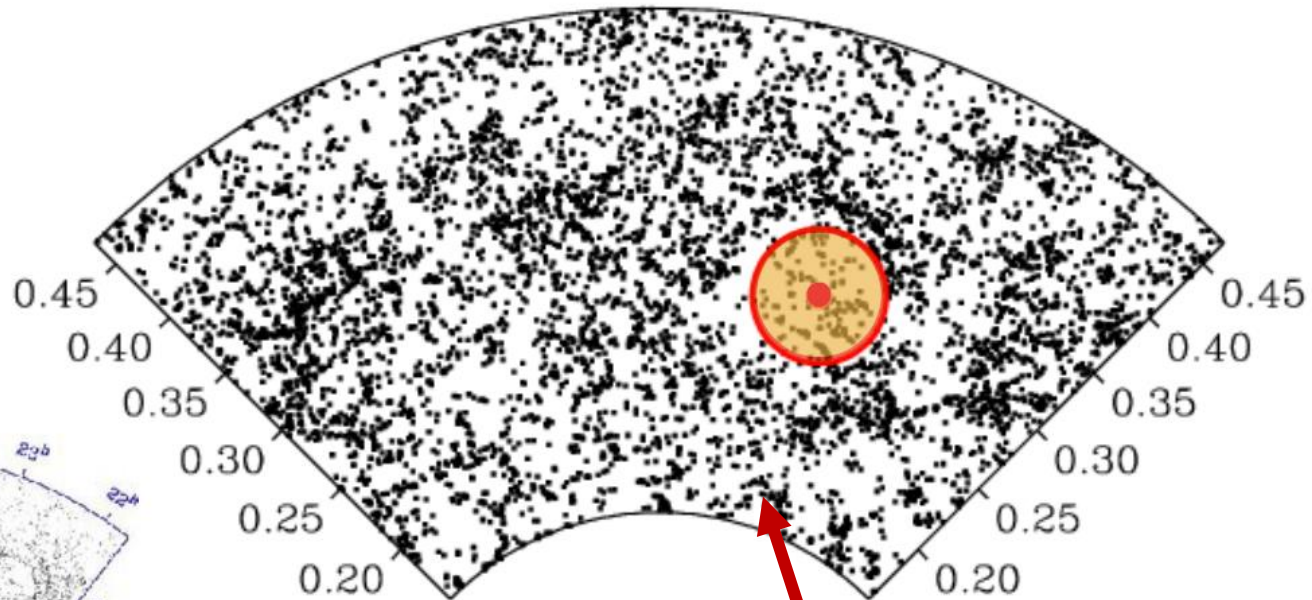
Early surveys
where not large
enough to see
the BAO scale



CfA survey (1989)



2dFGRS (2003)



SDSS - LRGs (2009)

Only from XXI century the
technology made posible the
measurement of the BAO
scale

BAO measurements require large volumes!

Current surveys start to have enough power to produce precision measurements of the BAO scale

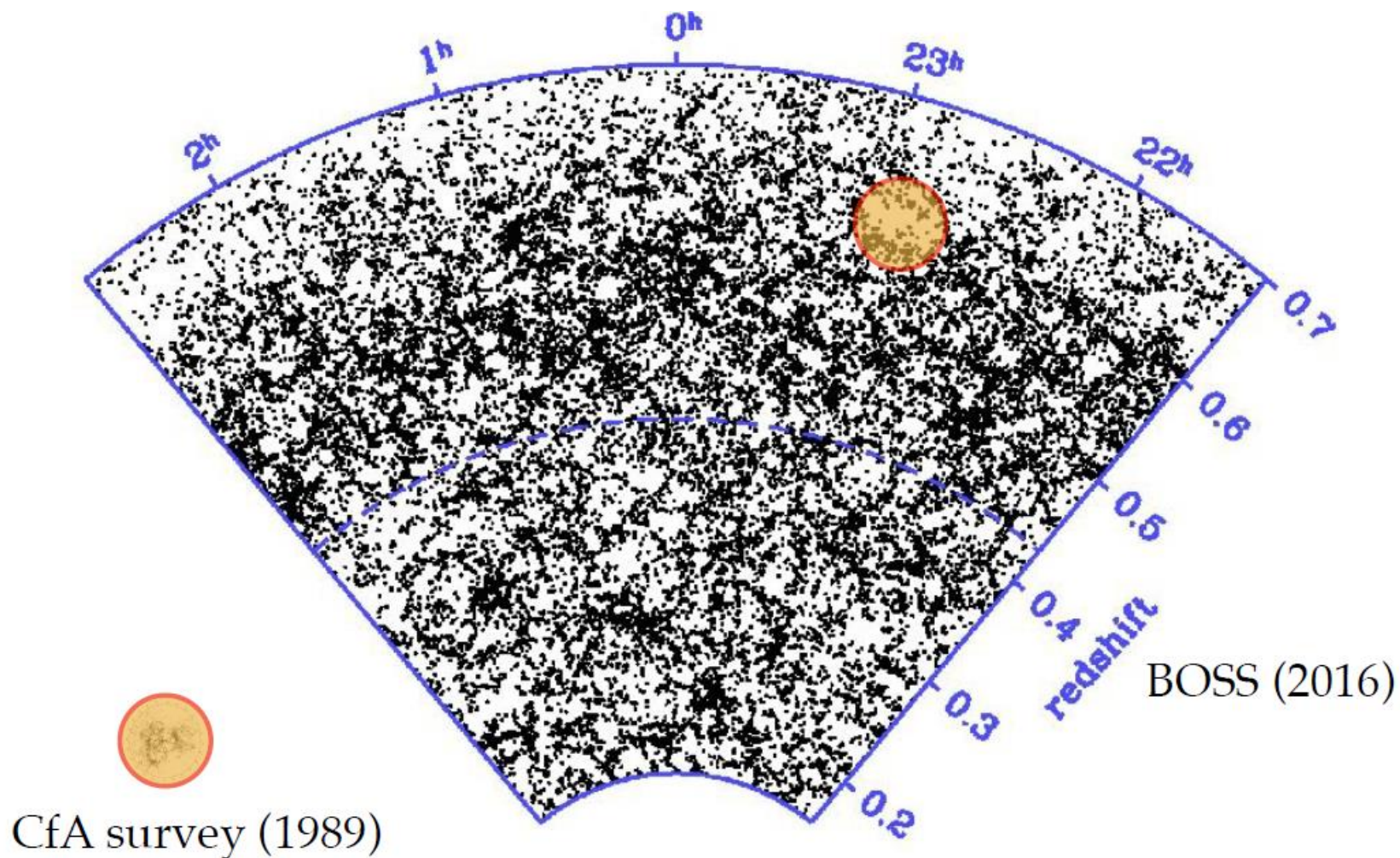
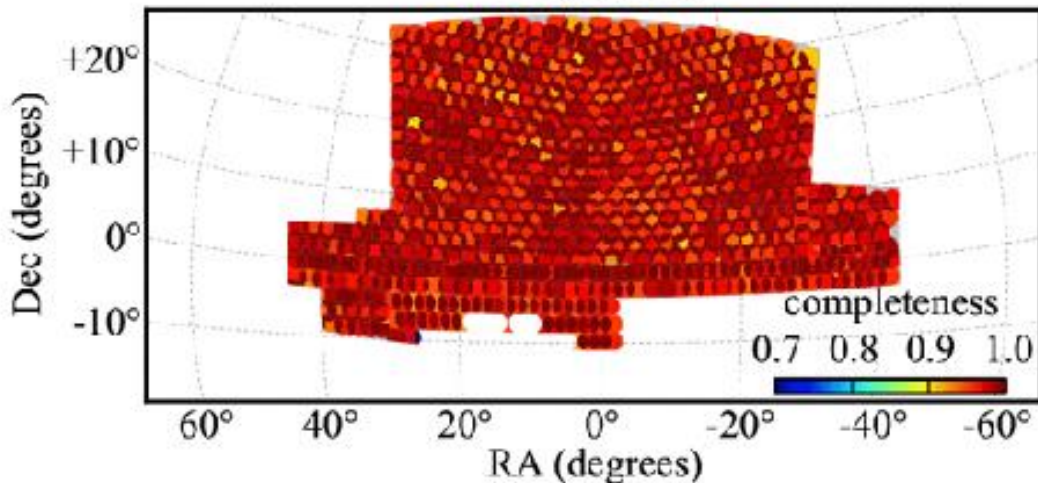
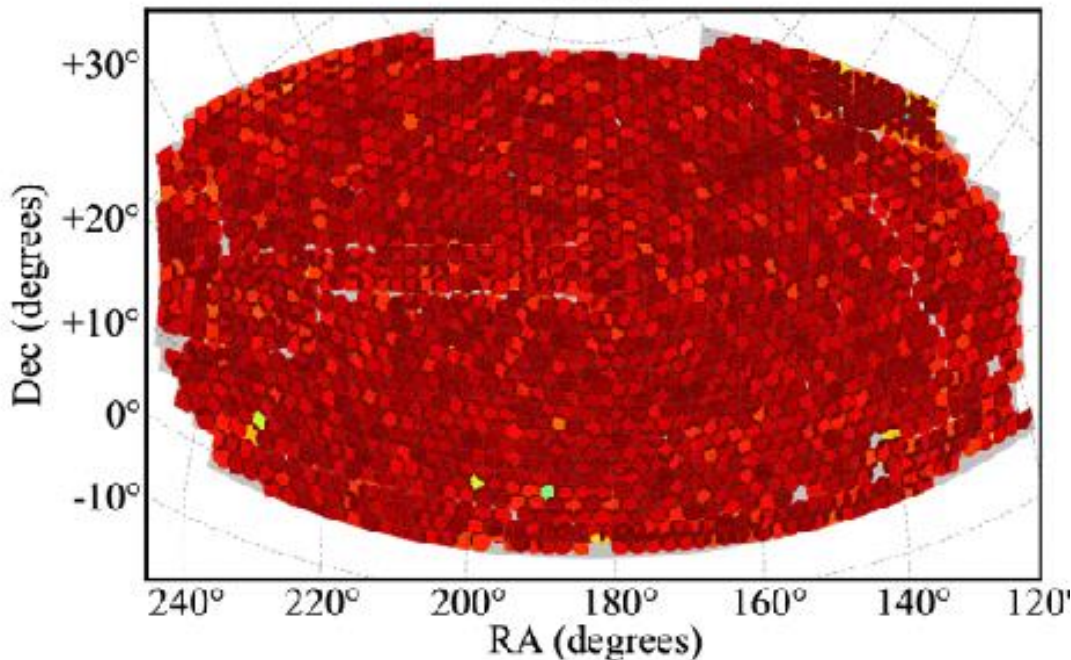


Figure taken from Ariel Sánchez

Redshift survey: BOSS

DR12



BOSS in a nutshell

- Designed to tackle CA through BAO measurements
- Total area of 10,200 deg².
- Positions for 1.2×10^6 LGs
 - LOWZ, with $0.1 < z < 0.43$
 - CMASS, with $0.43 < z < 0.7$
- A sample of 1.6×10^5 QSO, $2.3 < z < 2.8$

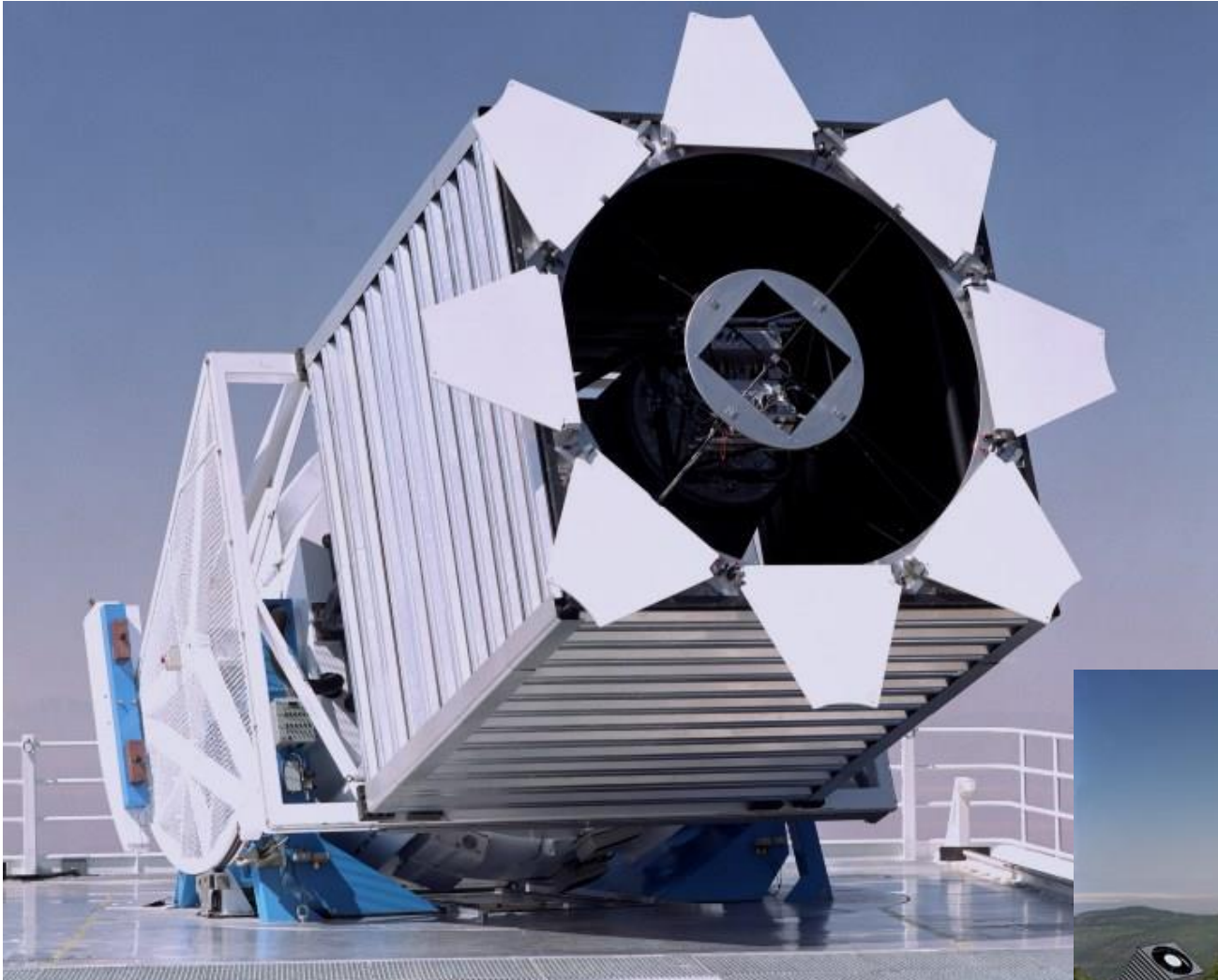
Redshift survey: BOSS (SDSS-III)

Apache Point Observatory
(New Mexico, USA)

Dedicated 2.5m Telescope

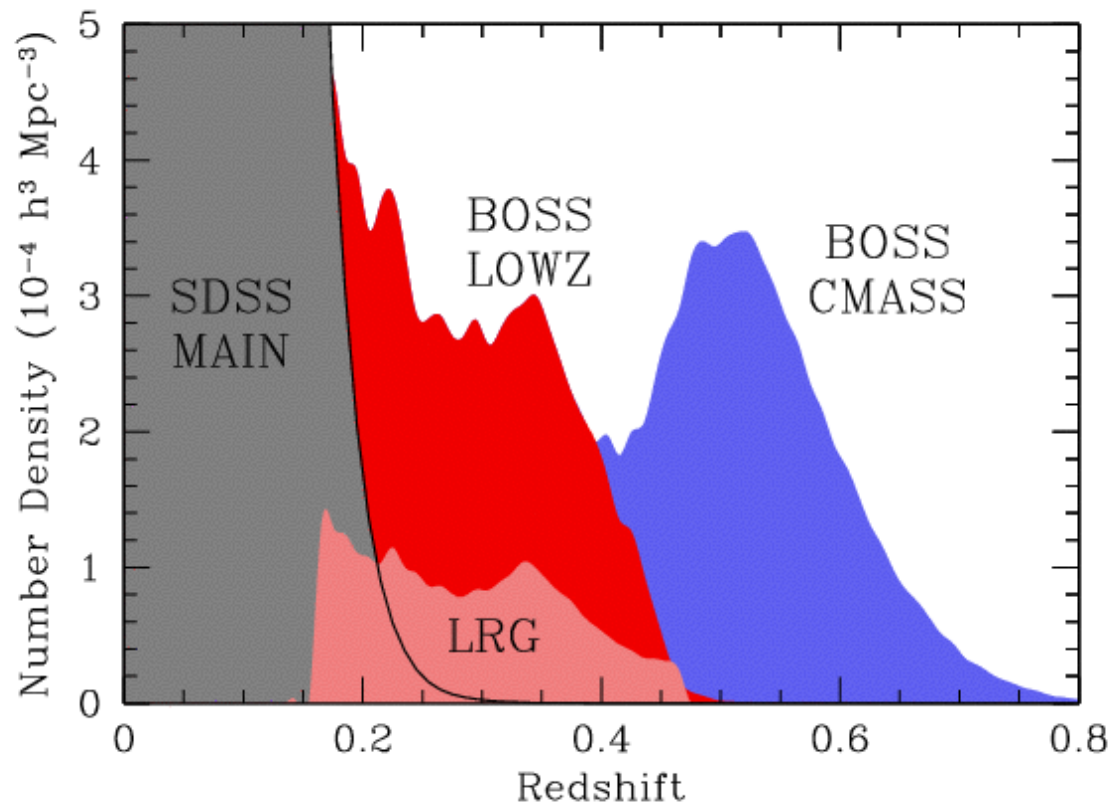
1000 spectra
simultaneously

BOSS took data from 2008
to 2014



There is currently a SDSS-IV phase, with the survey
eBOSS (extended BOSS)



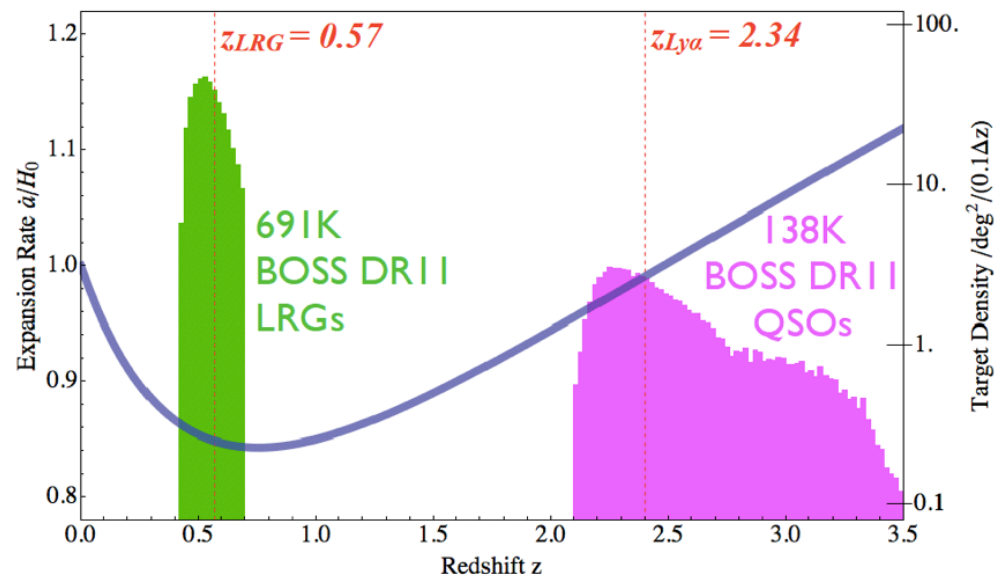


Several Galaxy samples, selected to map different redshift ranges

Luminous Red Galaxies ($z < 0.4$) → Brightest and reddest galaxies

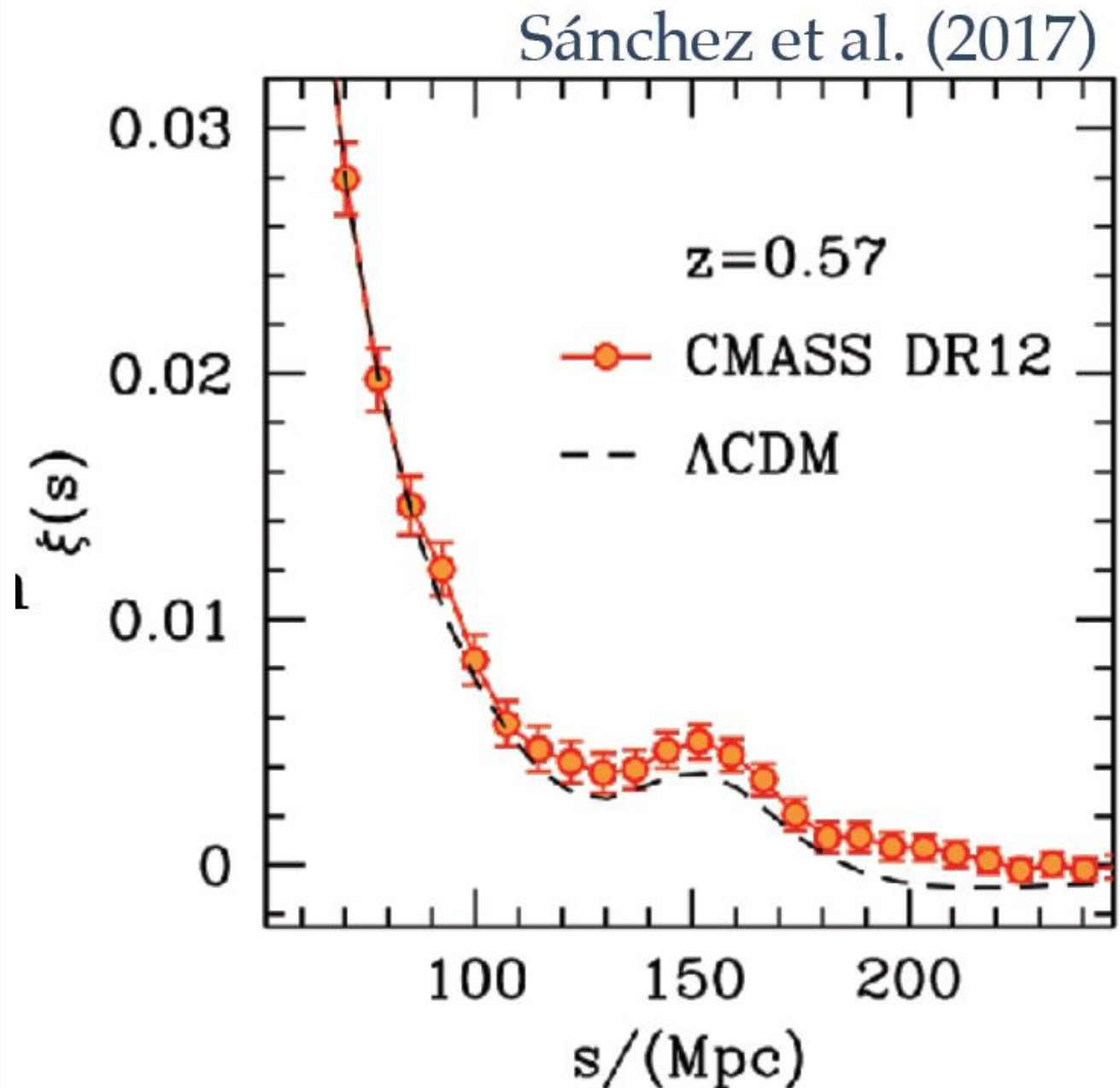
CMASS Galaxies ($0.4 < z < 0.7$) → More luminous and massive galaxies

In addition, a quasar sample that covers the redshift range $2.15 < z < 3.5$, to use the Ly- α forest as a cosmological probe



For each of these samples, compute the correlation function.

Identify and fit the BAO peak position



Other Effects: Non-linearities

The non-linear power spectrum can be written as

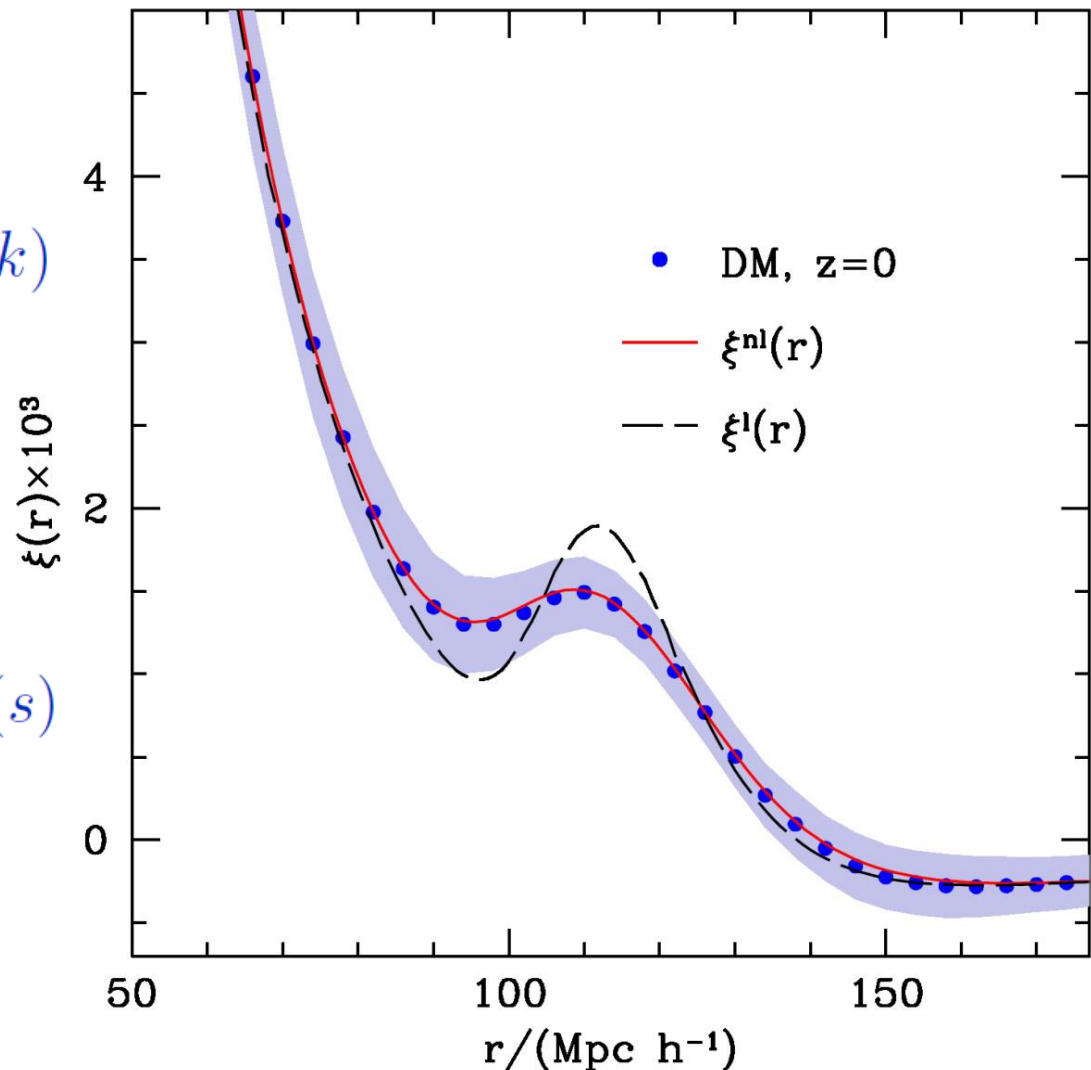
$$P(k) = P_L(k)G(k)^2 + P_{MC}(k)$$

The mode-coupling terms affect different scales

For the correlation function

$$\xi(s) = \xi_L(s) \otimes G(s)^2 + \xi_{MC}(s)$$

Non-linear evolution damps the BAO signal



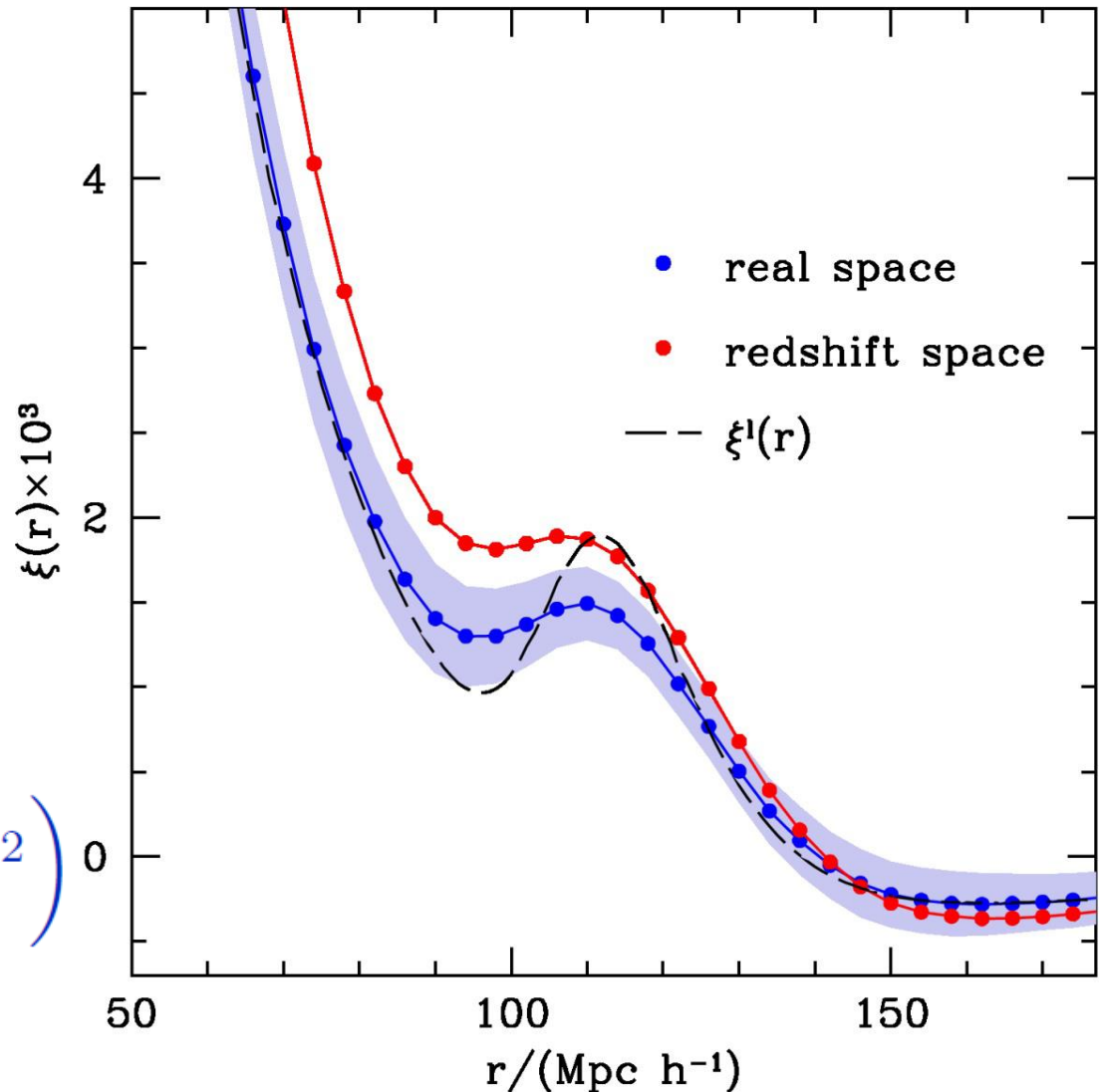
Other Effects: Anisotropic clustering

RSD main effect is to boost the clustering amplitude

RSD lead to an extra damping of the BAO peak, degrading the BAO signal

$$S \equiv \frac{\xi_s(r)}{\xi(r)} = \left(1 + \frac{2}{3}f + \frac{1}{5}f^2\right)$$

$$f = d \ln D / d \ln a$$



Other Effects: Galaxy bias

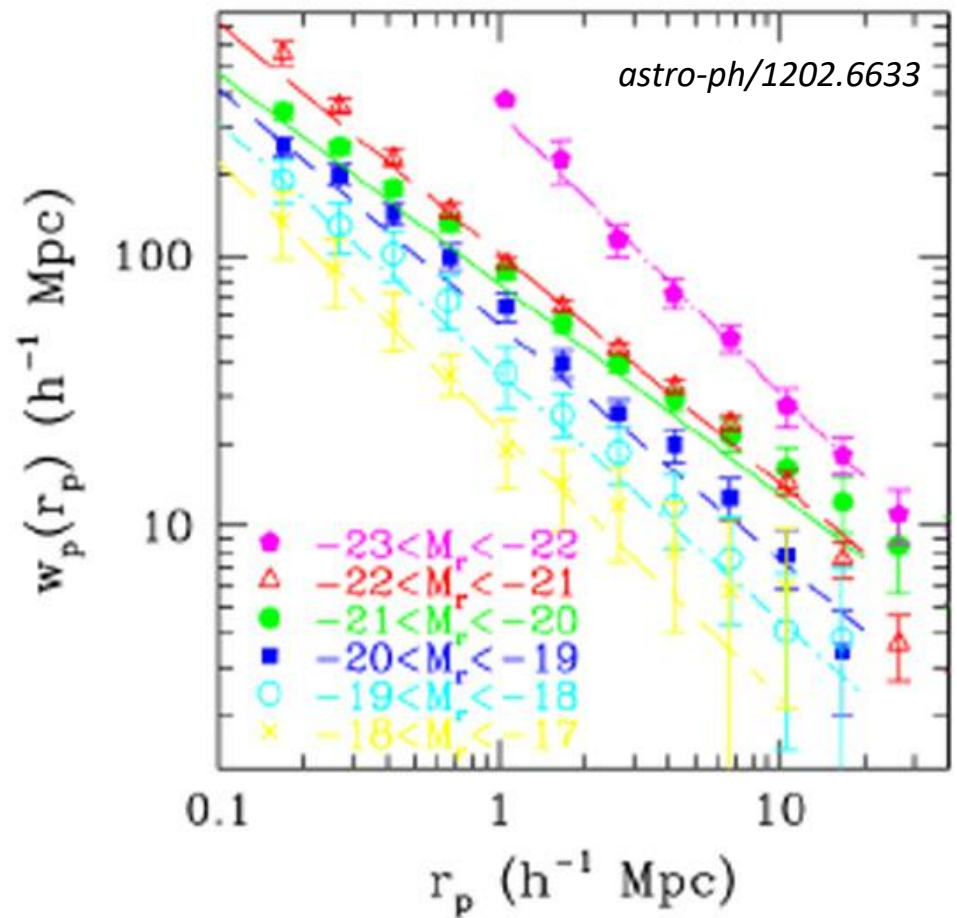
Our observations probe the
Galaxy density field

On large scales, a linear relation
is expected:

$$\delta_g(\mathbf{r}) = b\delta(\mathbf{r})$$

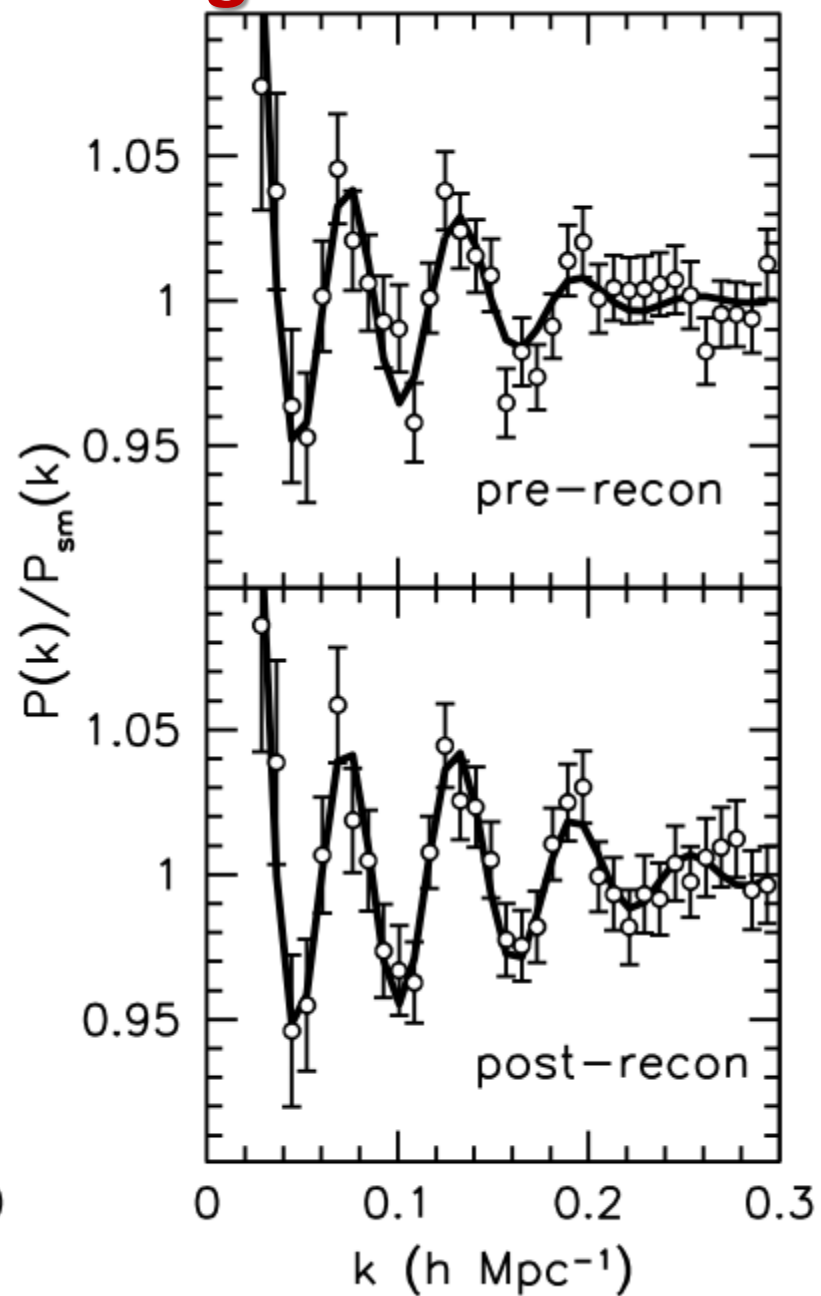
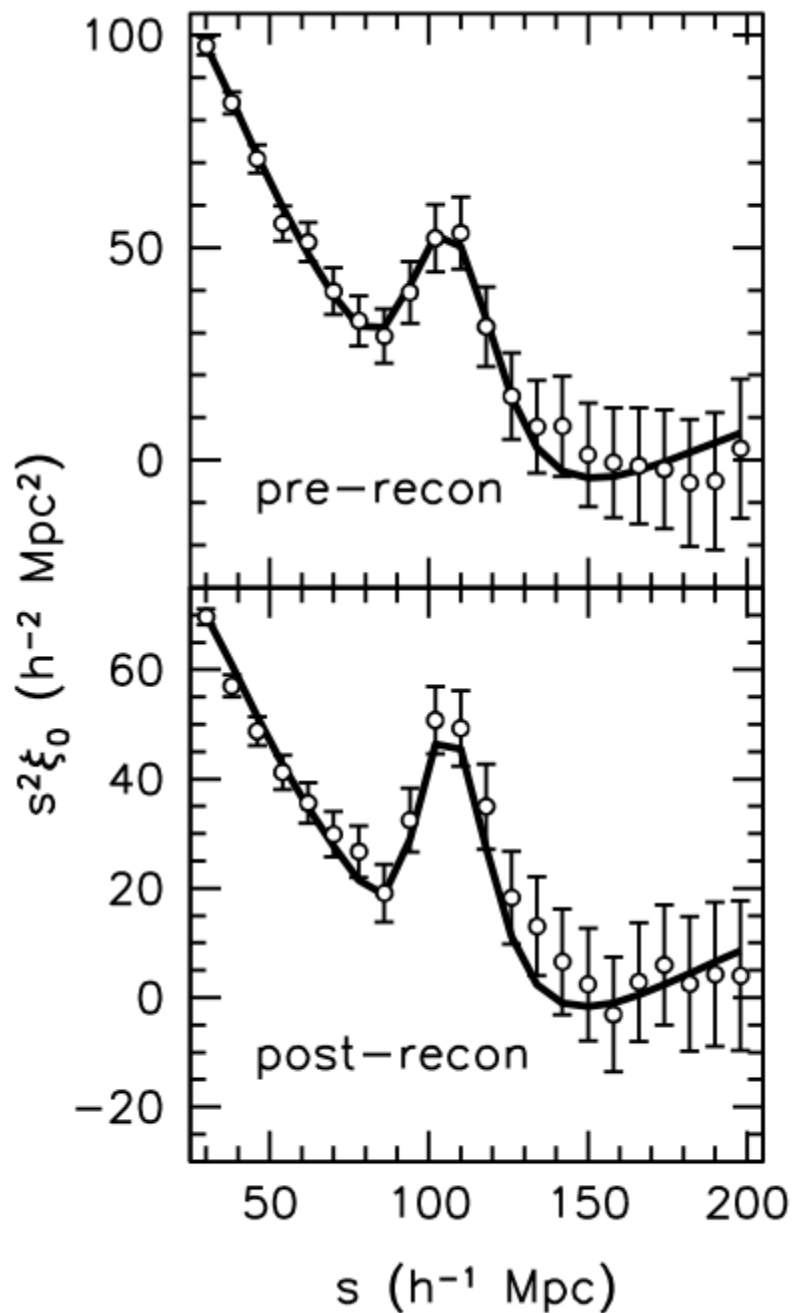
$$\xi_g(r) = b^2\xi(r)$$

The non-linear effects and the
RSD depend on the halo sample
→ And then, also on the selected
galaxy sample

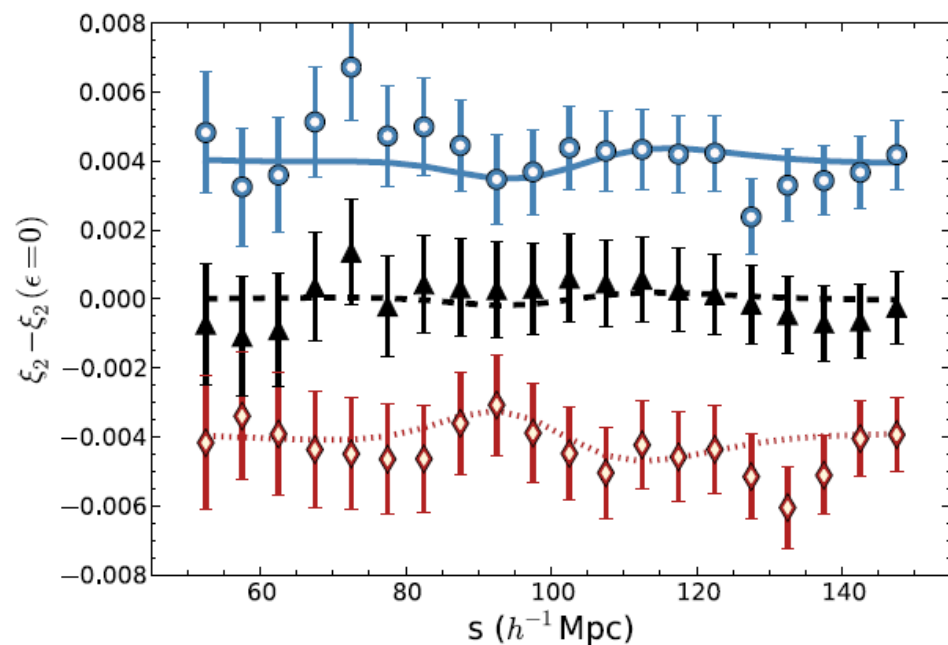
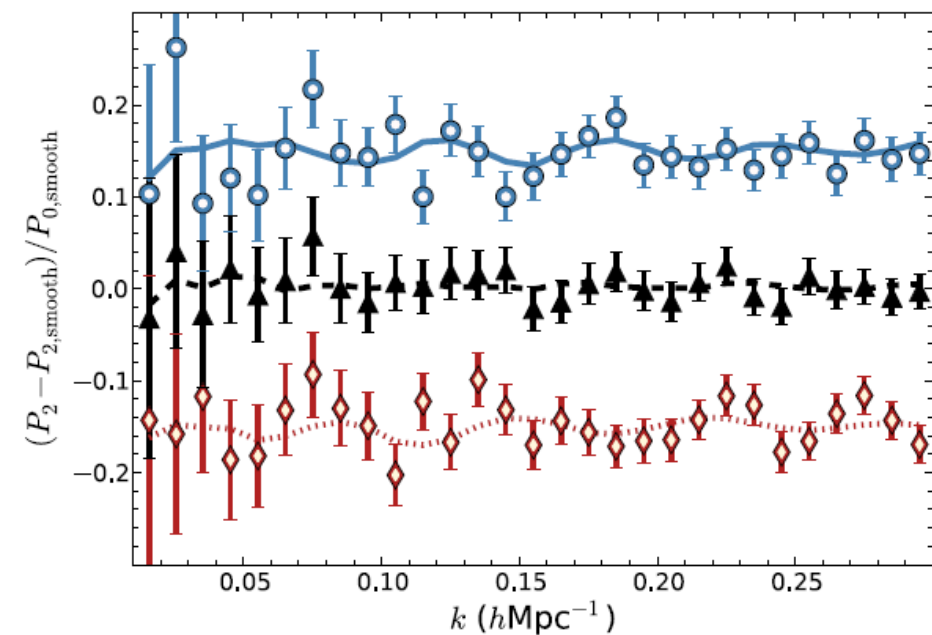
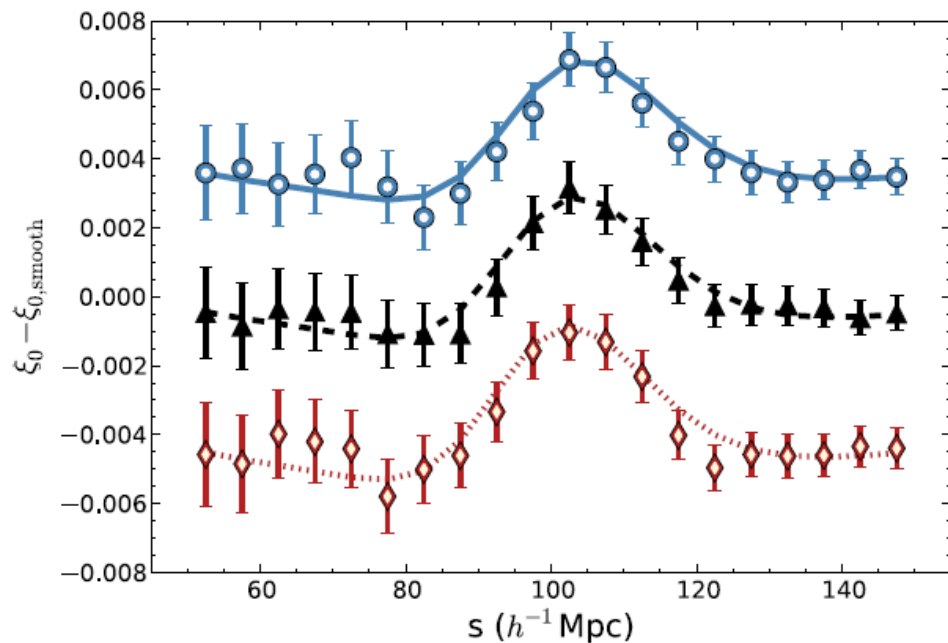
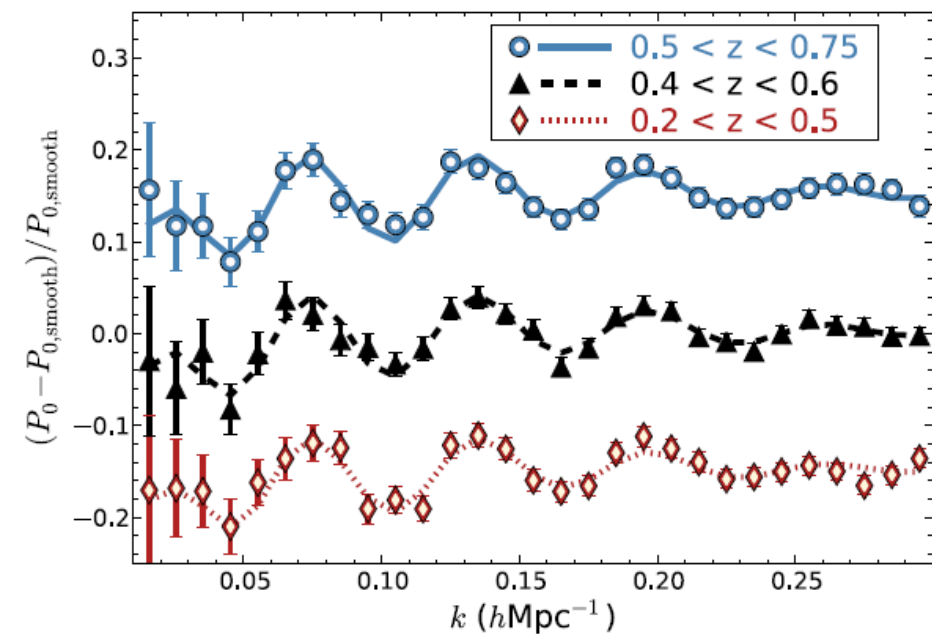


projected correlation function, $w_p(r_p)$, for
SDSS galaxies in different absolute magnitude
ranges, where brighter galaxies are seen to
be more clustered

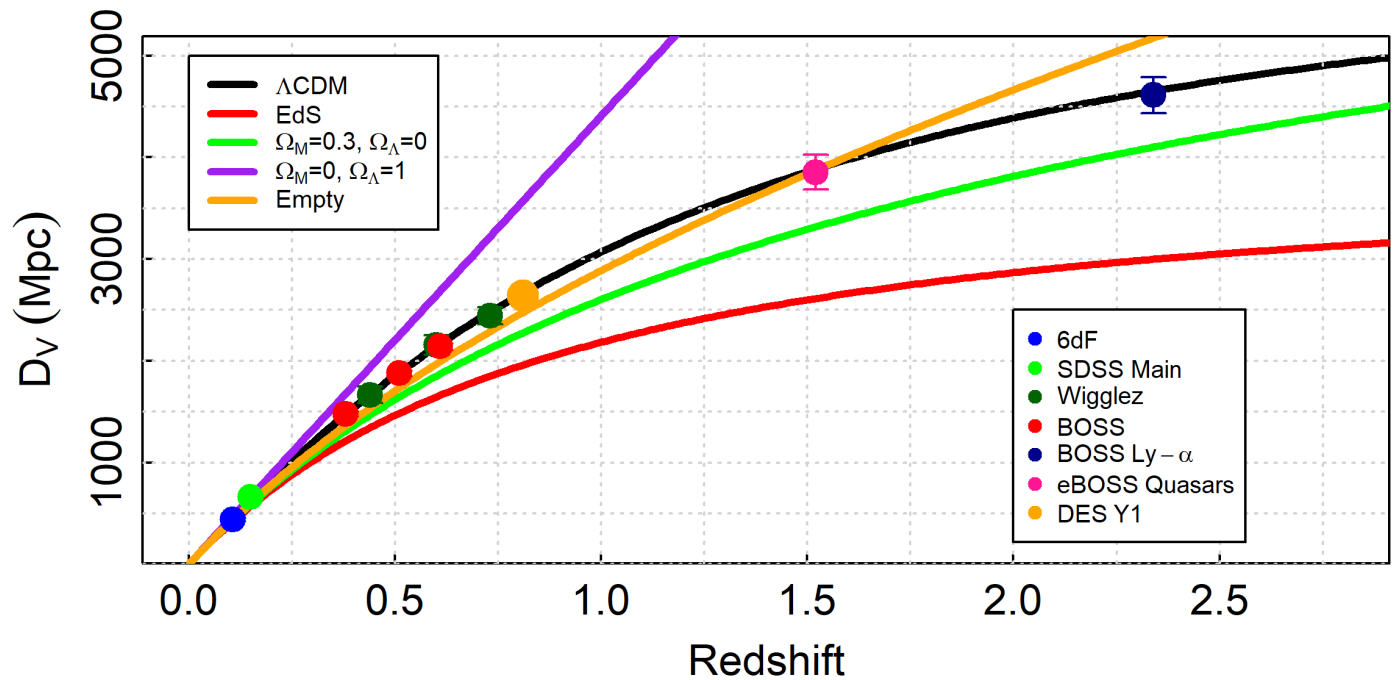
BOSS DR11 Clustering Results



BOSS Final Results

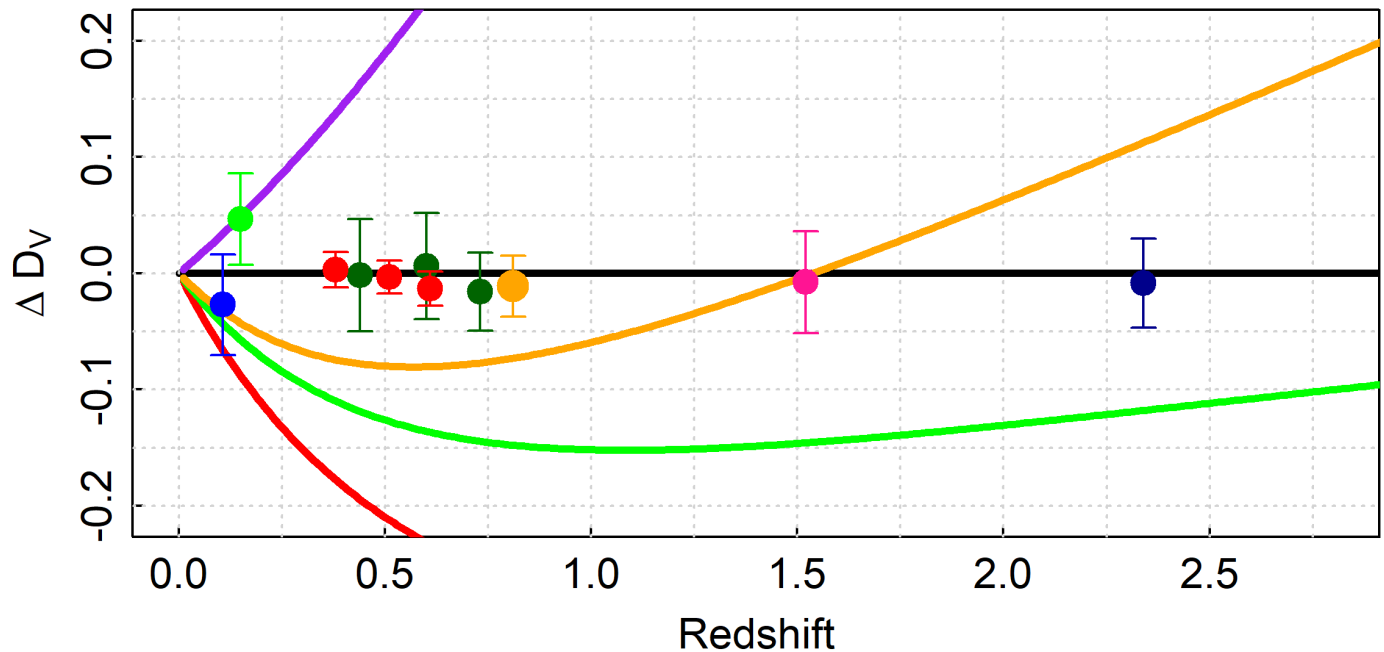


Current Hubble Diagram using BAO distances



Perfectly described by Λ CDM, but not by other cosmological parameters

Precisions of the percent order



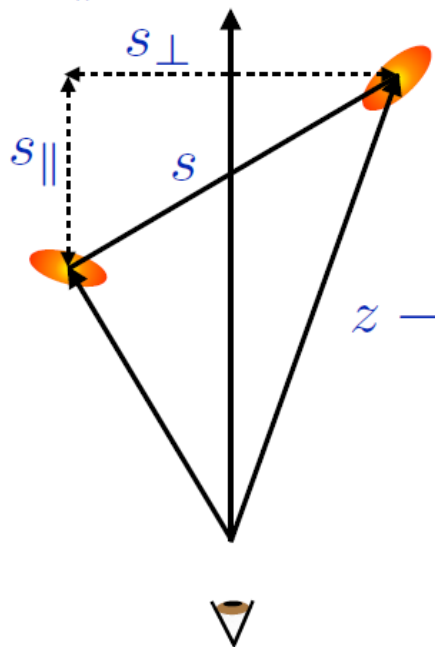
The full BAO power

Anisotropic clustering

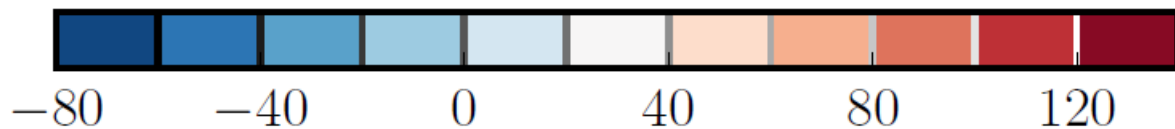
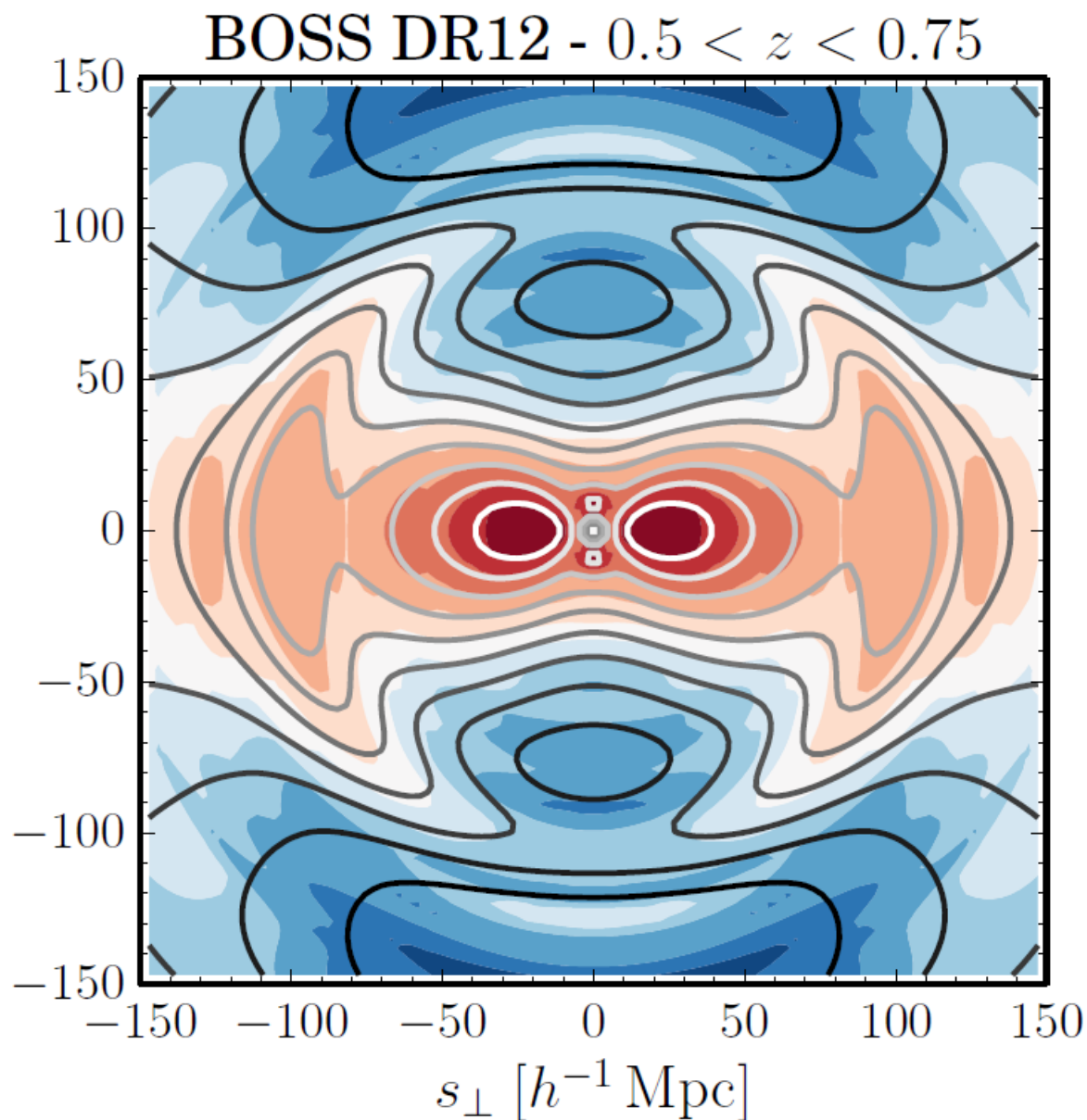
Measuring angular and radial BAO separately

Redshift space distortions

$$\xi(s_{\perp}, s_{\parallel})$$



$s_{\parallel} [h^{-1} \text{ Mpc}]$



The full BAO power

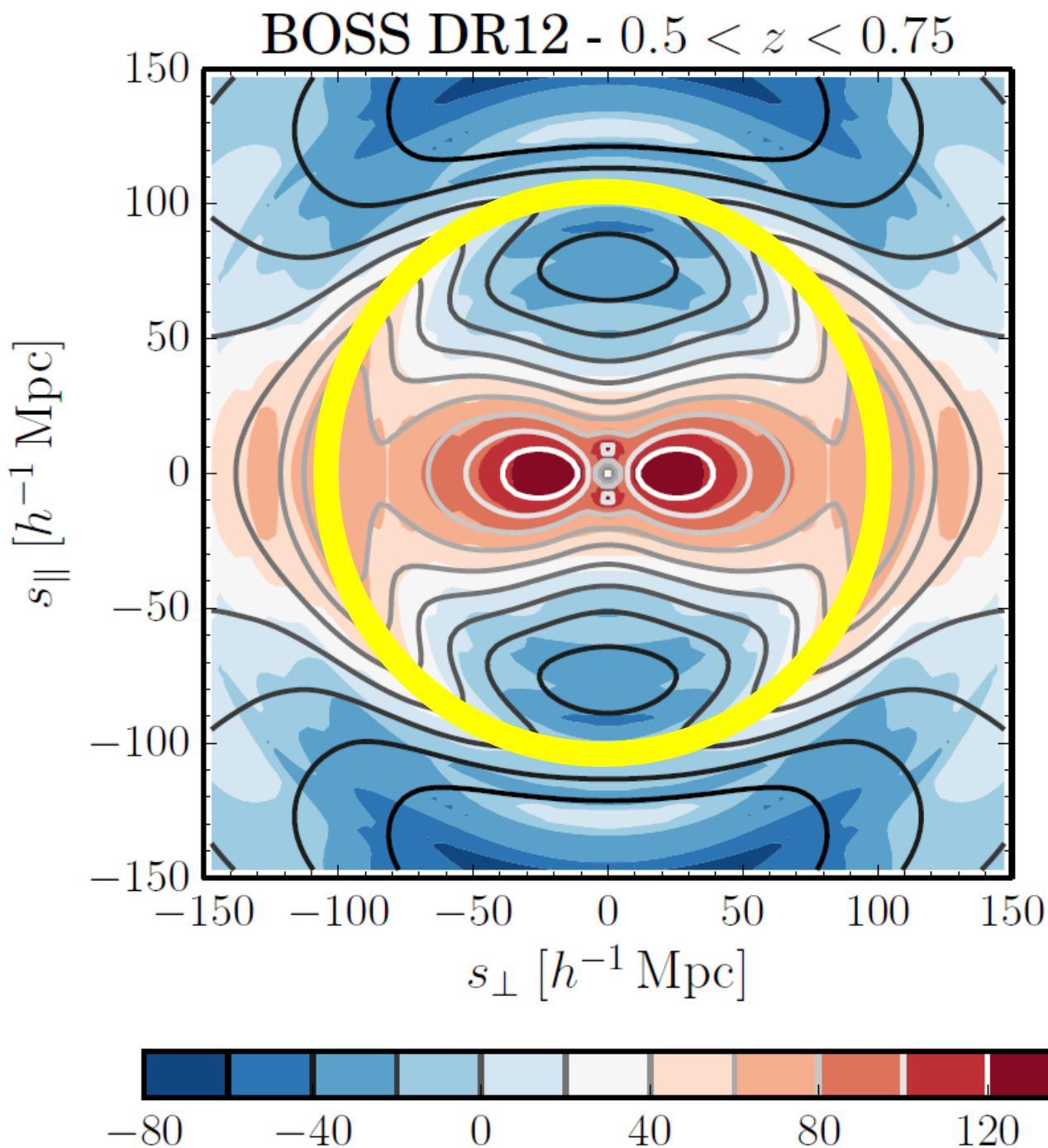
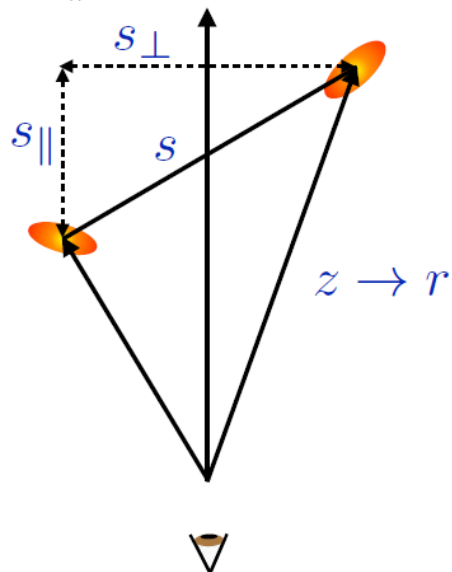
BOSS DR12 anisotropic correlation function

The BAO signal appears as a ring at $s=110$ Mpc/h

RSD distort the contours, which deviate from perfect circles

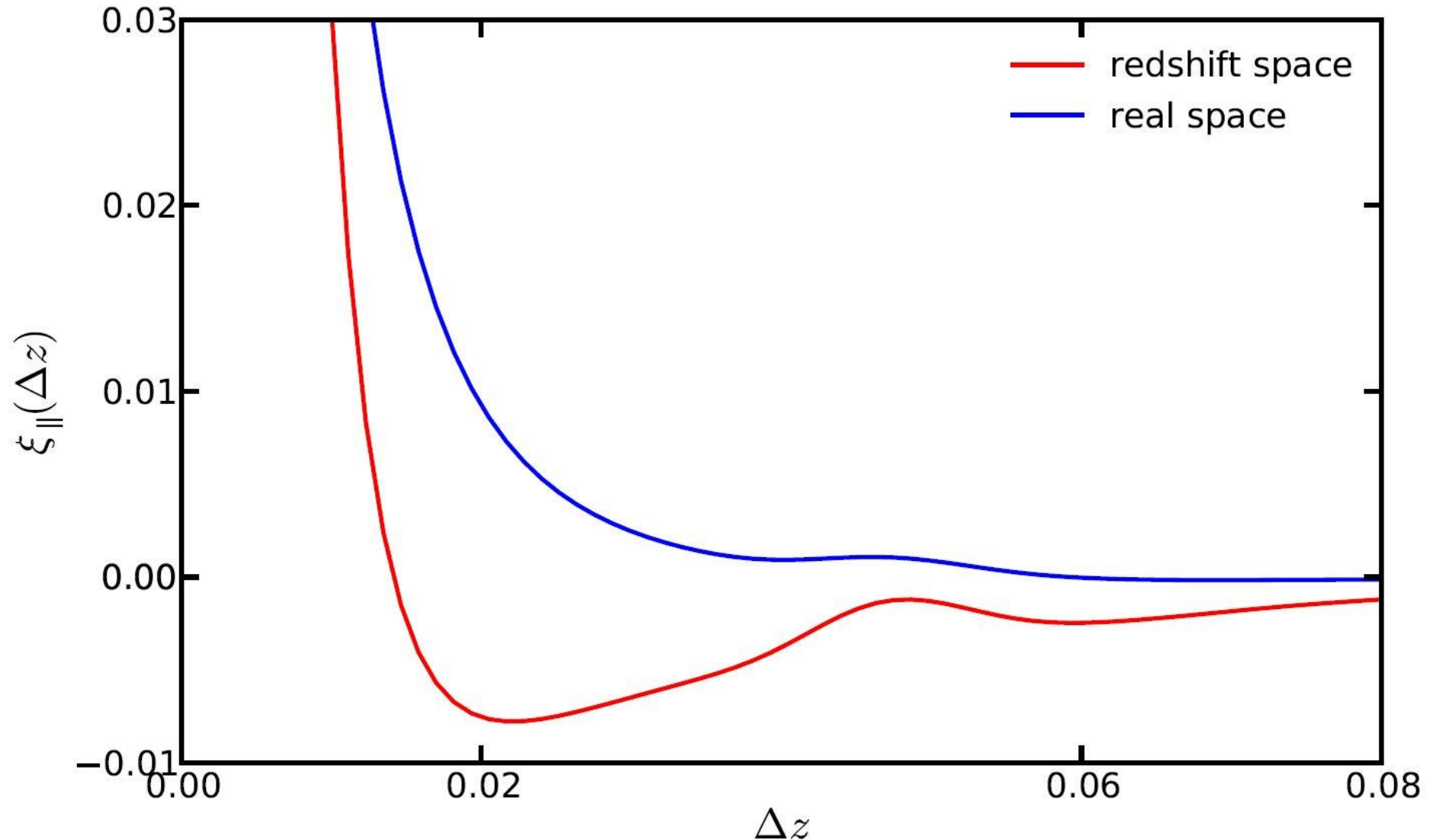
Usable for cosmology

$$\xi(s_{\perp}, s_{\parallel})$$



Redshift Space Distortions (RSD)

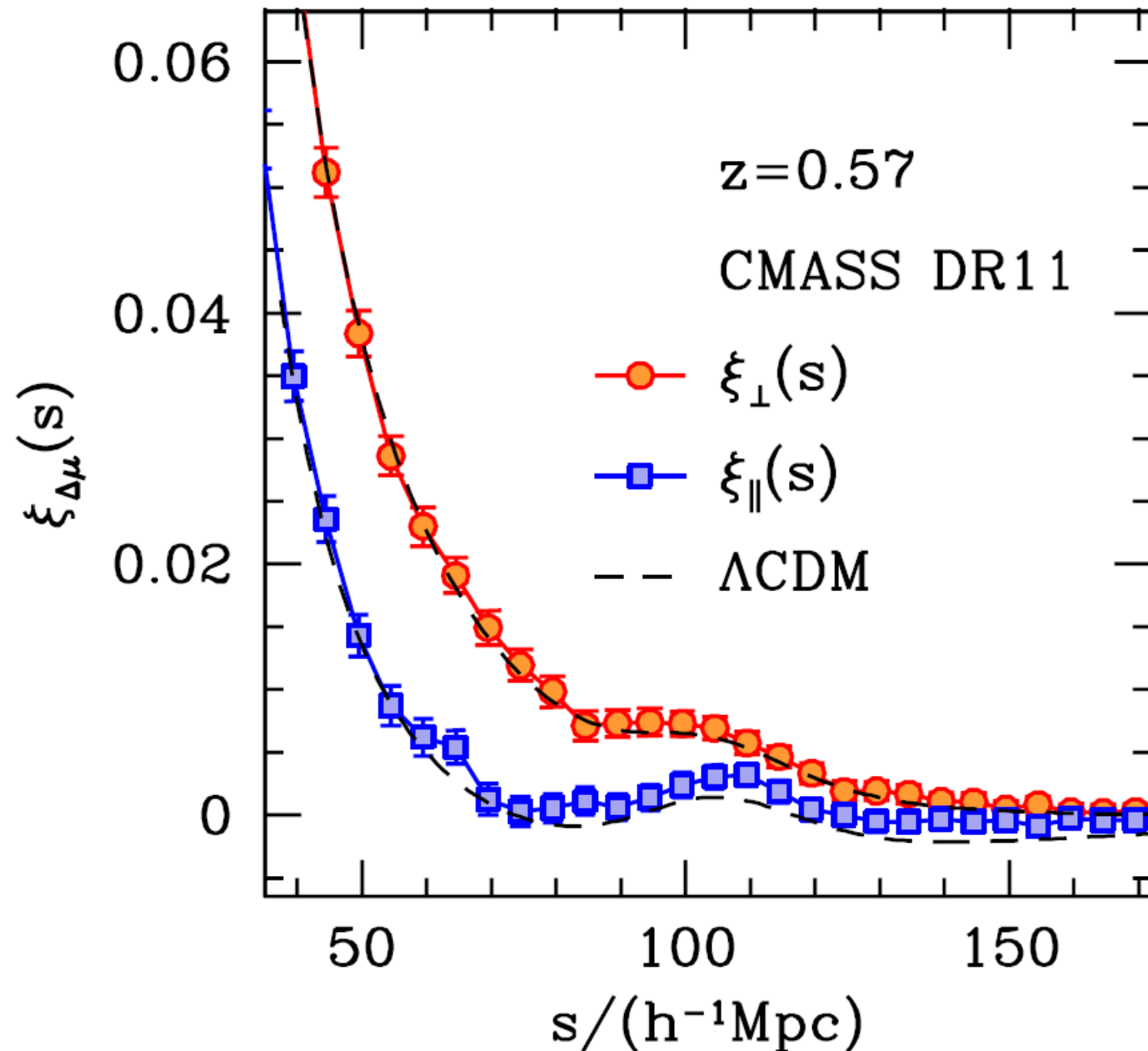
The shape of the correlation function changes dramatically when RSD are included
However the BAO peak position does not change
BAO is very robust against systematic errors

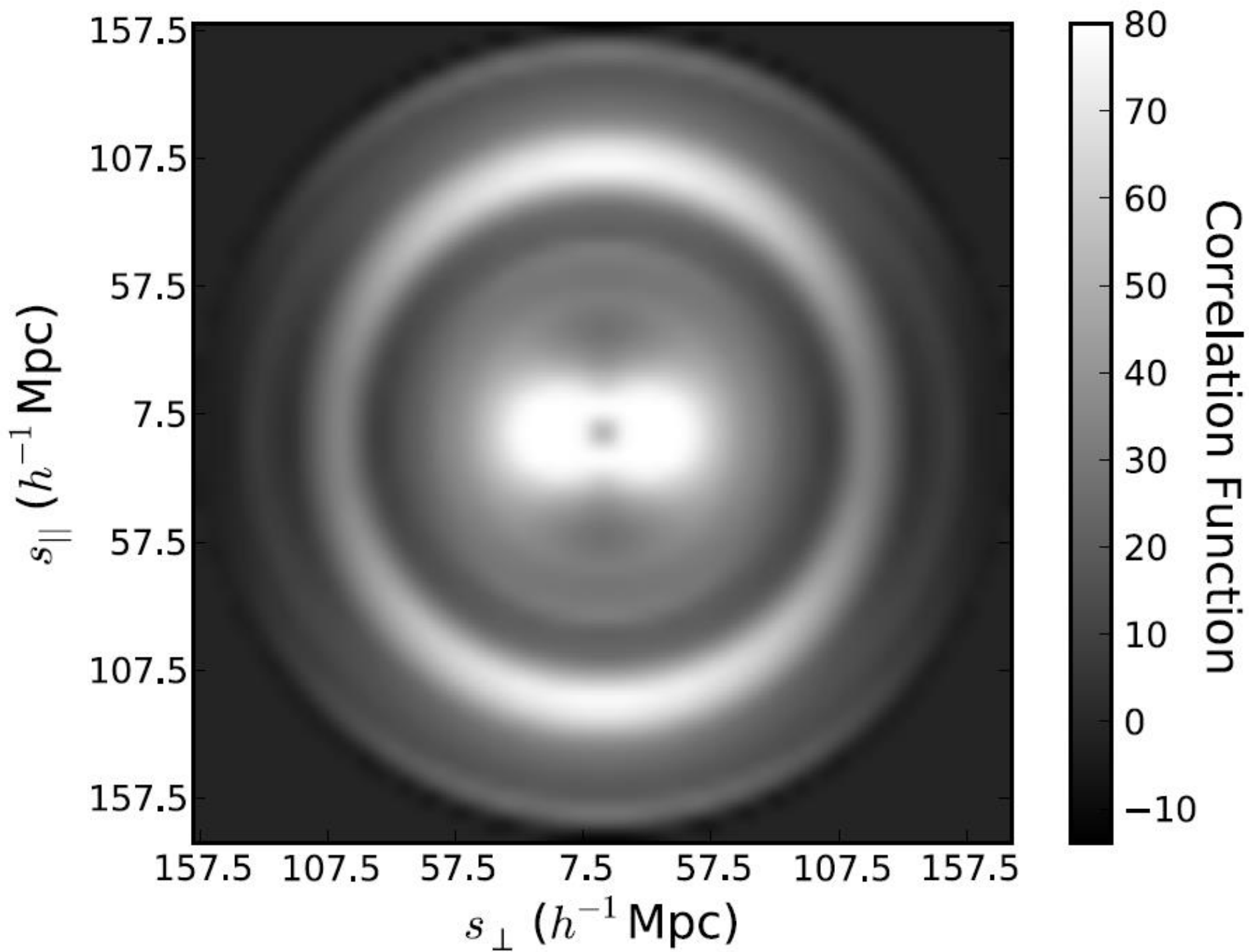


RSD have been measured in real data

Spectroscopic surveys are sensitive to RSD, since the radial distances are not measured directly, but using the Galaxy redshift

They are affected by the peculiar velocity of the galaxy

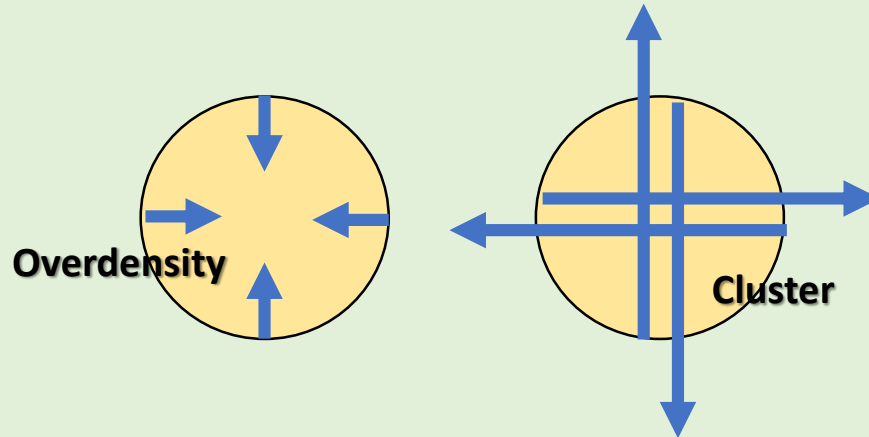




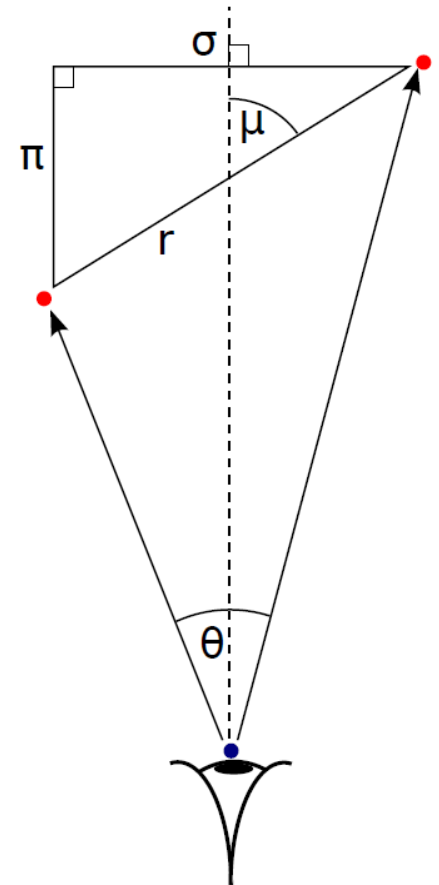
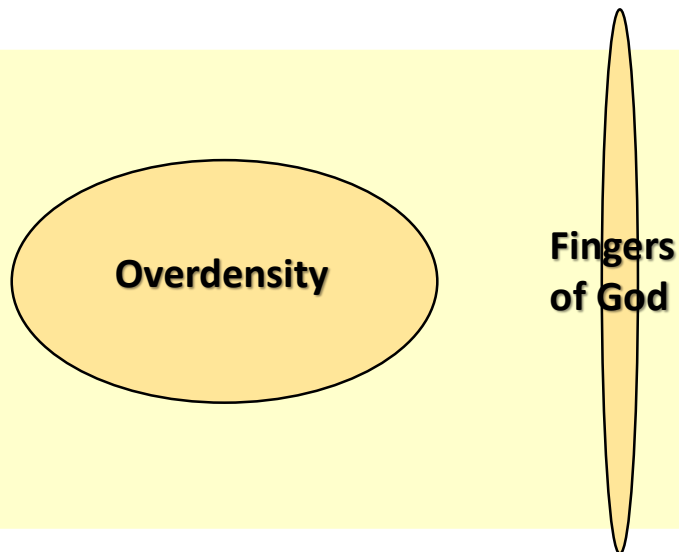
Why RSD?

They are a consequence of peculiar velocities coming from structure
They carry very valuable information about cosmology

**Real
Space**



**Redshift
Space**



RSD change the shape of the power spectrum and the correlation function

The velocity field is related to the density field

Separate the Fourier modes of the peculiar velocity field into longitudinal and transverse (irrotational and divergence-free in real space) components

$$v_{\mathbf{k},\parallel} \equiv \mathbf{v}_{\mathbf{k}} \cdot \frac{\mathbf{k}}{k}, \quad \mathbf{v}_{\mathbf{k},\perp} \equiv \mathbf{v}_{\mathbf{k}} - v_{\mathbf{k},\parallel} \frac{\mathbf{k}}{k}$$

Euler's equation (2.9) for the transverse component is

$$\dot{\mathbf{v}}_{\mathbf{k},\perp} + H \mathbf{v}_{\mathbf{k},\perp} = \frac{1}{a} \frac{d(a \mathbf{v}_{\mathbf{k},\perp})}{dt} = 0 \Rightarrow \mathbf{v}_{\mathbf{k},\perp} \propto \frac{1}{a}$$

Therefore the rotational component of the peculiar velocity vanishes rapidly and one can consider \mathbf{v} as a purely longitudinal vector. The continuity equation for $\mathbf{v}_{\mathbf{k}}$ relates it linearly to the density contrast as

$$v_{\mathbf{k}} = -i \frac{a H}{k} f \delta_{\mathbf{k}}$$

**f is the Growth rate and γ is the growth index.
For General Relativity, $\gamma \sim 0.55$**

$$f \equiv \frac{d \ln(\delta_{\mathbf{k}})}{d \ln(a)}$$

$$f(a) = \Omega_{\text{M}}(a)^{\gamma}$$

Including galaxy bias, the galaxy overdensity is related to the velocity field via the continuity equation

$$v_{\mathbf{k}} = -i \frac{a H}{k} \beta \delta_{g,\mathbf{k}}$$

$$\beta \equiv f/b$$

RSD change the shape of the power spectrum and the correlation function

The matter density field is estimated through redshift, and then includes the peculiar velocity influence. This distortion is correlated with the real density perturbation, and therefore changes the statistics of the observed matter distribution

The Kaiser effect

Assuming peculiar velocities are small, the observed redshift of an object z_o is altered from its comoving redshift z (the shift due only to the expansion) by $z_o = z + v_z$, where v_z is the projection of the object's peculiar velocity along the line of sight (in units of c). Thus, this object will be assigned a radial comoving distance given by

$$\chi_s \equiv \chi(z + v_z) \simeq \chi_r + \frac{v_z}{H(z)}$$

The number of galaxies cannot change from real space to redshift space

$$n_s(\mathbf{x}_s) d^3 x_s = n(\mathbf{x}) d^3 x$$

$$n_s(\mathbf{x}_s) = n(\mathbf{x}) J$$

$$d^3 x_s = dx_s x_s^2 \sin \theta d\theta d\phi$$

$$d^3 x = dx x^2 \sin \theta d\theta d\phi,$$

$$J = \frac{dx x^2}{dx_s x_s^2}$$

$$z = H_0 x + \mathbf{u} \cdot \hat{\mathbf{x}} \quad x_s = x + \frac{\mathbf{u} \cdot \hat{\mathbf{x}}}{H_0} = x \left(1 + \frac{\mathbf{u} \cdot \hat{\mathbf{x}}}{x H_0} \right)$$

$$J = \left[1 + \frac{\partial}{\partial x} \left(\frac{\mathbf{u} \cdot \hat{\mathbf{x}}}{H_0} \right) \right]^{-1} \left(1 + \frac{\mathbf{u} \cdot \hat{\mathbf{x}}}{x H_0} \right)^{-2} \xrightarrow{kx \gg 1} J \approx 1 - \frac{\partial}{\partial x} \left(\frac{\mathbf{u} \cdot \hat{\mathbf{x}}}{H_0} \right)$$

$$\delta_s(\mathbf{x}) = \delta(\mathbf{x}) - \frac{\partial}{\partial x} \left(\frac{\mathbf{u}(\mathbf{x}) \cdot \hat{\mathbf{x}}}{H_0} \right)$$

Distant observer approximation: The distance from the observer to the galaxies in a survey will usually be much larger than the distance between the galaxies. This means that \mathbf{x} will vary little from galaxy to galaxy, and we can approximate $\mathbf{u} \cdot \hat{\mathbf{x}}$ with $\mathbf{u} \cdot \hat{\mathbf{z}}$

$$\tilde{\delta}_s(\mathbf{k}) = \int d^3x e^{-i\mathbf{k} \cdot \mathbf{x}} \left[\delta(\mathbf{x}) - \frac{\partial}{\partial x} \left(\frac{\mathbf{u}(\mathbf{x}) \cdot \hat{\mathbf{z}}}{H_0} \right) \right] \quad \mathbf{u}(\mathbf{k}) = i f H_0 \tilde{\delta}(\mathbf{k}) \frac{\mathbf{k}}{k^2}$$

$$\begin{aligned}
\tilde{\delta}_s(\mathbf{k}) &= \tilde{\delta}(\mathbf{k}) - if \int d^3x e^{-i\mathbf{k}\cdot\mathbf{x}} \frac{\partial}{\partial x} \int \frac{d^3k'}{(2\pi)^3} e^{i\mathbf{k}'\cdot\mathbf{x}} \tilde{\delta}(\mathbf{k}') \frac{\mathbf{k}'}{k'^2} \cdot \hat{\mathbf{z}} \\
&= \tilde{\delta}(\mathbf{k}) - if \int d^3x e^{-i\mathbf{k}\cdot\mathbf{x}} \int \frac{d^3k'}{(2\pi)^3} e^{i\mathbf{k}'\cdot\mathbf{x}} i\mathbf{k}' \cdot \hat{\mathbf{x}} \tilde{\delta}(\mathbf{k}') \frac{\mathbf{k}'}{k'^2} \cdot \hat{\mathbf{z}} \\
&= \tilde{\delta}(\mathbf{k}) + f \int \frac{d^3k'}{(2\pi)^3} \tilde{\delta}(\mathbf{k}') k'^2 (\hat{\mathbf{k}}' \cdot \hat{\mathbf{z}})^2 \frac{1}{k'^2} \int e^{i(\mathbf{k}'-\mathbf{k})\cdot\mathbf{x}} \\
&= \tilde{\delta}(\mathbf{k}) + f \int \frac{d^3k'}{(2\pi)^3} \tilde{\delta}(\mathbf{k}') (\hat{\mathbf{k}}' \cdot \hat{\mathbf{z}})^2 (2\pi)^3 \delta^{(3)}(\mathbf{k}' - \mathbf{k}) \\
&= \tilde{\delta}(\mathbf{k}) + \tilde{\delta}(\mathbf{k}) f (\hat{\mathbf{k}} \cdot \hat{\mathbf{z}})^2 \\
&= [1 + f (\hat{\mathbf{k}} \cdot \hat{\mathbf{z}})^2] \tilde{\delta}(\mathbf{k}) \\
&\equiv [1 + f \mu_{\mathbf{k}}^2] \tilde{\delta}(\mathbf{k}),
\end{aligned}$$

$$\delta_{s,\mathbf{k}} = (1 + \beta \mu_{\mathbf{k}}^2) \delta_{r,\mathbf{k}} \quad \mu_{\mathbf{k}} \equiv \mathbf{k} \cdot \hat{\mathbf{n}}_z / k$$

$$\beta = \frac{f}{b} \approx \frac{\Omega_{m0}^{0.6}}{b}$$

Hence, redshift-space distortions induce an anisotropy in the observed power spectrum, which now is a function of both k and $\mu_{\mathbf{k}}$

$$P_s(k, \mu_{\mathbf{k}}, z) = (1 + \beta(z) \mu_{\mathbf{k}}^2)^2 P_r(k, z)$$

Redshift space distortions are sensitive to the growth of structures in the Universe

Provide a good test for modified gravity theories through the determination of the growth factor and the growth index

Power spectrum is normalized using the variance of Galaxy distribution smoothed on a scale of $8h^{-1}$ Mpc or

$$\sigma_8(z) = \sigma_{8,0} D(z)$$

What we really measure from RSD are $f\sigma_8$ and $b\sigma_8$

$$P_s(k, \mu_{\mathbf{k}}, z) = (1 + \beta(z) \mu_{\mathbf{k}}^2)^2 P_r(k, z)$$


$$\mu_{\mathbf{k}} \equiv \mathbf{k} \cdot \hat{\mathbf{n}}_z / k$$

$$\beta = \frac{f}{b} \approx \frac{\Omega_{m0}^{0.6}}{b}$$

A very common way of studying RSD is by the use of the multipole expansion

$$(1 + \beta \mu_k^2)^2 = \left(1 + \frac{2}{3}\beta + \frac{1}{5}\beta^2\right) \mathcal{P}_0(\mu_k) + \left(\frac{4}{3}\beta + \frac{4}{7}\beta^2\right) \mathcal{P}_2(\mu_k) + \frac{8}{35}\beta^2 \mathcal{P}_4(\mu_k)$$

Legendre polynomials



Each term can be independently measured due to the different angular dependence

$$\xi(r, \mu) = \sum_l \xi_l(r) \mathcal{P}_l(\mu) \quad \xi_l(r) = \frac{i^l}{2\pi^2} \int dk P(k) k^2 j_l(kr)$$

$$\xi_s(r, \mu) = b(z)^2 \left\{ \left[1 + \frac{2}{3}\beta + \frac{1}{5}\beta^2\right] \mathcal{P}_0(\mu) \xi_0(r) + \left[\frac{4}{3}\beta + \frac{4}{7}\beta^2\right] \mathcal{P}_2(\mu) \xi_2(r) + \frac{8}{35} \mathcal{P}_4(\mu) \xi_4(r) \right\}$$

Non-Linear Effects: Fingers of God

On small (non-linear) scales these velocities are large enough to compensate Hubble's law and the spheres are turned inside out and deformed in shape, forming structures that point towards the observers, commonly known as fingers of God

Difficult to model. In general:

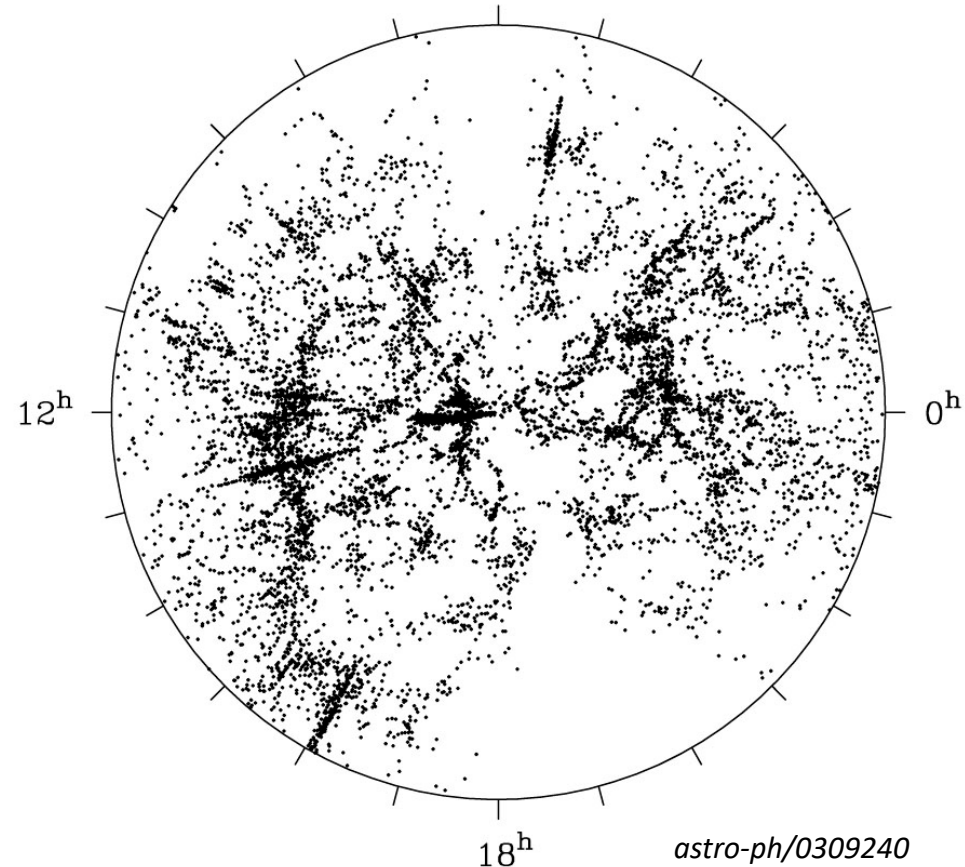
$$P_s(k, \mu_{\mathbf{k}}, z) = (1 + \beta(z) \mu_{\mathbf{k}}^2)^2 F(k, \mu_{\mathbf{k}}) P_r(k, z)$$

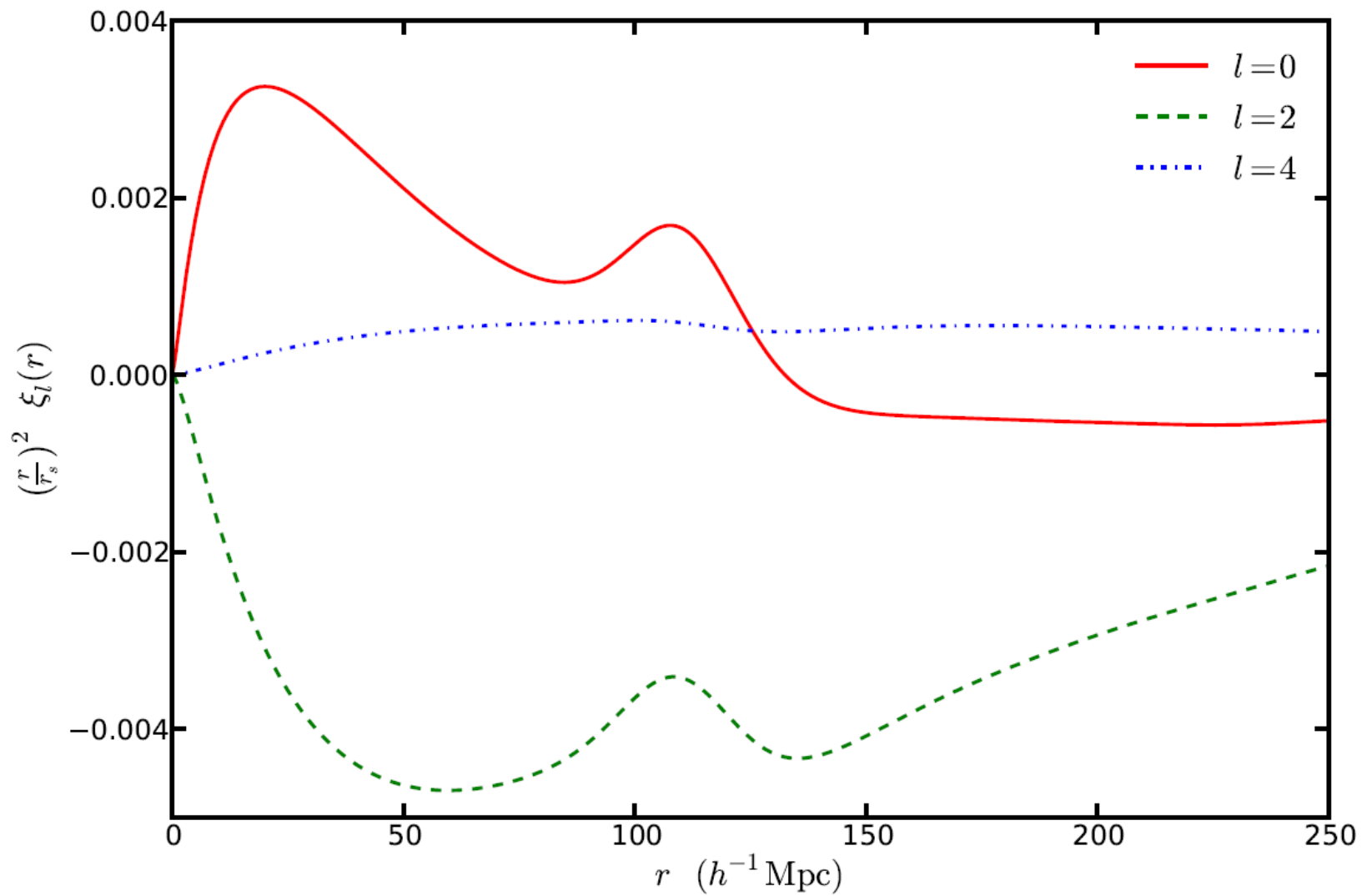
CfA: $0^\circ < \delta < 30^\circ$ 6^h $v < 12\,000 \text{ km s}^{-1}$

A usual $F(k, \mu)$ is

$$F(k, \mu_{\mathbf{k}}) = \frac{1}{(1 + k^2 \mu_{\mathbf{k}}^2 \Sigma_v^2)^2}$$

Streaming model





First three non-zero multipoles of the two-point correlation function in redshift space as predicted in the Kaiser approximation

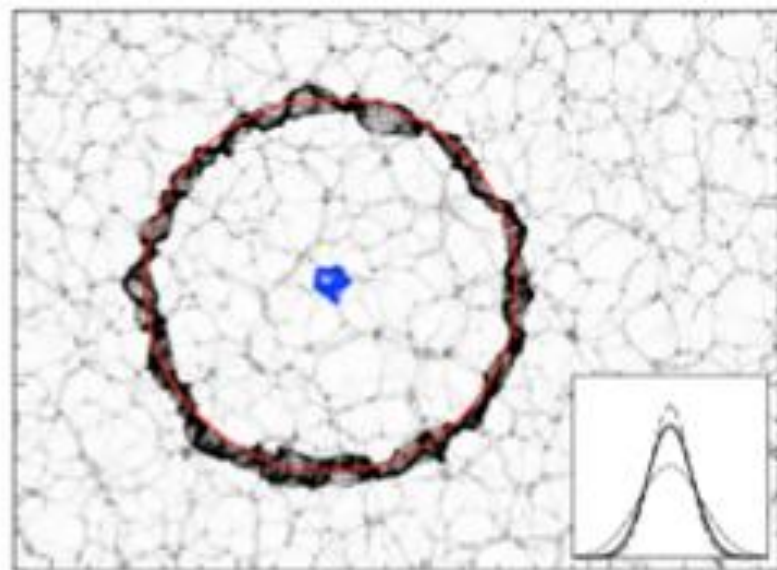
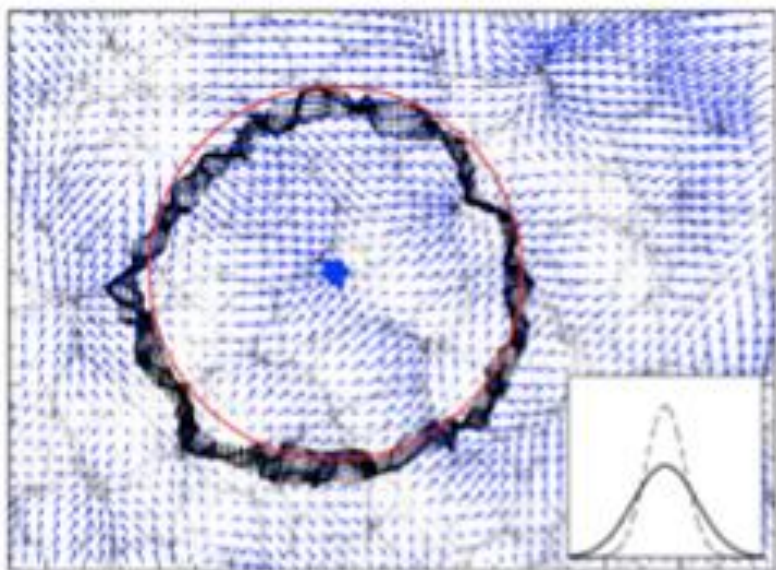
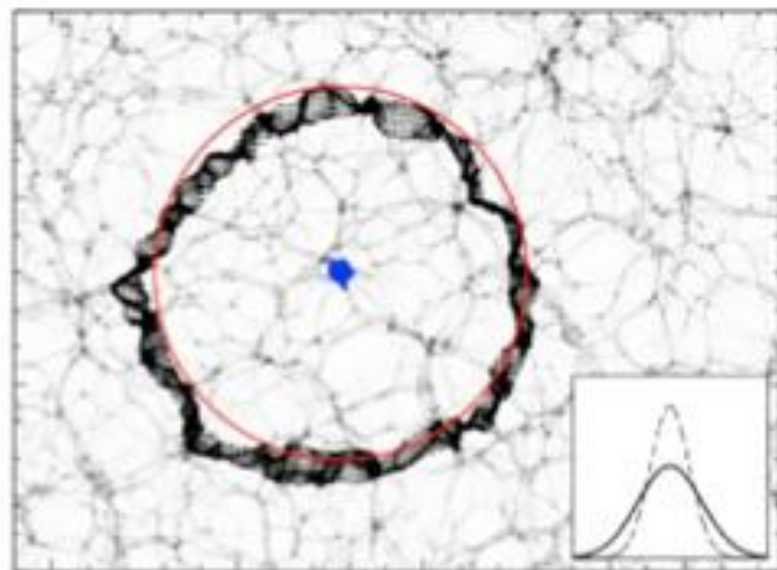
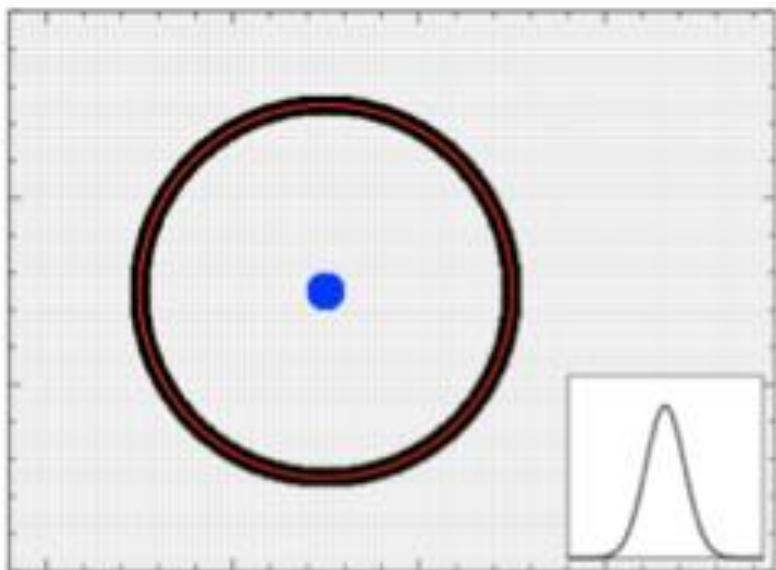
Reconstruction techniques

- The damping of the BAO limits the attainable accuracy.
- Reconstruction attempts to “un-do” these distortions.
- Construct a *displacement field* Ψ as

$$\nabla \cdot \Psi + \frac{f(z)}{b} \nabla \cdot (\Psi_s \hat{s}) = -\frac{\delta_g}{b}$$

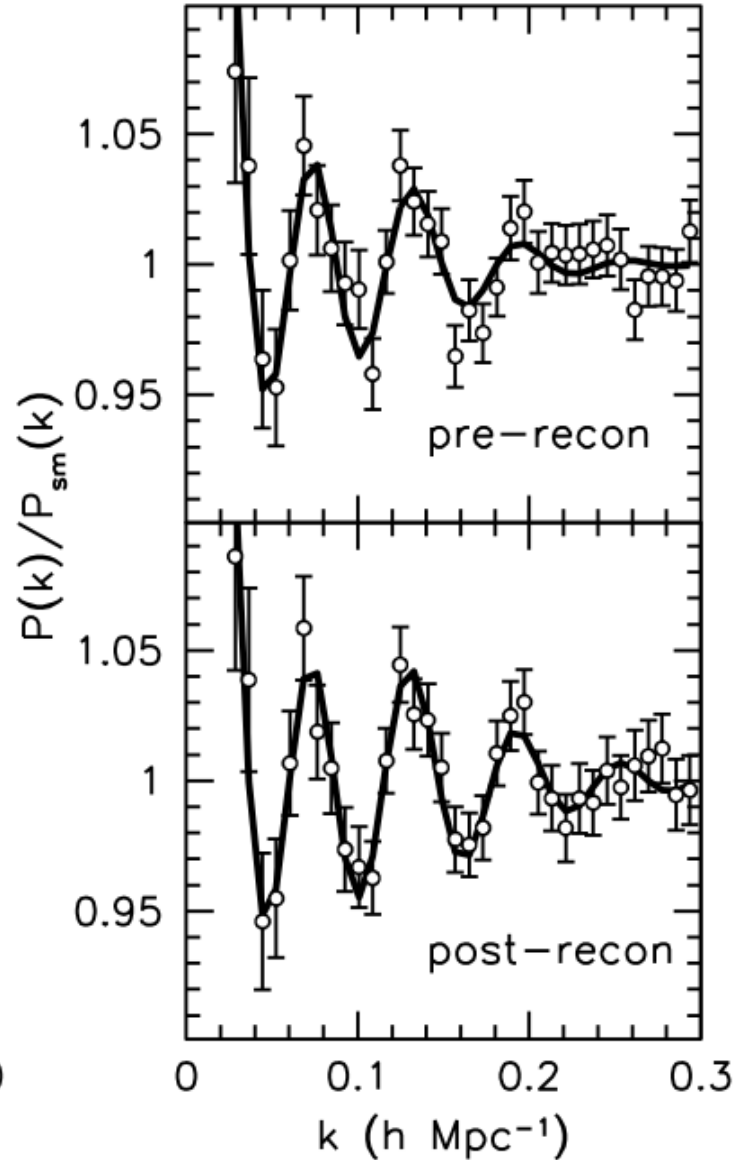
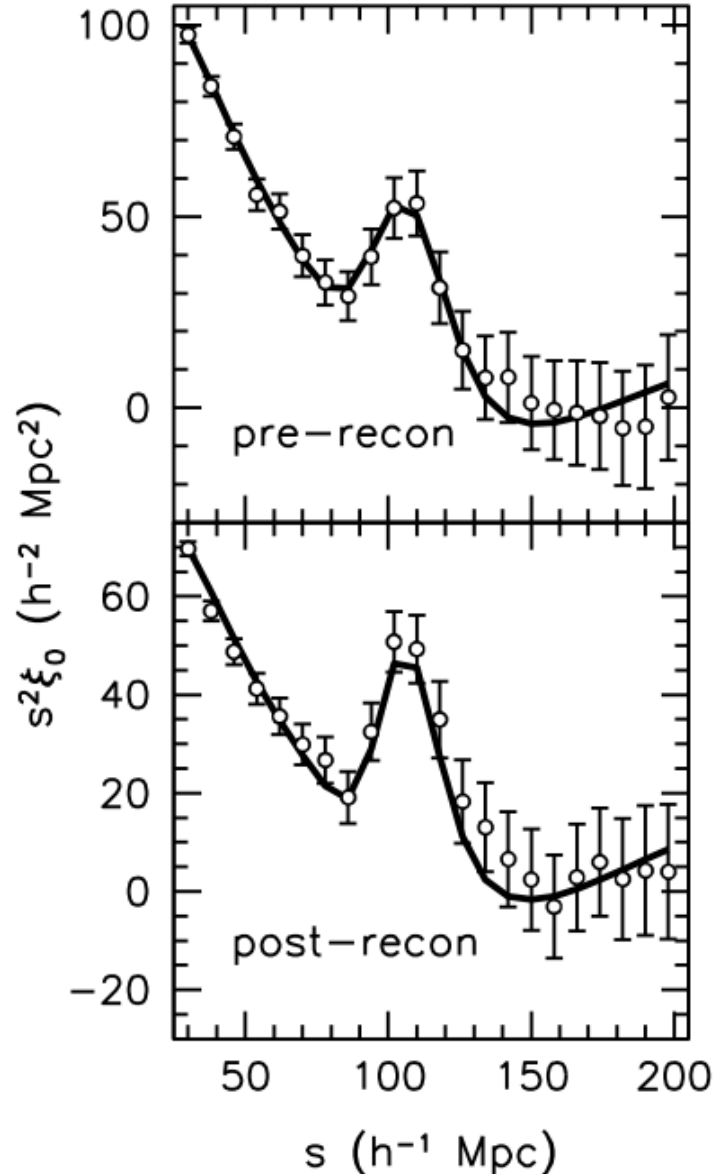
- Significantly improve BAO distance measurements.
- Requires the knowledge of b and $f(z)$.

Reconstruction of the BAO ring



Reconstruction of the BAO ring

After reconstruction the BAO signal is enhanced both in the correlation function and in the power spectrum

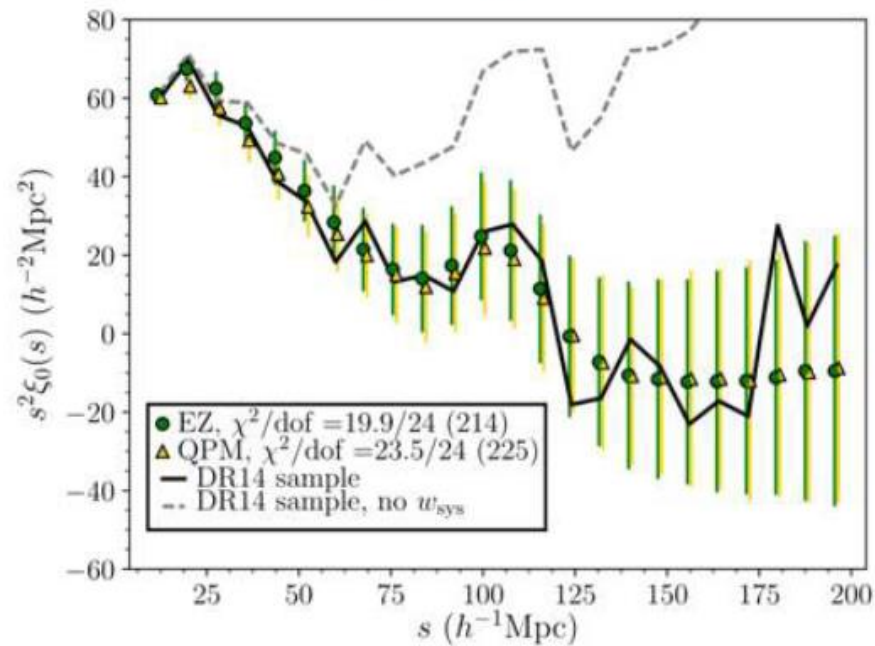


BAO measurements in 2018 (eBOSS measurements)

Slide taken from M. Blanton, CosmoAndes 2018

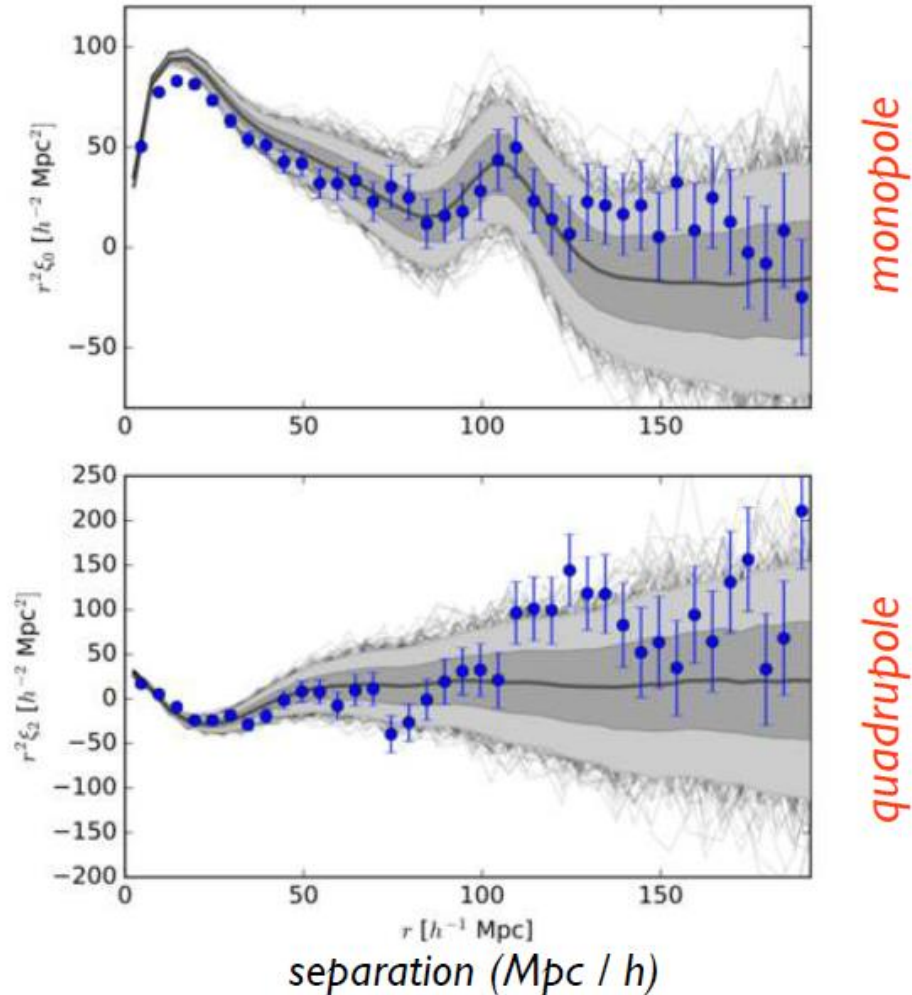
quasar correlation function

Ata et al. (2017); SDSS-IV



separation (Mpc / h)

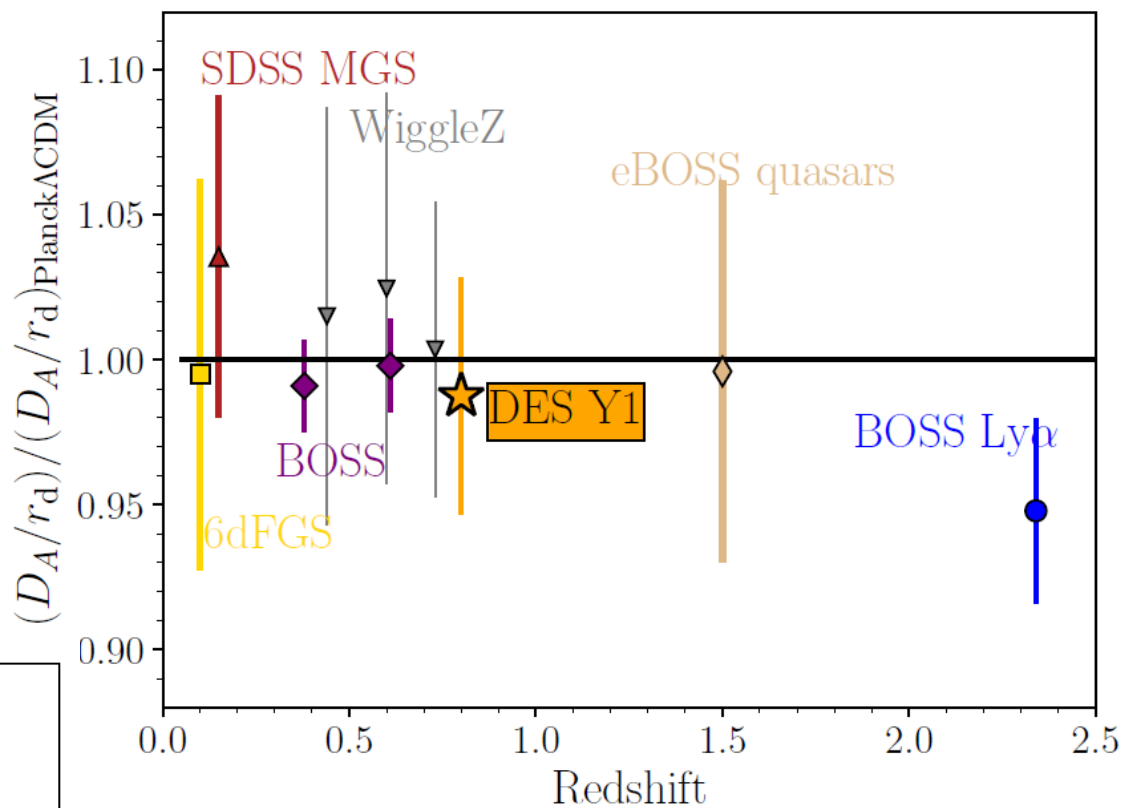
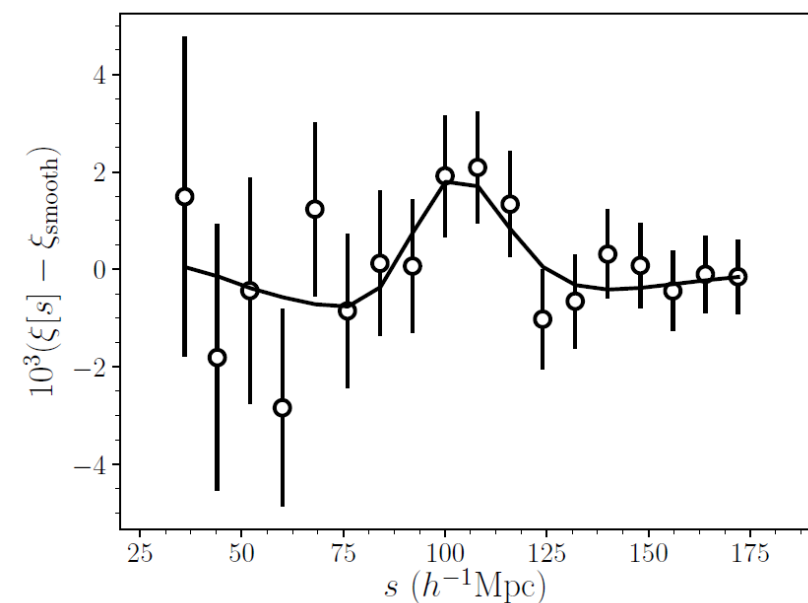
luminous red galaxy correlation function
Bautista et al. (2018); SDSS-IV



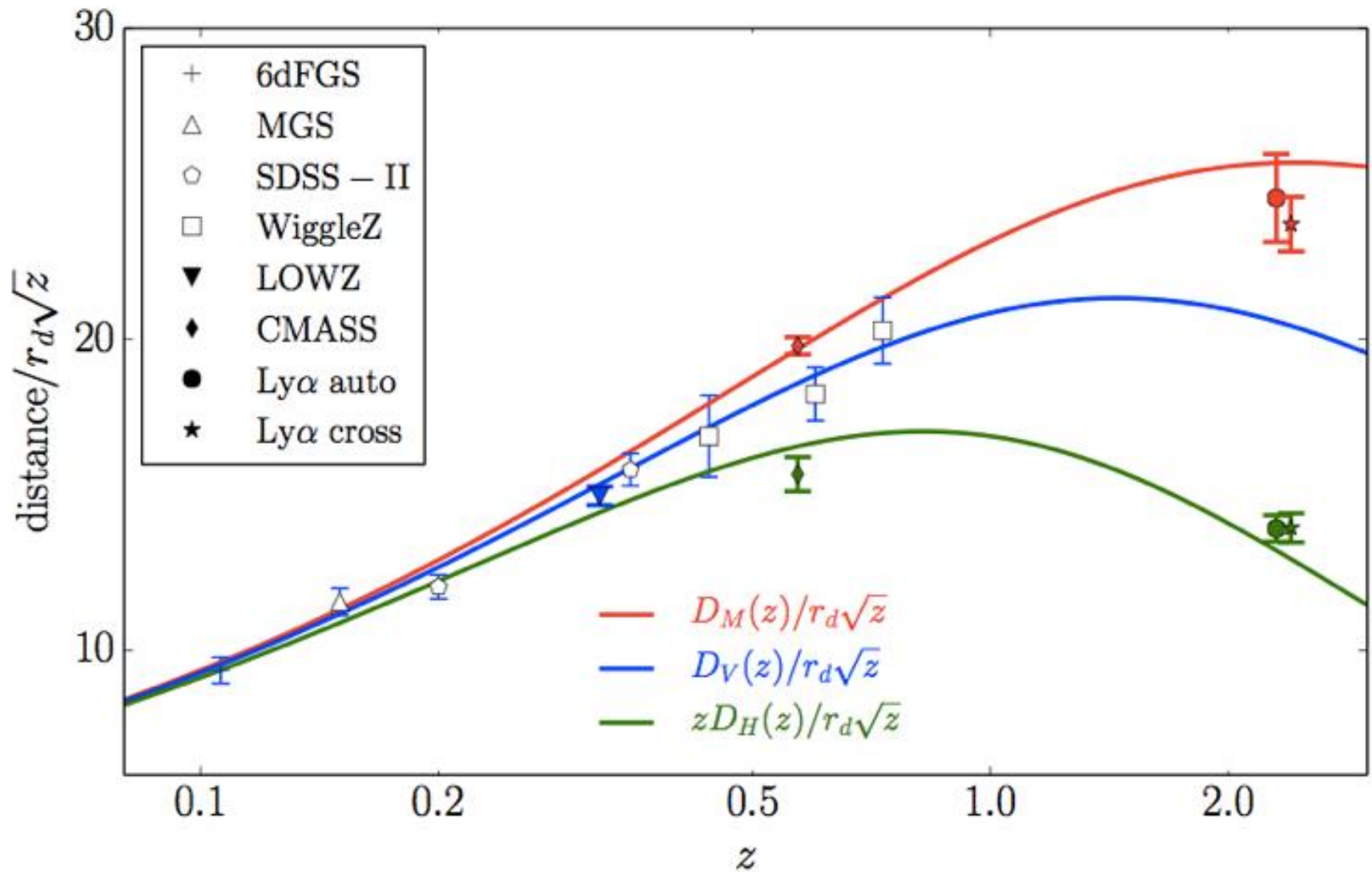
after reconstruction

Include quasars as tracers of the matter density fields

BAO with Quasars from eBOSS

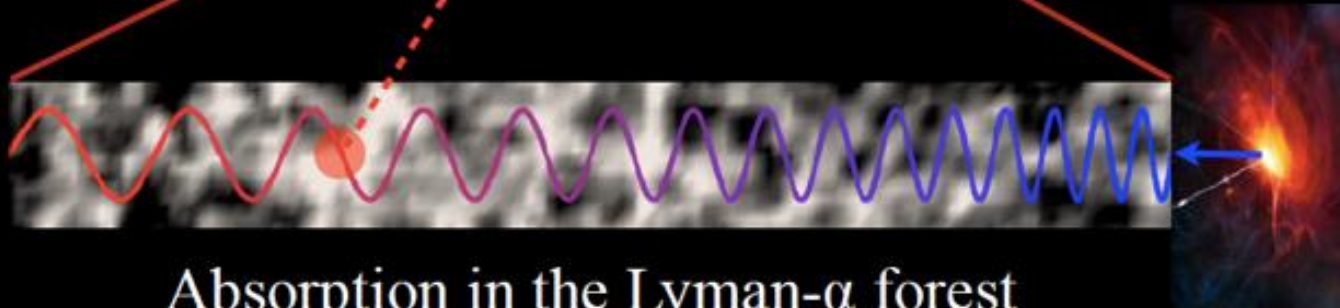
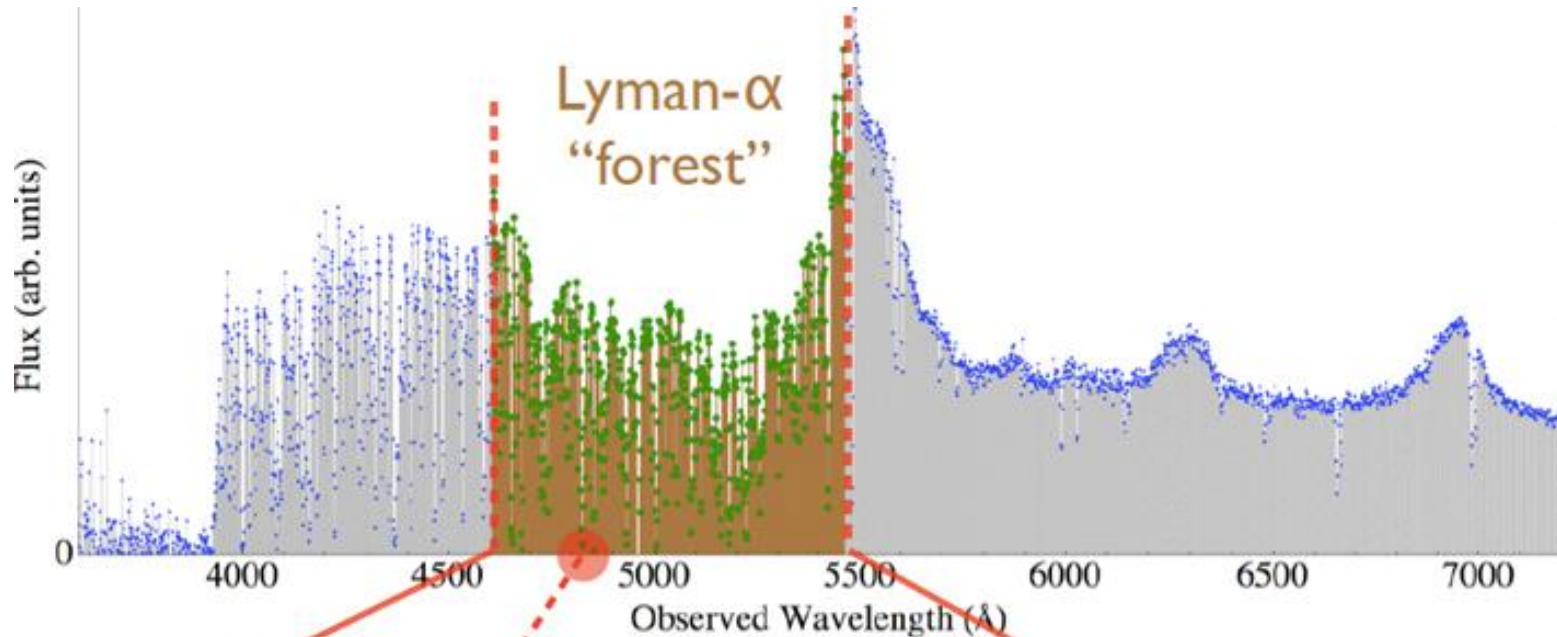


Hubble diagram for different definitions of Distances



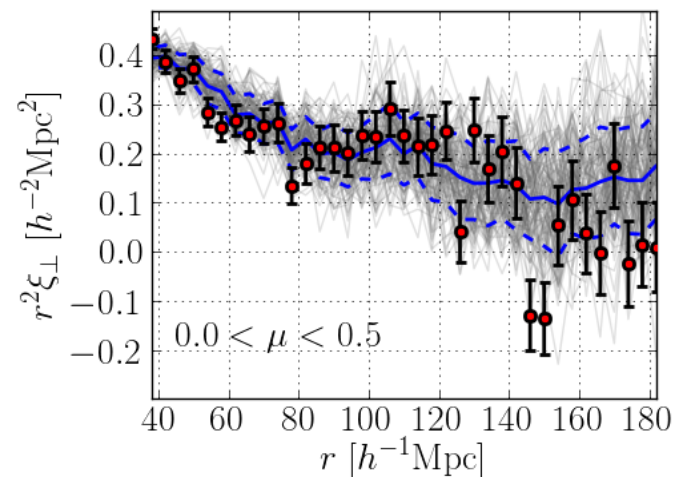
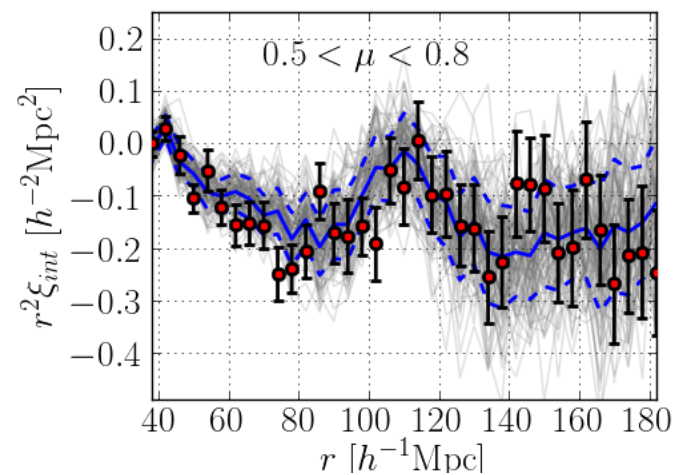
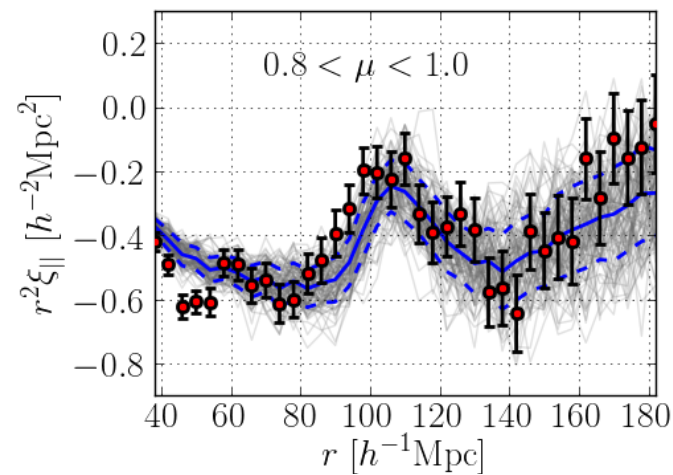
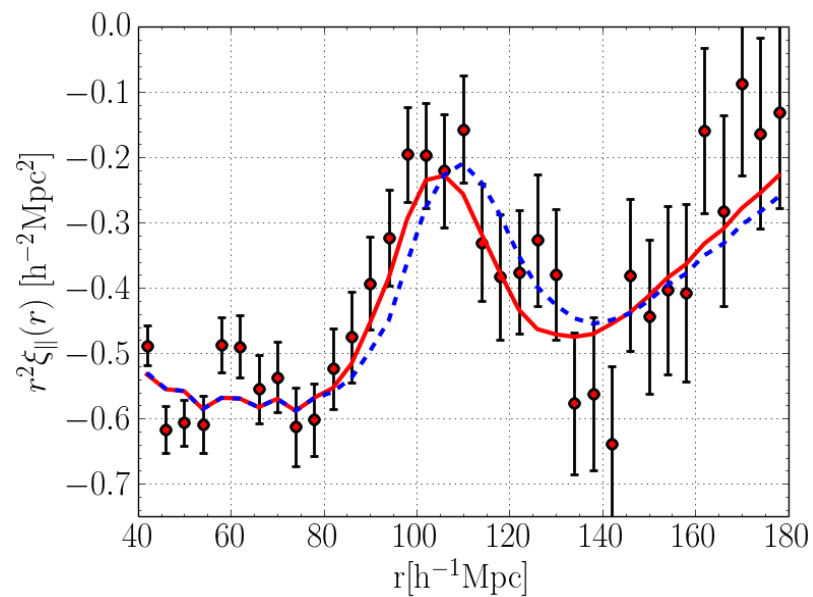
Other BAO methods: The Lyman Alpha Forest

Use the Lyman Alpha absorption lines in quasars spectra to trace matter
Allow to extend the BAO reach beyond redshift 2

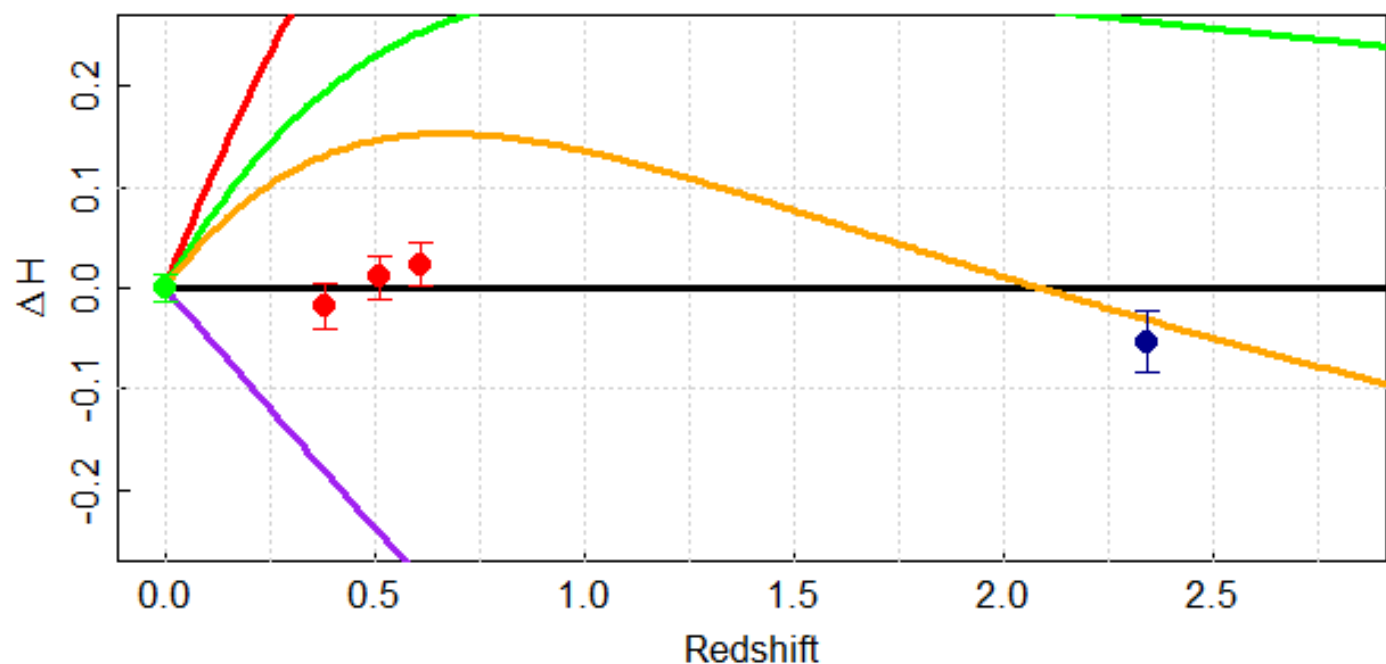
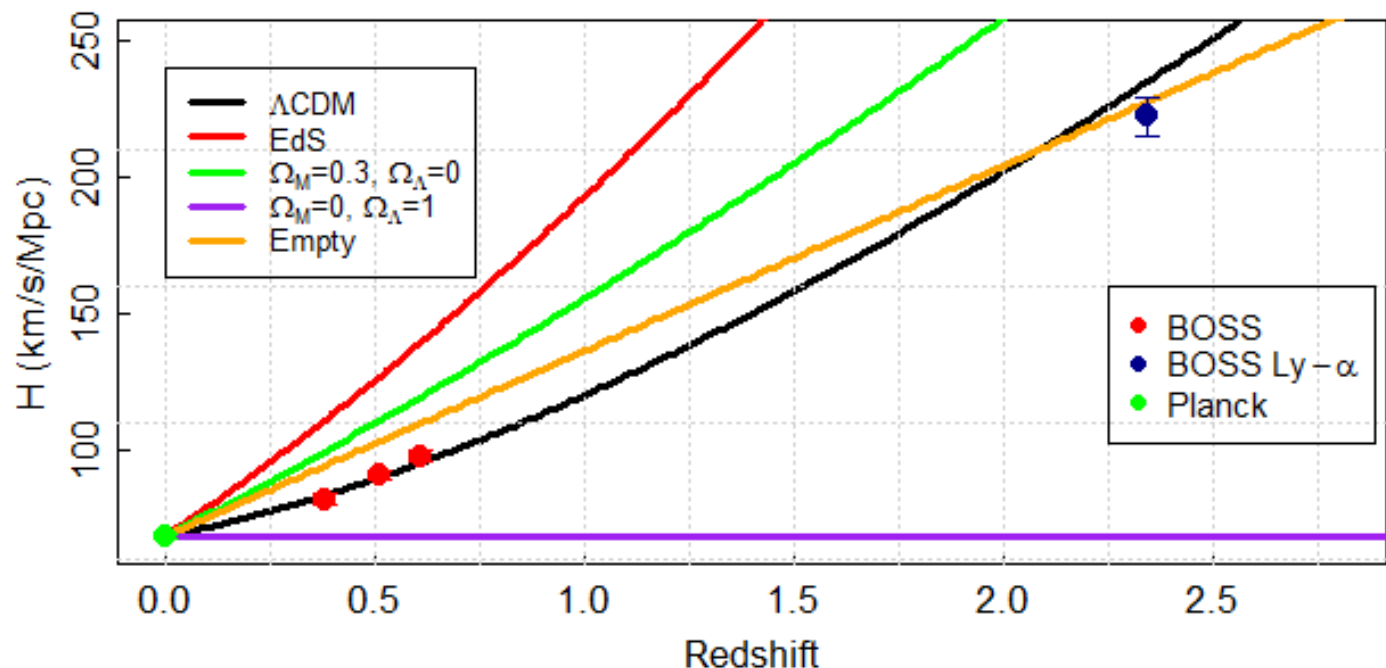


Absorption in the Lyman- α forest
at λ_{obs} measures H-I density at $1+Z_{\text{abs}} = \lambda_{\text{obs}}/\lambda_{\alpha}$

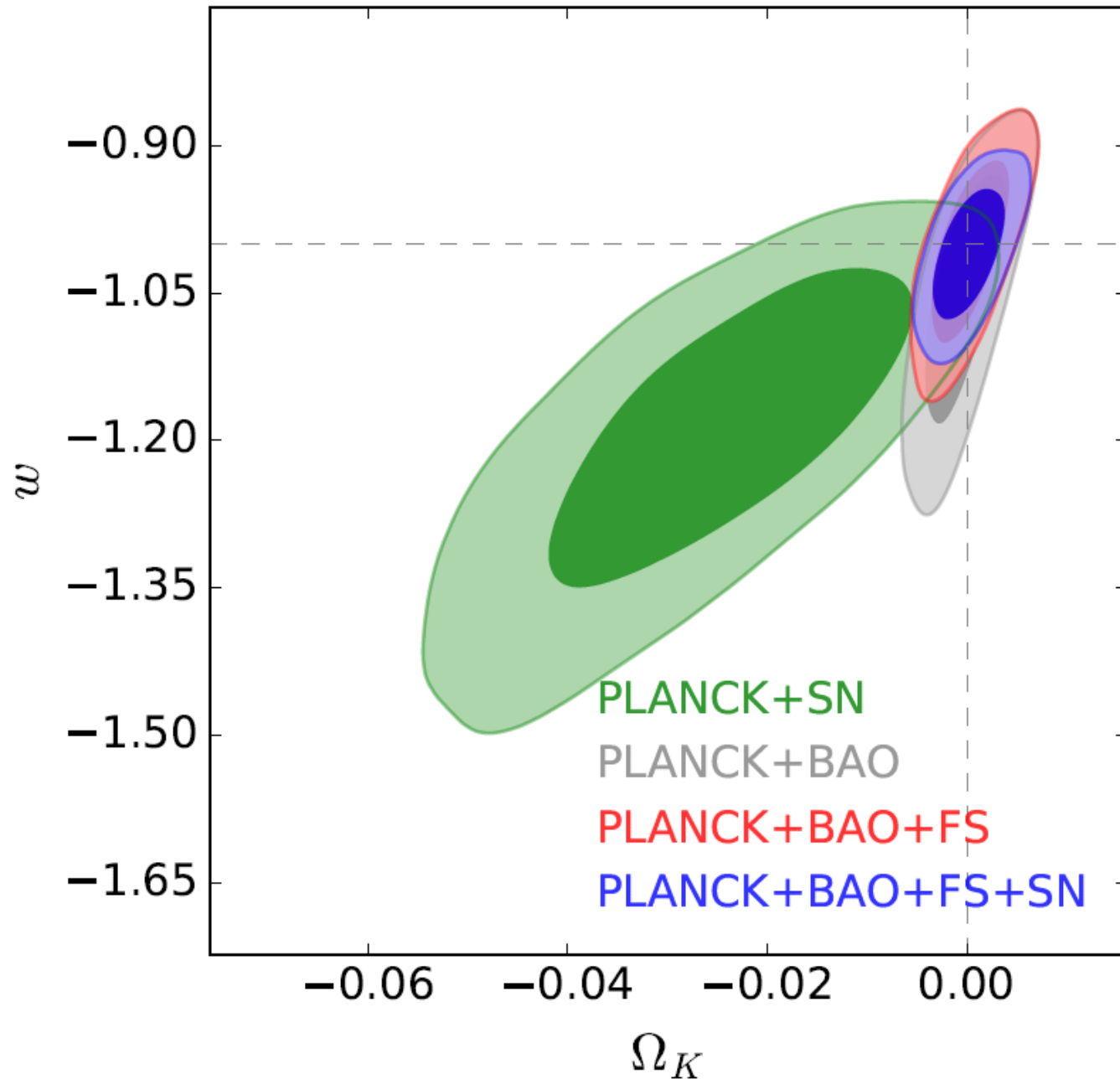
Measured correlation function averaged over three angular regions



Current Hubble Parameter Measurements using BAO Standard Ruler

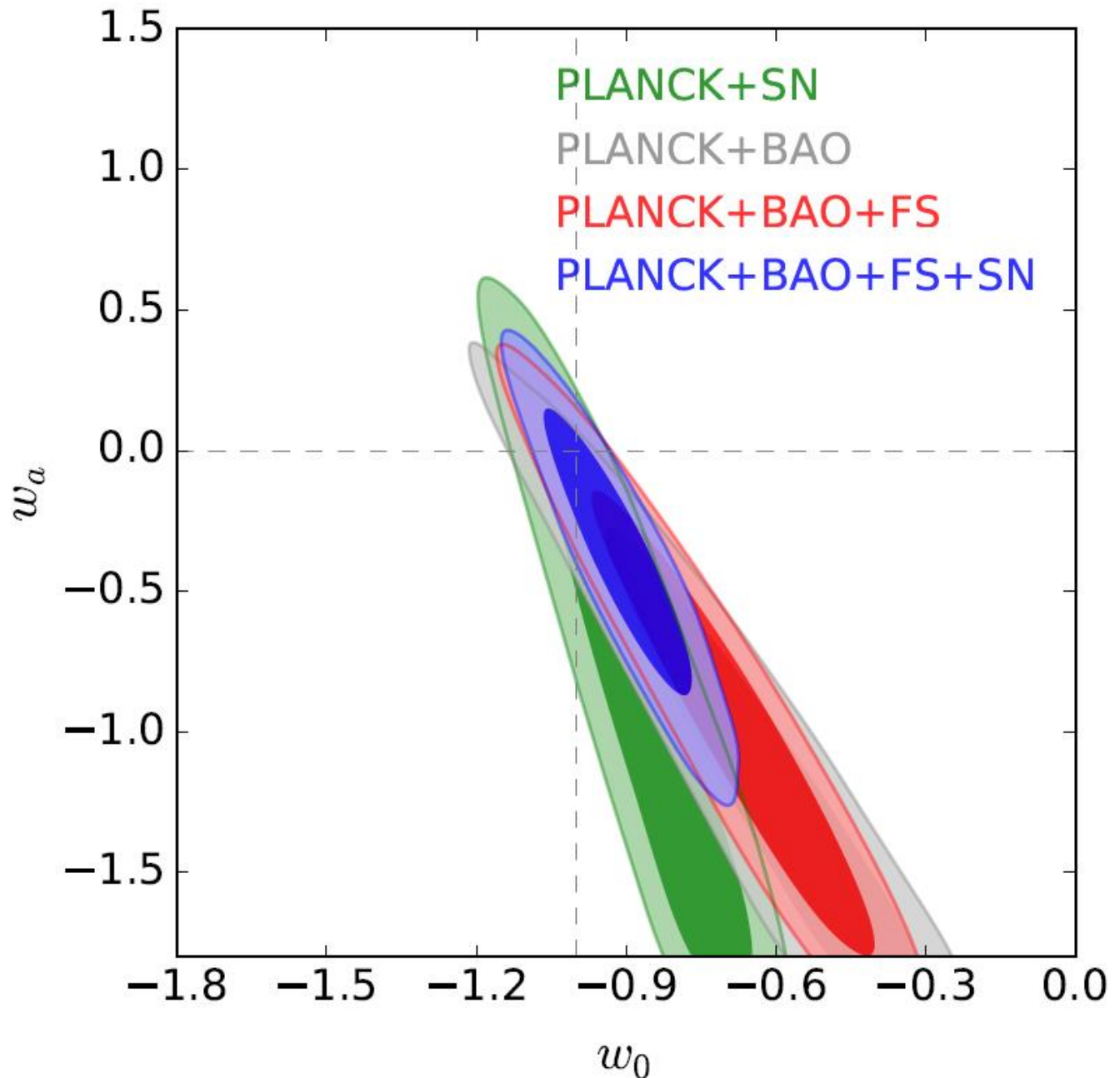


Cosmological Parameters Constraints using BAO



Cosmological Parameters Constraints using BAO

Current constraints are compatible with the dark energy being the cosmological constant



Cosmological Parameters Constraints using BAO

Limits here or smaller rule out the inverse mass ordering for neutrinos

